Supporting Information

Mechanically tunable porous gels constructed via the dual coordination/covalent polymerization of coumarin-functionalized rhodium-organic cuboctahedra

David W. Burke,[a,*] Masataka Yamashita,[b] Zaoming Wang,[a] Mako Kuzumoto,[b] Kenji Urayama,[b] Kei Saito,[c] and Shuhei Furukawa[a,d,*]

[a] *Institute for Integrated Cell-Material Sciences (WPI-iCeMS), Kyoto University, Yoshida, Sakyo-ku, Kyoto 606-8501, Japan.*

[b] *Department of Material Chemistry, Graduate School of Engineering, Kyoto University, Katsura, Nishikyo-ku, Kyoto 615-8510, Japan*

[c] *Graduate School of Advanced Integrated Studies in Human Survivability (GSAIS), Kyoto University, Sakyo-ku, Kyoto 606-8306, Japan*

[d] *Department of Synthetic Chemistry and Biological Chemistry, Graduate School of Engineering, Kyoto University, Katsura, Nishikyo-ku, Kyoto 615-8510, Japan.*

Contents

1. Materials and Instruments

1.1. Materials

All reagents were purchased from commercial suppliers (Nacalai Tesque, Inc., TCI Co., Ltd., and WAKO Pure Chemical Industries Ltd.; 95% purity or higher) and used without further purification.

1.2. Instruments

Nuclear Magnetic Resonance Spectroscopy. Solution-state ^{1}H, ^{13}C, COSY, HSQC, HMBC, and DOSY NMR spectra were collected using a Bruker Avance III 500 MHz spectrophotometer, and each spectrum was referenced to the residual solvent peak. Solid-state ^{13}C Cross-Polarization/Magic-Angle Spinning (CP/MAS) NMR spectra were collected using a JEOL JNM-ECZ600R spectrophotometer (600 MHz) equipped with a JEOL 3.2 mm double resonance MAS probe. All solid-state measurements were performed with a MAS frequency of 14 kHz.

Mass Spectrometry. Electrospray ionization (ESI) and atmospheric-pressure chemical ionization (APCI) mass spectra were collected using an Exactive Plus mass spectrometer (Thermo Fischer Scientific) in positive detection mode. Cold-spray ionization (CSI) mass spectra were collected using a micrOTOF II mass spectrometer (Bruker Daltonics) in positive detection mode. Matrix-assisted laser desorption/ionization time-of-flight (MALDI-TOF) mass spectra were collected using either an ultrafleXtreme MALDI-TOF mass spectrometer (Bruker Daltonics) in linear positive mode equipped with a 337 nm nitrogen gas laser for sample ionization, or a Shimadzu MALDI-8030 in linear positive mode equipped with a 355 nm laser for sample ionization. A *trans*-2-[3-(4-tert-butylphenyl)-2-methyl-2-propenylidene]malononitrile (DCTB) matrix was employed for all MALDI-TOF measurements, along with sodium trifluoroacetate as a cationizing agent.

Infrared Spectroscopy. Infrared spectra were collected using an FT/IR-6100 spectrometer (JASCO) in attenuated total reflection (ATR) mode under vacuum.

Ultraviolet-Visible Spectroscopy. Ultraviolet-visible (UV-Vis) spectra were collected using a V-670 spectrophotometer (JASCO) at 20 °C. For UV-Vis titration experiments, the samples were stirred at 300 rpm while each spectrum was collected. For all other experiments, samples were measured without stirring.

Scanning Electron Microscopy. Scanning electron microscopy (SEM) images were collected using either a JEOL JSM-7001F Scanning Electron Microscope or a Hitachi High-Tech Schottky Field Emission Scanning Electron Microscope SU5000. All samples were coated with osmium (19 nm) using an HPC-20 Osmium Plasma Coater prior to imaging.

Supercritical CO_2 Drying. Supercritical CO_2 drying was performed using a Tousimis Autosamdri-931 critical point dryer. Methanol-solvated gels were first placed inside of the sample chamber, which was filled with methanol, sealed, and cooled to 0 °C. The solvent was then exchanged with liquid CO_2 twice; after each exchange, CO_2 was held inside the chamber for 2 hours to facilitate the complete removal of methanol from the gel. The temperature of the chamber was then raised to 40 °C to generate supercritical CO_2, and subsequently vented to afford the activated aerogels.

Gas Sorption. N_2 sorption isotherms (77 K) were collected using a BELSORP-max volumetric adsorption instrument (MicrotracBEL Corporation) equipped with a BELCRYO temperature control unit and a CryoMini

Compressor (Model SA112, Iwatani Industrial Gases Corporation). Brunauer-Emmett-Teller (BET) surface areas for aerogel samples were calculated from the N_2 adsorption data via BETSI analysis, as previously described in the literature.[1] CO_2 sorption isotherms (195 K) were collected using a BELSORP MINI X volumetric adsorption instrument (MicrotracBEL Corporation). Samples were submerged in a dry ice/isopropanol bath throughout the CO_2 sorption measurement to maintain the temperature at 195 K. All samples were activated at 120 °C under vacuum overnight prior to data collection.

Photoirradiation Experiments. Photoirradiation experiments at λ = 350 nm were performed using either an Asahi Spectra MAX-303 Compact Xenon Light Source equipped with a 350 nm filter (irradiance = 10 mW/cm^2 unless otherwise noted), or an Imoto Model IMC-0091 Photoreactor equipped with 18 Toshiba FL8BLB/N black lights (total irradiance of 4 mW/cm^2, λ_{max} = 350 nm). Prior to each experiment, the irradiance produced by the light source was confirmed using a Thorlabs 100MD power meter.

Rheological Measurements. Rheological measurements for all MOP gels (swollen in DMF) were performed in shearing mode at 25 °C using a stress-controlled MCR502 rheometer (Anton-Paar) in parallel-plate geometry. Prior to each measurement, diamond sheets (Sankyo Corporation DIA-150) were taped to both the top and bottom plates to ensure that the rheometer could grip the gel effectively. Each gel (15 mm diameter) was gently placed on the diamond sheet attached to the rheometer's bottom plate, and then the top plate (15 mm diameter) was slowly lowered until just touching the surface of the gel. First, frequency sweep measurements (oscillation frequency ω = 0.1-10 rad/s, strain amplitude γ = 1%) were performed to determine the storage (G') and loss moduli (G'') of the pristine gels as a function of oscillation frequency. For all tested gels, G' was found to be frequency independent and approximately one order of magnitude larger than G'', as is characteristic for crosslinked polymer gels. Next, the gels were compressed by further lowering the top probe to 60% of its original height. Compression enables the diamond sheet-covered plates to grip the gel effectively even at high strain amplitudes (γ > 100%), facilitating the characterization of the mechanical strength of each sample. Once the gels were compressed, another frequency sweep was first performed (ω = 0.1-10 rad/s, γ = 1%) to check G' and G'' of the gel and confirm that it had not fractured during compression. In all cases, the gels were found to exhibit frequency-independent G' values that were an order of magnitude larger than G'', confirming that they were still intact. Notably, compression was found to increase the moduli of all gels (**Figure S47a**). Finally, strain amplitude sweep measurements (ω = 1 rad/s, γ = 0.1-400%) were performed to identify the onset of fracture for each of the compressed gels (**Figure S47b**), which is assigned to the strain amplitude at which G'' achieves its maximum value.

2. Synthetic Protocols

2.1. Synthesis of Small Molecule Building Blocks

2.1.1. Synthesis of Rhodium Acetate [$Rh_2(OAc)_4(MeOH)_2$]

Rhodium acetate [Rh_2(acetate)$_4$(methanol)$_2$] was synthesized according to literature precedent.[2]

2.1.2. Synthesis of 1,4-bis(imidazol-1-ylmethyl)benzene (bix)

Bix was synthesized according to literature precedent.[3]

2.1.3. Synthesis of 1-dodecylimidazole (diz)

Diz was synthesized according to literature precedent.[3]

Scheme S1. Synthesis of C_{10}-Coumarin-bdcH_2

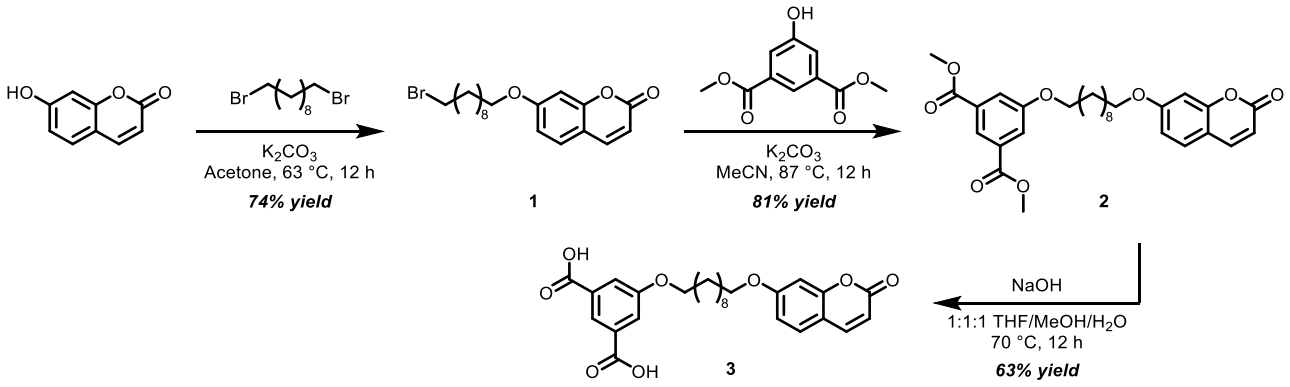

2.1.4. Synthesis of 7-((10-bromodecyl)oxy)-2H-chromen-2-one (1)

This protocol was adapted from a procedure initially reported by Park and coworkers.[4] Umbelliferone (1.62 g, 10.0 mmol), 1,10-dibromodecane (30.0 g, 100 mmol), and K_2CO_3 (19.9 g, 144 mmol) were combined in a round bottom flask. Acetone (100 mL) was then added to dissolve the organic components. The resulting reaction mixture was heated to reflux for 12 h, after which the reaction was centrifuged to remove undissolved K_2CO_3, then evaporated to a viscous, yellow oil. This oil was redissolved in dichloromethane and washed with water to remove residual K_2CO_3. Next, the DCM layer was dried over Na_2SO_4, evaporated to a viscous yellow oil, and purified by column chromatography (silica gel, hexane → 1:1 hexane/ethyl acetate). The solids isolated after column chromatography were still found to contain a small amount of unreacted 1,10-dibromodecane, and were therefore washed twice with hexane (30 mL each), collected by centrifugation, and dried under vacuum, affording the product (**1**) as a white powder (2.81 g, 74% yield). ^{1}H NMR ($CDCl_3$, 500 MHz) δ 7.63 (d, J = 9.4 Hz, 1H), 7.36 (d, J = 8.6 Hz, 1H), 6.83 (dd, J = 8.6, 2.4 Hz, 1H), 6.80 (d, J = 2.4 Hz, 1H), 6.24 (d, J = 9.4 Hz, 1H), 4.01 (t, J = 6.5 Hz, 2H), 3.41 (t, J = 6.8 Hz, 2H), 1.90 – 1.76 (m, 4H), 1.50 – 1.26 (m, 12H). ^{13}C{^{1}H} NMR ($CDCl_3$, 125 MHz) δ 162.58, 161.42, 156.09, 143.57, 128.83, 113.15, 113.08, 112.52, 101.48, 68.79, 34.15, 32.95, 29.53, 29.47, 29.40, 29.10, 28.86, 28.28, 26.07. HRMS (APCI) calcd for $C_{19}H_{26}BrO_3$ $[M+H]^+$: 381.1060; found: 381.1063.

2.1.5. Synthesis of dimethyl 5-((10-((2-oxo-2H-chromen-7-yl)oxy)decyl)oxy)isophthalate (2)

This protocol was adapted from a procedure initially reported by Park and coworkers.[4] **1** (1.73 g, 4.54 mmol), dimethyl 5-hydroxyisophthalate (0.63 g, 3.00 mmol), K_2CO_3 (0.45 g, 3.26 mmol), and acetonitrile (30 mL) were combined in a round bottom flask and heated to reflux for 12 h. Next, the reaction mixture was evaporated to dryness, then redissolved in $CHCl_3$ and centrifuged to remove undissolved K_2CO_3. The remaining organic

solution was washed with water to remove residual K_2CO_3, then dried over Na_2SO_4, dry loaded onto silica gel, and purified by column chromatography (silica gel, dichloromethane → 5% methanol in dichloromethane), affording the product (**2**) as a white powder (1.24 g, 81% yield). ^{1}H NMR ($CDCl_3$, 500 MHz) δ 8.25 (t, J = 1.5 Hz, 1H), 7.74 (d, J = 1.4 Hz, 2H), 7.63 (d, J = 9.4 Hz, 1H), 7.35 (d, J = 8.5 Hz, 1H), 6.83 (dd, J = 8.5, 2.4 Hz, 1H), 6.80 (d, J = 2.4 Hz, 1H), 6.24 (d, J = 9.5 Hz, 1H), 4.04 (t, J = 6.5, 2H), 4.01 (t, J = 6.5, 2H), 3.93 (s, 6H), 1.86 – 1.76 (m, 4H), 1.52 – 1.29 (m, 12H). ^{13}C{^{1}H} NMR ($CDCl_3$, 125 MHz) δ 166.34, 162.56, 161.39, 159.36, 156.06, 143.56, 131.83, 128.81, 122.87, 119.96, 113.12, 113.04, 112.49, 101.46, 68.78, 68.72, 52.51, 29.56, 29.55, 29.41, 29.20, 29.09, 26.08, 26.06. HRMS (ESI) calcd for $C_{29}H_{34}O_8Na$ $[M+Na]^+$: 533.2146; found: 533.2137.

2.1.6. Synthesis of 5-((10-((2-oxo-2H-chromen-7-yl)oxy)decyl)oxy)isophthalic acid (C_{10}-Coumarin-bdcH_2, 3)

This protocol was adapted from a procedure initially reported by Park and coworkers.[4] **2** (1.21 g, 2.37 mmol) was combined with a 1:1 tetrahydrofuran/methanol mixture (90 mL) in a round bottom flask. A solution of NaOH (3.83 g, 95.8 mmol) in 45 mL H_2O was then added to the flask. The resulting reaction mixture was heated at 70 °C for 12 h, at which point the solution color had become red. Both tetrahydrofuran and methanol were then removed by rotary evaporation. The remaining aqueous solution was diluted with additional H_2O (100 mL), then acidified to pH = 1 via dropwise addition of concentrated HCl. At this point, the crude product precipitated from solution as white solids, which were isolated by vacuum filtration. The crude product was recrystallized in methanol (250 mL), affording the pure product (**3**, C_{10}-Coumarin-bdcH_2) as a white powder (0.72 g, 63% yield). ^{1}H NMR (DMSO-d_6, 500 MHz) δ 13.27 (s, br, 2H), 8.05 (t, J = 1.4 Hz, 1H), 7.97 (d, J = 9.5 Hz, 1H), 7.62 (d, J = 1.5 Hz, 2H), 7.60 (d, J = 8.6 Hz, 1H), 6.96 (d, J = 2.4 Hz, 1H), 6.93 (dd, J = 8.6, 2.4 Hz, 1H), 6.27 (d, J = 9.6 Hz, 1H), 4.06 (t, J = 6.5 Hz, 4H), 1.77 – 1.67 (m, 4H), 1.47 – 1.22 (m, 12H). ^{13}C{^{1}H} NMR (DMSO-d_6, 125 MHz) δ 166.39, 161.89, 160.28, 158.78, 155.41, 144.31, 132.57, 129.43, 122.07, 119.00, 112.69, 112.34, 112.21, 101.11, 68.27, 68.07, 28.86, 28.65, 28.45, 28.39, 25.37, 25.34. HRMS (APCI) calcd for $C_{27}H_{31}O_8$ $[M+H]^+$: 483.2013; found: 483.2013.

Scheme S2. Synthesis of C_3-Coumarin-bdcH_2

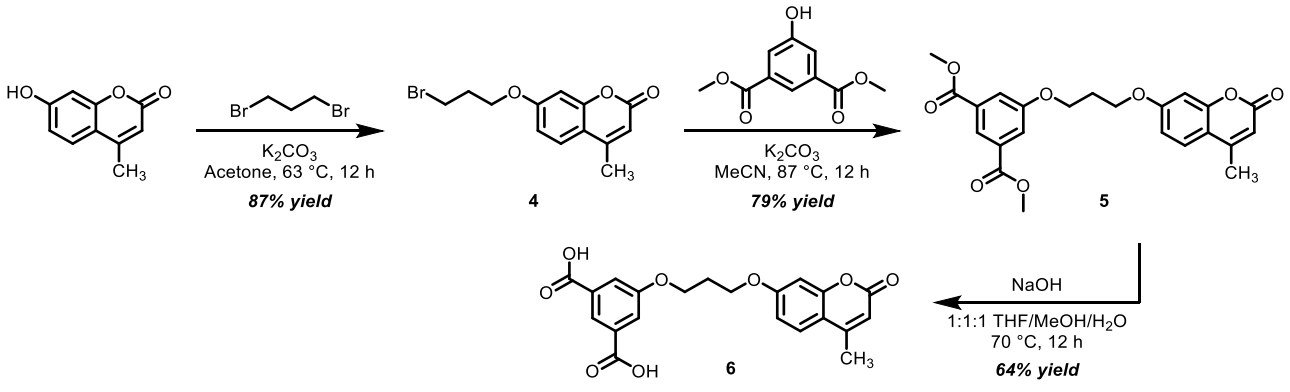

2.1.7. Synthesis of 7-(3-bromopropoxy)-4-methyl-2H-chromen-2-one (4)

This protocol was adapted from a procedure initially reported by Park and coworkers.[4] 4-methylumbelliferone (1.31 g, 7.44 mmol), 1,3-dibromopropane (15.00 g, 74.3 mmol), and K_2CO_3 (14.79 g, 107 mmol) were combined in a round bottom flask. Acetone (75 mL) was then added to dissolve the organic components. The resulting reaction mixture was heated to reflux for 12 h, after which the reaction was centrifuged to remove undissolved K_2CO_3, then evaporated to a viscous, yellow oil. This oil was redissolved in dichloromethane and

washed with water to remove residual K_2CO_3. Finally, the DCM layer was dried over Na_2SO_4, evaporated to a viscous yellow oil, and purified by column chromatography (silica gel, hexane → 1:1 hexane/ethyl acetate), affording the product (**4**) as a white powder (1.91 g, 87% yield). ^{1}H NMR ($CDCl_3$, 500 MHz). δ 7.50 (d, J = 8.7 Hz, 1H), 6.86 (dd, J = 8.7, 2.5 Hz, 1H), 6.83 (d, J = 2.5 Hz, 1H), 6.14 (q, J = 1.3 Hz, 1H), 4.18 (t, J = 5.8 Hz, 2H), 3.61 (t, J = 6.4 Hz, 2H), 2.40 (d, J = 1.3 Hz, 3H), 2.36 (p, J = 6.1 Hz, 2H). ^{13}C{^{1}H} NMR ($CDCl_3$, 125 MHz) δ 161.78, 161.29, 155.33, 152.58, 125.71, 113.89, 112.50, 112.19, 101.68, 65.96, 32.10, 29.66, 18.76. HRMS (APCI) calcd for $C_{13}H_{14}BrO_3$ $[M+H]^+$: 297.0121; found: 297.0122.

2.1.8. Synthesis of dimethyl 5-(3-((4-methyl-2-oxo-2H-chromen-7-yl)oxy)propoxy)isophthalate (5)

This protocol was adapted from a procedure initially reported by Park and coworkers.[4] **4** (0.55 g, 1.85 mmol), 0.27 g dimethyl 5-hydroxyisophthalate (0.27 g, 1.28 mmol), K_2CO_3 (0.19 g, 1.37 mmol), and acetonitrile (10 mL) were combined in a round bottom flask and heated to reflux for 12 h. Next, the reaction mixture was evaporated to dryness, then redissolved in $CHCl_3$ and centrifuged to remove undissolved K_2CO_3. The remaining organic solution was washed with water to remove residual K_2CO_3, then dried over Na_2SO_4, dry loaded onto silica gel, and purified by column chromatography (silica gel, dichloromethane → 5% methanol in dichloromethane), affording the product (**5**) as a white powder (0.44 g, 79% yield). ^{1}H NMR ($CDCl_3$, 500 MHz) δ 8.27 (t, J = 1.4 Hz, 1H), 7.76 (d, J = 1.5 Hz, 2H), 7.49 (d, J = 8.7 Hz, 1H), 6.87 (dd, J = 8.7, 2.5 Hz, 1H), 6.83 (d, J = 2.5 Hz, 1H), 6.13 (q, J = 1.2 Hz, 1H), 4.26 (t, J = 6.0 Hz, 2H), 4.24 (t, J = 6.1 Hz, 2H), 3.93 (s, 6H), 2.39 (d, J = 1.2 Hz, 3H), 2.33 (p, J = 6.0 Hz, 2H). ^{13}C{^{1}H} NMR ($CDCl_3$, 125 MHz) δ 166.23, 161.95, 161.36, 158.99, 155.43, 152.58, 132.00, 125.71, 123.30, 119.96, 113.89, 112.62, 112.23, 101.72, 64.89, 52.57, 29.09, 18.79. HRMS (ESI) calcd for $C_{23}H_{22}O_8Na$ $[M+Na]^+$: 449.1207; found: 449.1198.

2.1.9. Synthesis of 5-(3-((4-methyl-2-oxo-2H-chromen-7-yl)oxy)propoxy)isophthalic acid (C_3-Coumarin-bdcH_2, 6)

This protocol was adapted from a procedure initially reported by Park and coworkers.[4] **5** (0.40 g, 0.94 mmol) was combined with a 1:1 tetrahydrofuran/methanol mixture (30 mL) in a round bottom flask. A solution of NaOH (1.47 g, 36.8 mmol) in 15 mL H_2O was then added to the flask. The resulting reaction mixture was heated at 70 °C for 12 h, at which point the solution color had become red. Both tetrahydrofuran and methanol were then removed by rotary evaporation. The remaining aqueous solution was diluted with additional H_2O (15 mL), then acidified to pH = 1 via dropwise addition of concentrated HCl. At this point, the crude product precipitated from solution as white solids, which were isolated by vacuum filtration. The crude product was recrystallized in methanol (150 mL), affording the pure product (**6**, C_3-Coumarin-bdcH_2) as a white powder (0.24 g, 64% yield). ^{1}H NMR (DMSO-d_6, 500 MHz) δ 13.27 (s, br, 2H), 8.07 (t, J = 1.5 Hz, 1H), 7.70 – 7.64 (m, 3H), 7.01 (d, J = 2.4 Hz, 1H), 6.99 (dd, J = 8.7, 2.5 Hz, 1H), 6.20 (d, J = 1.4 Hz, 1H), 4.31 – 4.23 (m, 4H), 2.39 (d, J = 1.2 Hz, 3H), 2.23 (p, J = 6.3 Hz, 2H). ^{13}C{^{1}H} NMR (DMSO-d_6, 125 MHz) δ 166.40, 161.56, 160.14, 158.59, 154.73, 153.32, 132.62, 126.39, 122.33, 119.10, 113.16, 112.35, 111.17, 101.30, 65.00, 64.82, 28.32, 18.10. HRMS (APCI) calcd for $C_{21}H_{19}O_8$ $[M+H]^+$: 399.1074; found: 399.1075.

2.2. Synthesis of Metal Organic Polyhedra

2.2.1. Synthesis of C_{10}-Coumarin-RhMOP

To each of three 30 mL glass scintillation vials was added C_{10}-Coumarin-bdcH_2 (119 mg, 0.25 mmol), $[Rh_2(OAc)_4(MeOH)_2]$ (50 mg, 0.10 mmol), and N,N-dimethylacetamide (DMA, 18 mL). The resulting mixtures were sonicated until all components had fully dissolved to afford blue-green solutions. Next, Na_2CO_3 (26 mg, 0.25 mmol) was added to each vial. The vials were then capped, sonicated for 30 seconds, and heated in an oven at 100 °C for 48 h, at which point each solution had turned dark green. Each green solution was

syringe filtered (0.2 μm PTFE) into a 50 mL centrifuge tube to remove Na_2CO_3, then diluted to 45 mL with methanol, resulting in the immediate precipitation of fine blue solids, which were allowed to sediment overnight. The solids were then isolated by centrifugation, combined, and washed via redispersion and sedimentation in EtOH (30 mL × 2), 1 M NaOH (30 mL × 2), H_2O (30 mL × 2), acetone (30 mL × 2), and diethyl ether (30 mL × 2). The solids were then redispersed in diethyl ether (30 mL) and allowed to sit overnight. Finally, the solids were isolated by centrifugation and dried under vacuum at 80 °C for 12 h, affording the pure product as a blue-green powder (0.326 g, 94% yield).

2.2.2. Synthesis of C_3-Coumarin-RhMOP

To each of three 30 mL glass scintillation vials was added C_3-Coumarin-bdcH_2 (98 mg, 0.25 mmol), $[Rh_2(OAc)_4(MeOH)_2]$ (50 mg, 0.10 mmol), and N,N-dimethylacetamide (DMA, 18 mL). The resulting mixtures were sonicated until all components had fully dissolved to afford blue-green solutions. Next, Na_2CO_3 (26 mg, 0.25 mmol) was added to each vial. The vials were then capped, sonicated for 30 seconds, and heated in an oven at 100 °C for 48 h, at which point each solution had turned dark green. The solutions were syringe filtered (0.2 μm PTFE) to remove Na_2CO_3, then combined in a single glass vial. The solvent (DMA) was then removed from the sample using a spiral plug evaporator at 75 ºC. The isolated material was dispersed in methanol (30 mL), resulting in the precipitation of fine blue solids, which were isolated by centrifugation. The solids were then washed via redispersion and sedimentation in EtOH (30 mL × 2), 1 M NaOH (30 mL × 2), H_2O (30 mL × 2), acetone (30 mL × 2), and diethyl ether (30 mL × 2). The solids were then redispersed in diethyl ether (30 mL) and allowed to sit overnight. Finally, the solids were isolated by centrifugation and dried under vacuum at room temperature for 22 h, then 80 ºC for 12 h, affording the pure product as a blue-green powder (0.296 g, 100% yield).

2.2.3. Synthesis of 12:12 C_{10}-Coumarin/OH-RhMOP

To a 30 mL glass scintillation vial was added C_{10}-Coumarin-bdcH_2 (60 mg, 0.125 mmol), 5-hydroxyisophthalic acid (23 mg, 0.125 mmol), $[Rh_2(OAc)_4(MeOH)_2]$ (50 mg, 0.10 mmol), and N,N-dimethylacetamide (DMA, 18 mL). The resulting mixture was sonicated until all components had fully dissolved to afford a blue-green solution. Next, Na_2CO_3 (26 mg, 0.25 mmol) was added to the vial. The vial was then capped, sonicated for 30 seconds, and heated in an oven at 100 °C for 48 h, at which point the solution had turned dark green. The solution was syringe filtered (0.2 μm PTFE) to remove Na_2CO_3, then diluted with 100 mL diethyl ether, resulting in the precipitation of fine blue solids. These solids were isolated by centrifugation, combined, and washed via redispersion and sedimentation in methanol (13 mL × 3), H_2O (13 mL × 3), methanol (13 mL × 3), and finally diethyl ether (13 mL × 2). The solids were then redispersed in diethyl ether (13 mL) and allowed to sit overnight. Finally, the solids were isolated by centrifugation and dried under vacuum at 80 °C for 12 h, affording the pure product as a blue-green powder (0.044 g, 52% yield).

Note: All MOP powder yields are calculated using cage molecular weights that do not account for residual solvent molecules coordinated to the open metal sites. In reality, a few solvent molecules (typically Et_2O, see **Figures S1**, **S8**, and **S14**) remain coordinated to the open metal sites even after heating under vacuum at 80 ºC, such that the calculated percent yields are slight overestimates. If the cages are activated at higher temperatures (150 ºC) to dissociate more coordinating solvent molecules, their solubility decreases.

2.2.4. Synthesis of HRhMOP

HRhMOP powder was synthesized according to literature precedent.[5]

2.3. Synthesis of RhMOP Gels, Aerogels, and Thin Films

2.3.1. Synthesis of pristine C_{10}-Coumarin-RhMOP / bix gel (bix gel, 0.4 mM MOP)

C_{10}-Coumarin-RhMOP (67 mg, 4.8 μmol) was dissolved in dimethylformamide (DMF, 6 mL). Separately, bix (14 mg, 59 μmol, 12 equivalents) was dissolved in DMF (6 mL). The MOP solution was then added into the bix solution with vigorous stirring, affording a purple DMF solution of (C_{10}-Coumarin-RhMOP)(bix)$_{12}$ (12 mL, 0.4 mM). This solution was divided evenly between ten 24 mL disposable syringes, which were capped and heated in an oven at 80 ºC for 72 h. At this point, the reaction mixture inside each syringe had solidified into a purple gel. Each syringe was then cut open, and the gels inside were combined in a glass vial containing fresh DMF (30 mL). The solvent was exchanged with fresh DMF three more times (30 mL each) to remove free bix molecules released during the polymerization process, affording pristine bix gel. **Note**: for rheological measurements only, gels (15 mm diameter) were prepared by dividing the 12 mL reaction mixture evenly between fourteen 12 mL syringes.

2.3.2. Synthesis of coumarin/bix gel (0.4 mM MOP)

Syringes (24 mL volume) containing bix gel (prior to DMF washes, prepared from 67 mg C_{10}-Coumarin-RhMOP and 14 mg bix) were cut open using a pair of scissors, and each gel was pushed to the 8 mL mark of the syringe by compressing the plunger. DMF (2 mL) was added to the surface of each gel, and then each syringe was placed face-up inside an Imoto Model IMC-0091 Photoreactor and irradiated at 350 nm (irradiance = 4 mW/cm^2) for 5 h. After the photopolymerization process was completed, the DMF layer was removed from the surface of each gel, and all gels were combined in a glass vial containing 25 mL fresh DMF. The solvent was exchanged with fresh DMF three more times (30 mL each) to remove free bix molecules released during the polymerization process, affording coumarin/bix gel.

2.3.3. Synthesis of coumarin gel (0.4 mM MOP)

Coumarin/bix gels in 24 mL syringes (prior to DMF washes, prepared from 67 mg C_{10}-Coumarin-RhMOP and 14 mg bix) were combined in a glass vial containing DMF (25 mL), after which trifluoroacetic acid (TFA, 2.5 mL) was added. The gels were then allowed to soak in this solvent mixture for 1 h. At this point, the gels had changed color from purple to green, indicating that bix had dissociated from the open metal sites. Moreover, the solvent mixture was found to be blue-green in color, indicating that some unreacted MOPs had dissolved after coordination crosslinker dissociation. The solvent was exchanged once more with fresh DMF (25 mL) and TFA (2.5 mL), and the gels were allowed to sit for 12 h. Next, the gels were washed with fresh DMF four times (30 mL each) to remove all TFA and dissociated bix, affording coumarin gel.

2.3.4. Readdition of bix to coumarin gel (0.4 mM MOP) for rheological measurements

To an individual disc of coumarin gel in a 12 mL syringe (15 mm diameter, prepared by dividing a mixture of 67 mg C_{10}-Coumarin-RhMOP and 14 mg bix evenly between fourteen 12 mL syringes) was added fresh DMF (0.2 mL) and a solution of bix in DMF (0.1 mL, 21 mM, 6 equivalents). The syringe was then covered with parafilm and allowed to sit for 12 h. At this point, the gel had changed color from green to blue/grey, indicating that some bix molecules were coordinating to the cages in a monodentate fashion. Next, another aliquot of the bix/DMF solution (0.1 mL, 21 mM, 6 equivalents) was added, resulting in a further color change of the gel from blue/grey to purple/red. Once the gel had turned purple/red, additional DMF (3 mL) was added to the surface of the gel. The syringe was then capped with a silicone stopper and heated in an oven at 80 ºC for 6 h to promote the reformation of the coordination crosslinks between cages. After heating the gels were allowed to cool to room temperature. Next, the solvent was exchanged with fresh DMF (1 mL × 4) to remove unbound bix molecules, and the resulting gel was used for rheological measurements.

2.3.5. Supercritical CO_2 activation of C_{10}-Coumarin-RhMOP gels to produce aerogels (0.4 mM MOP)
DMF-washed bix, coumarin/bix, or coumarin gels were exchanged with methanol six times (50 mL each), then placed inside the Tousimis Autosamdri-931 critical point dryer and activated (see **1.2 Instruments** for detailed activation conditions), affording the corresponding bix, coumarin/bix, or coumarin aerogels. Yields for aerogel samples prepared from 67 mg C_{10}-Coumarin-RhMOP and 14 mg bix are provided below:

bix aerogel ($(C_{10}$-Coumarin-RhMOP$)(bix)_{5.6}$): 62 mg (85% yield)

coumarin/bix aerogel ($(C_{10}$-Coumarin-RhMOP$)(bix)_{5.6}$): 64 mg (87% yield)

coumarin aerogel ($(C_{10}$-Coumarin-RhMOP$)(bix)_{2.4}$): 38 mg (55% yield)

2.3.6. Direct photopolymerization of C_{10}-Coumarin-RhMOP solutions into thin films
C_{10}-Coumarin-RhMOP (56 mg, 4.0 μmol) was dissolved in DMF (0.2 mL), affording a 20 mM solution of the cage. This sample was transferred to a 1 mm quartz cuvette, briefly sparged with argon, sealed, and irradiated at 350 nm for 12 h using an Asahi Spectra MAX-303 Compact Xenon Light Source equipped with a 350 nm filter (irradiance = 10 mW/cm^2). At this point, an insoluble, blue-green thin film had formed on the surface of the cuvette facing the light source. The excess MOP solution was first removed from the cuvette via syringe, and then the film was washed with fresh DMF (0.5 mL × 3) and methanol (0.5 mL × 3). The film was then extracted from the cuvette using tweezers, further washed with methanol (3 mL × 3), and activated by supercritical CO_2 drying. Yield: 0.4 mg (0.7%)

2.3.7. Photopatterning coumarin gel in a glass dish.
C_{10}-Coumarin-RhMOP (34 mg, 2.4 μmol) was dissolved in dimethylformamide (DMF, 3 mL). Separately, bix (7 mg, 29 mmol, 12 equivalents) was dissolved in DMF (3 mL). The MOP solution was then added into the bix solution with vigorous stirring, affording a purple DMF solution of (C_{10}-Coumarin-RhMOP)$(bix)_{12}$ (6 mL, 0.4 mM). This solution was transferred to a glass petri dish (6 cm diameter), which was capped with a second, wider glass dish and sealed inside a Ziplock back. The sample was placed inside an oven at 80 ºC for 48 h, with a beaker placed on top of the sample to hold down the top glass dish and minimize solvent evaporation. At this point, the reaction mixture had solidified into a purple gel, which was adhered to the bottom surface of the glass petri dish. The glass dish was then inverted so that its base was facing upward. A flower-shaped photomask was placed on the base of the dish, and each portion of the exposed gel was irradiated at 350 nm (irradiance = 4 mW/cm^2) for 5 h using an Asahi Spectra MAX-303 Compact Xenon Light Source equipped with a 350 nm filter. After the photopolymerization was complete, the gel was turned upright, and DMF (10 mL) and TFA (1 mL) were added to its surface, inducing the rapid dissociation of bix. After the sampled had changed color from purple to green, the acidic solvent was replaced with fresh DMF (10 mL), resulting in the dissolution of unreacted MOP and the appearance of a flower-shaped sample of coumarin gel, which matched the shape of the photomask. To the surface of the flower petals was applied 4-*t*-butylpyridine, which resulted in an immediate color change from green to purple.

2.3.8. Screening harsh conditions for dissociating bix from coumarin/bix gels
In an attempt to remove all bix molecules from coumarin/bix gel, four additional bix dissociation conditions were tested, as described below:

Condition 1 – DMSO: Coumarin/bix gel (prepared from 6 mL of 0.4 mM (C_{10}-Coumarin-RhMOP)$(bix)_{12}$) was transferred to a glass vial along with DMF (25 mL) and TFA (2 mL), then allowed to sit for 1.5 h. The solvent was then replaced with DMF (20 mL), followed by a mixture of DMF (20 mL) and TFA (2 mL), at which point the gel was left to sit for 12 h. Next, the solvent was removed and the gels were washed with strongly-coordinating DMSO (20 mL × 4; gel changed color from green to red), tetrahydrofuran (20 mL × 14; gel changed color from red to green), and MeOH (25 mL × 6). Finally, the gel was activated by supercritical CO_2 drying to produce the corresponding aerogel, which was decomposed via heating in a mixture of DMSO-d_6 (600 μL) and 35% DCl in D_2O (50 μL) at 100 ºC for 1 h. The decomposed solution was characterized by ^{1}H NMR spectroscopy (**Figure S43**), revealing an aerogel composition of (C_{10}-Coumarin-RhMOP)$(bix)_{1.9}$

Condition 2 – HCl: Coumarin/bix gel (prepared from 6 mL of 0.4 mM (C_{10}-Coumarin-RhMOP)$(bix)_{12}$) was transferred to a glass vial along with DMF (25 mL). The solvent was then replaced with a mixture of DMF (7 mL) and concentrated HCl (3 mL). After soaking for 30 minutes, the solvent was exchanged with fresh DMF (10 mL) for 30 minutes, then a mixture of DMF (7 mL) and concentrated HCl (3 mL) for 30 minutes, and finally DMF (25 mL × 2, 1 h each). The gel was then washed with MeOH (25 mL × 6) and activated by supercritical CO_2 drying to produce the corresponding aerogel. The aerogel was decomposed via heating in a mixture of DMSO-d_6 (600 μL) and 35% DCl in D_2O (50 μL) at 100 ºC for 1 h, then characterized by ^{1}H NMR spectroscopy (**Figure S43**), revealing an aerogel composition of (C_{10}-Coumarin-RhMOP)$(bix)_{1.8}$

Condition 3 – Heating in TFA: Coumarin/bix gel (30% of gel prepared from 12 mL of 0.4 mM (C_{10}-Coumarin-RhMOP)$(bix)_{12}$) was transferred to a glass vial containing DMF (10 mL) and TFA (1 mL) and allowed to soak for 12 h. The solvent was then replaced with a fresh mixture of DMF (10 mL) and TFA (1 mL), and allowed to sit for an additional 24 h. At this point, the solvent was replaced once more with DMF (10 mL) and TFA (1 mL), and the submerged gel was heated at 80 ºC in an aluminum bead bath for 2 h. Immediately afterwards, while the solvent was still hot, it was exchanged for fresh DMF (10 mL) and TFA (1 mL), and heated again at 80 ºC for 2 h. At this point, the acidic solvent was removed, and the gel was washed with MeOH (50 mL × 5). The gel was then activated by heating under vacuum at 70 ºC for 12 h. Finally, the dried gel was decomposed via heating in a mixture of DMSO-d_6 (600 μL) and 35% DCl in D_2O (50 μL) at 100 ºC for 1 h, then characterized by ^{1}H NMR spectroscopy (**Figure S43**), revealing a composition of (C_{10}-Coumarin-RhMOP)$(bix)_{1.5}$

Condition 4 – TFA for 1 month: Coumarin/bix gel (40% of gel prepared from 12 mL of 0.4 mM (C_{10}-Coumarin-RhMOP)$(bix)_{12}$) was transferred to a glass vial containing DMF (10 mL) and TFA (1 mL) and allowed to soak for 12 h. The solvent was then replaced with a fresh mixture of DMF (10 mL) and TFA (1 mL), and the gels were allowed to soak for 36 days, at which point the gel had become light green/yellow in color, likely due to the partial degradation of the dirhodium paddlewheels after long-term exposure to concentrated TFA. The gel was washed with MeOH (50 mL × 5), then activated to the corresponding aerogel via supercritical CO_2 drying. The aerogel was decomposed via heating in a mixture of DMSO-d_6 (600 μL) and 35% DCl in D_2O (50 μL) at 100 ºC for 1 h, then characterized by ^{1}H NMR spectroscopy (**Figure S43**), revealing an aerogel composition of (C_{10}-Coumarin-RhMOP)$(bix)_{1.4}$

2.3.9. Synthesis of HRhMOP/bix gel (0.4 mM MOP)

HRhMOP/bix gel was synthesized according to literature precedent.[5]

3. Experimental Protocols

3.1. Decomposition of MOP powders and aerogels

3.1.1. MOP powder decomposition

C_{10}-Coumarin-RhMOP (10 mg, 0.71 μmol), C_3-Coumarin-RhMOP (10 mg, 0.83 μmol), or 12:12 C_{10}-Coumarin/OH-RhMOP (10 mg, 0.96 μmol) was placed in a glass vial, followed by 600 μL DMSO-d_6 and 50 μL 35% DCl in D_2O. The vial was then sealed and heated at 100 ºC for 1 h, at which point the solution had turned yellow in color and all solids had dissolved, indicating that the dirhodium paddlewheels had decomposed. The resulting solution was measured by ^{1}H NMR spectroscopy immediately after heating (**Figures S7**, **S13**, and **S18**).

3.1.2. C_{10}-Coumarin-RhMOP aerogel decomposition

Bix aerogel (10 mg), coumarin/bix aerogel (11 mg), or coumarin aerogel (12 mg) was placed in a glass vial, followed by 600 μL DMSO-d_6 and 50 μL 35% DCl in D_2O. The vial was then sealed and heated at 100 ºC for 1 h, at which point the solution had turned yellow in color and all solids had dissolved, indicating that the dirhodium paddlewheels had decomposed. The resulting solution was measured by ^{1}H NMR spectroscopy immediately after heating (**Figure S40**).

3.2. UV-Vis Experiments

3.2.1. Titration of Coumarin-RhMOPs with diz

C_{10}-Coumarin-RhMOP (11.7 mg, 0.84 μmol), C_3-Coumarin-RhMOP (10.0 mg, 0.83 μmol), or 12:12 C_{10}-Coumarin/OH-RhMOP (8.7 mg, 0.84 μmol) was added to a 1 cm quartz cuvette along with a stir bar and dissolved in DMF (2.50 mL), affording a 334 μM solution of the cage. Separately, diz (98.5 mg, 417 μmol) was dissolved in DMF (4.98 mL), affording an 83.6 mM solution, such that 10 μL corresponds to 1 equivalent of diz relative to the MOP. The MOP solution was then titrated with the diz solution in 1 equivalent (10 μL) increments up to 14 total equivalents of ligand added. At each step, the solution was stirred for 1 minute (300 rpm) to ensure adequate mixing, and then a UV-Vis spectrum was collected (20 ºC). Additional spectra were collected after a total of 16, 18, 21, and 24 equivalents of diz were added (**Figures S5**, **S11**, and **S16**).

3.2.2. UV-Vis controls for calculating coumarin photodimerization reaction yields

For C_{10}-Coumarin-RhMOP: Solutions of C_{10}-Coumarin-RhMOP (0.417 mM), 5-hydroxyisophthalic acid (10 mM), C_{10}-Coumarin-Br (**1**, 10 mM), and C_{10}-Coumarin-bdcH_2 (**3**, 10 mM) were separately prepared in DMF. Each solution was further diluted by mixing 60 μL with 10 mL DMF, then measured by UV-Vis spectroscopy at 20 ºC. Given that a 0.417 mM solution of C_{10}-Coumarin-RhMOP contains 24 equivalents (10 mM concentration) of C_{10}-Coumarin side chains, the ratio of absorption intensity of C_{10}-Coumarin-Br (**1**, 10 mM) relative to C_{10}-Coumarin-RhMOP (0.417 mM) provides the percentage of the cage's UV absorption at 320 nm that can be attributed to the coumarin side chains (74%, **Figure S36**). Likewise, the ratio of absorption intensity of C_{10}-Coumarin-Br (**1**, 10 mM) to C_{10}-Coumarin-bdcH_2 (10 mM) provides the percentage of the C_{10}-Coumarin-bdcH_2 absorption that can be attributed to the coumarin moiety (89%, **Figure S36**).

For C_3-Coumarin-RhMOP: Solutions of C_3-Coumarin-RhMOP (0.417 mM), 5-hydroxyisophthalic acid (10 mM), C_3-Coumarin-Br (**4**, 10 mM), and C_3-Coumarin-bdcH_2 (**6**, 10 mM) were separately prepared in DMF. Each solution was further diluted by mixing 60 μL with 10 mL DMF, then measured by UV-Vis spectroscopy at 20 ºC. Given that a 0.417 mM solution of C_3-Coumarin-RhMOP contains 24 equivalents (10 mM concentration) of C_3-Coumarin side chains, the ratio of absorption intensity of C_3-Coumarin-Br (**4**, 10 mM)

relative to C_3-Coumarin-RhMOP (0.417 mM) provides the percentage of the cage's UV absorption at 320 nm that can be attributed to the coumarin side chains (84%, **Figure S36**).

For 12:12 C_{10}-Coumarin/OH-RhMOP: Solutions of 12:12 C_{10}-Coumarin/OH RhMOP (0.833 mM), 5-hydroxyisophthalic acid (20 mM), C_{10}-Coumarin-Br (**1**, 10 mM), and C_{10}-Coumarin-bdcH_2 (**3**, 10 mM) were separately prepared in DMF. Each solution was further diluted by mixing 60 μL with 10 mL DMF, then measured by UV-Vis spectroscopy at 20 ºC. Given that a 0.833 mM solution of 12:12 C_{10}-Coumarin/OH RhMOP contains 12 equivalents (10 mM concentration) of C_{10}-Coumarin side chains, the ratio of absorption intensity of C_{10}-Coumarin-Br (**1**, 10 mM) relative to 12:12 C_{10}-Coumarin/OH RhMOP (0.833 mM) provides the percentage of the cage's UV absorption at 320 nm that can be attributed to the coumarin side chains (63%, **Figure S36**).

3.3. Solution-State Photoirradiation Experiments

3.3.1. Tracking C_{10}-Coumarin-bdcH_2 self-dimerization by ^{1}H NMR and UV-Vis spectroscopy

C_{10}-Coumarin-bdcH_2 (9.7 mg, 20 mmol) was dissolved in DMSO-d_6 (1 mL), affording a 20 mM solution, which was transferred to an NMR tube and irradiated at 350 nm using an Imoto Model IMC-0091 Photoreactor (4 mW/cm^2) for 72 h in 24 h increments. At 0 h, 24 h, 48 h, and 72 h timepoints, the sample was measured by ^{1}H NMR spectroscopy (**Figures S19c**, **S20**, and **S21**). At 0 h and 72 h timepoints, the sample was further characterized by COSY spectroscopy experiments (**Figures S22-24**). Furthermore, a 60 μL aliquot of the sample was mixed with 10 mL DMF at each time point, then further diluted (2 mL diluted sample + 2 mL DMF) and measured by UV-Vis spectroscopy (**Figure S19b**).

3.3.2. Tracking C_{10}-Coumarin-RhMOP self-dimerization by ^{1}H NMR and UV-Vis spectroscopy

C_{10}-Coumarin-RhMOP (49 mg, 3.5 μmol) was dissolved in DMF-d_7 (0.7 mL), affording a 5 mM solution. Separately, an analogous non-deuterated 5 mM solution was prepared by dissolving C_{10}-Coumarin-RhMOP (70 mg, 5.0 μmol) in DMF (1.0 mL). Both solutions were transferred to NMR tubes and irradiated at 350 nm using an Imoto Model IMC-0091 Photoreactor (4 mW/cm^2) for 72 h in 24 h increments. At 0 h, 24 h, 48 h, and 72 h timepoints, the deuterated sample was measured by ^{1}H and ^{13}C NMR spectroscopy (**Figures 3b**, **S25**, and **S28**). At 0 h and 72 h timepoints, the deuterated sample was further characterized by DOSY, COSY, HSQC, and HMBC spectroscopy experiments (**Figures S26-27** and **S29-33**). At all time points, a 0.1 mL aliquot of the non-deuterated sample was mixed with 0.9 mL DMF, then further diluted (60 μL diluted sample + 15 mL DMF) and measured by UV-Vis spectroscopy (**Figure 3c**).

3.3.3. Quantum yield experiments

Solutions of C_{10}-Coumarin-RhMOP, C_3-Coumarin-RhMOP, 12:12 C_{10}-Coumarin/OH-RhMOP (both 0.417 mM and 0.833 mM for all cages, and an additional 0.586 mM solution for C_{10}-Coumarin-RhMOP), and C_{10}-Coumarin-bdcH_2 (10 mM and 20 mM) were prepared in DMF. For each experiment, either 1.00 mL, 0.94 mL, or 0.90 mL (indicated below) of the pristine solution was transferred to a quartz cuvette (1 cm) along with a stir bar, while the remaining solution was stored as a control. The solution in the cuvette was sparged briefly with argon (~30 seconds), capped, and irradiated at 350 nm (10 mW/cm^2) using an Asahi Spectra MAX-303 Compact Xenon Light Source equipped with a 350 nm filter for 12 h with stirring, unless otherwise noted. Once the photoreaction was complete, both pristine and irradiated samples were diluted and measured by UV-Vis spectroscopy (**Figures S37-38**). Dilution conditions for each sample/concentration are provided below:

C_{10}-Coumarin-RhMOP (0.833 mM, 0.94 mL, with stirring): 60 μL sample + 10 mL DMF

C_{10}-Coumarin-RhMOP (0.586 mM, 0.94 mL, with stirring): 60 µL sample + 10 mL DMF
C_{10}-Coumarin-RhMOP (0.417 mM, 1.00 mL, with stirring): 60 µL sample + 10 mL DMF

C_3-Coumarin-RhMOP (0.833 mM, 1.00 mL, with stirring): 60 µL sample + 10 mL DMF, then 2 mL diluted sample + 2 mL DMF
C_3-Coumarin-RhMOP (0.417 mM, 1.00 mL, no stirring): 0.8 mL sample + 1.6 mL DMF, then 0.2 mL diluted sample + 15 mL DMF

12:12 C_{10}-Coumarin/OH-RhMOP (0.833 mM, 0.94 mL, with stirring): 60 µL sample + 10 mL DMF
12:12 C_{10}-Coumarin/OH-RhMOP (0.417 mM, 1.00 mL, with stirring): 120 µL sample + 10 mL DMF

C_{10}-Coumarin-bdcH_2 (20 mM, 0.90 mL, with stirring): 20 µL sample + 10 mL DMF
C_{10}-Coumarin-bdcH_2 (10 mM, 1.00 mL, with stirring): 40 µL sample + 10 mL DMF

4. Sample Calculations

4.1 Percent Yields for Coumarin Photodimerization Reactions

As a representative example, the calculation of coumarin dimerization yield for a C_{10}-Coumarin-RhMOP solution (0.417 mM in DMF, 1.00 mL) irradiated at 350 nm (10 mW/cm^2) for 12 h (See **3.3.3. Quantum yield experiments and calculations**, **Figure S37**) is described here. First, the absorbance of the sample before (a_{0h}) and after (a_{12h}) irradiation are measured. The observed reduction in the coumarin π→π* peak at 320 nm corresponds to the formation of coumarin dimers, which do not absorb at 320 nm. First, the percent reduction in absorption intensity of the sample at 320 nm is calculated as follows:

$$\%\, reduction = \left(\frac{a_{0h} - a_{12h}}{a_{0h}}\right)(100\%) = \left(\frac{1.16583 - 0.512121}{1.16583}\right)(100\%) = 56\%$$

Since the C_{10}-Coumarin-RhMOP is composed of multiple components that absorb 320 nm light (coumarin side chain, isophthalic acid, and dirhodium paddlewheel complex), the relative contribution of the coumarin residue itself to the absorbance of the cage at 320 nm must be calculated. To do this, solutions of C_{10}-Coumarin-RhMOP (0.417 mM, containing 24 coumarin side chains) and an identical amount of free coumarin tether (compound **1**, 10 mM) were each identically diluted and measured by UV-Vis spectroscopy (see **3.2.2. UV-Vis controls for calculating coumarin photodimerization reaction yields**, **Figure S36**). The absorbance ratio of the coumarin solution (a_{coumarin}) to the cage solution (a_{cage}) at 320 nm provides the percentage of cage absorbance that can be attributed to coumarin side chains:

$$\%\, coumarin\ contribution = \left(\frac{a_{coumarin}}{a_{cage}}\right)(100\%) = \left(\frac{0.880063}{1.18796}\right)(100\%) = 74\%$$

This suggests that 74% of the C_{10}-Coumarin-RhMOP absorbance at 320 nm can be attributed to the coumarin side chains. Hence, a 74% reduction in absorbance of an irradiated C_{10}-Coumarin-RhMOP sample at 320 nm corresponds to the complete dimerization of all MOP-bound coumarin side chains. Therefore, the photodimerization percent yield can be calculated by dividing the percent reduction in absorbance that occurs upon irradiation by the total percentage of MOP absorbance corresponding to the coumarin side chains:

$$\%\, yield = \left(\frac{\%\, reduction}{\%\, coumarin\ contribution}\right)(100\%) = \left(\frac{56\%}{74\%}\right)(100\%) = 76\%\ yield$$

All photodimerization yields reported in this manuscript were calculated as described above.

4.2. Quantum Yields for Coumarin Photodimerization

As a representative example, the calculation of coumarin dimerization quantum yield for a C_{10}-Coumarin-RhMOP solution (0.417 mM in DMF, 1.00 mL) irradiated at 350 nm (10 mW/cm^2) for 12 h (See **3.3.3. Quantum yield experiments and calculations**, **Figure S37**) is described here. In this case, a 1 cm^3 aliquot of MOP solution was placed in a quartz cuvette with 1 cm width and 1 cm depth, such that the surface area of the MOP solution facing the light source was 1 cm^2. This surface was irradiated at 350 nm (irradiance = 10 mW/cm^2) for 12 hours (43200 seconds). To calculate the quantum yield for the photodimerization process, the number of photons absorbed by the sample during the reaction must first be calculated. To do this, the total

energy from the light source arriving at the sample (E_{total}) must be calculated from the irradiance (E_e), sample surface area (A), and irradiation time (t) as follows:

$$E_{total} = (E_e)(A)(t) = (0.01\,J\,s^{-1}\,cm^{-2})(1\,cm^2)(43200\,s) = 432\,J$$

Next, E_{total} can be divided by the energy of a single photon (E_{photon}) to calculate the total number of photons absorbed by the sample (N_{photon}). E_{photon} can be calculated directly using the Planck Equation ($E = h\nu$), where h is Planck's constant and ν is the frequency of a 350 nm photon:

$$N_{photon} = \frac{E_{total}}{E_{photon}} = \frac{E_{total}}{h\nu_{350\,nm}} = \frac{E_{total}}{(h)\left(\frac{c}{\lambda}\right)} = \frac{432\,J}{(6.626 \times 10^{-34}\,J\,s)\left(\frac{2.998 \times 10^8\,m\,s^{-1}}{3.50 \times 10^{-7}\,m}\right)}$$
$$= 7.61 \times 10^{20}\,photons$$

Since each equivalent of C_{10}-Coumarin-RhMOP is functionalized with 24 equivalents of coumarin, a 0.417 mM solution of C_{10}-Coumarin-RhMOP contains a 10 mM concentration of coumarin side chains. The total number of coumarin molecules in solution ($N_{coumarin}$) can be calculated from the coumarin concentration (C), solution volume (V), and Avogadro's number (N_A) as follows:

$$N_{coumarin} = (C)(V)(N_A) = (0.01\,mol\,L^{-1})(0.001\,L)(6.022 \times 10^{23}\,mol^{-1}) = 6.02 \times 10^{18}\,molecules$$

The number of reacted (dimerized) coumarin molecules (N_{dimer}) is given by the product of $N_{coumarin}$ and the percent yield of the photodimerization reaction (see **4.1 Percent Yields for Coumarin Photodimerization Reactions**):

$$N_{dimer} = (N_{coumarin})(\%\,yield) = (6.02 \times 10^{18}\,molecules)(0.76) = 4.58 \times 10^{18}\,molecules$$

Each coumarin dimerization reaction occurs between one triplet excited state coumarin molecule and one ground state coumarin molecule.[6] Hence, the number of dimerization reactions ($N_{reaction}$) is equal to half of the total number of dimerized coumarin molecules (N_{dimer}):

$$N_{reaction} = \frac{N_{dimer}}{2} = \frac{4.58 \times 10^{18}\,molecules}{2} = 2.29 \times 10^{18}\,reactions$$

The quantum yield (Φ) for the photodimerization reaction can then be calculated by dividing the total number of reactions by the total number of photons absorbed by the sample:

$$\Phi = \frac{N_{reaction}}{N_{photon}} = \frac{2.29 \times 10^{18}\,reactions}{7.61 \times 10^{20}\,photons} = 0.0030$$

Note: The quantum yield calculation protocol includes several assumptions which introduce inherent error into the absolute value of the numbers. Namely, the protocol assumes that every photon which strikes the surface of the cuvette is absorbed by the sample. Moreover, this method assumes that the irradiance produced by the light source is uniform over the entire exposed surface area of the cuvette, whereas in reality, the irradiance drops slightly around the cuvette's edges. Likewise, the protocol assumes that the filtered light source is monochromatic ($\lambda = 350$ nm), though in reality, a narrow distribution of wavelengths centered at 350 nm is produced. While these factors will influence the absolute value of each calculated quantum yield, since every sample is irradiated in an identical manner, the relative differences between the values obtained for each MOP at different concentrations facilitate a qualitative comparison of each cage's ability to support coumarin photodimerization reactions.

4.3 MOP:bix Ratios in Decomposed Coumarin-RhMOP Gels based on ^{1}H NMR Peak Integrations

As a representative example, the calculation of the MOP:bix ratio in a decomposed sample of bix aerogel (10 mg, see **3.1.2. C_{10}-Coumairn-RhMOP aerogel decomposition**, **Figure S40**) is described here. In the ^{1}H NMR spectrum of the decomposed aerogel (**Figure S40**), proton 1 of the isophthalic acid residue can be fixed to an integral value of 24, since each MOP contains 24 of these equivalent protons. Next, the relative integrations of bix protons a, b, d, and e are measured, as these peaks are not heavily overlapped with decomposition byproducts. By dividing the relative integration of each bix signal (I_x) by the number of equivalent protons (N_x) in one molecule of bix, then averaging the values, the number of bix molecules per MOP (N_{bix}) can be calculated:

$$N_{bix} = \frac{\left(\frac{I_a}{N_a} + \frac{I_b}{N_b} + \frac{I_d}{N_d} + \frac{I_e}{N_e}\right)}{4} = \frac{\left(\frac{10.24}{2} + \frac{11.37}{2} + \frac{23.29}{4} + \frac{22.36}{4}\right)}{4} = 5.6\ bix\ molecules$$

Therefore, the molecular composition of the bix aerogel can be written as (C_{10}-Coumarin-RhMOP)(bix)$_{5.6}$. All other MOP:bix ratios were calculated via the same protocol.

5. Additional Characterization Data

5.1. Structural Characterization Data for C_{10}-Coumarin-RhMOP

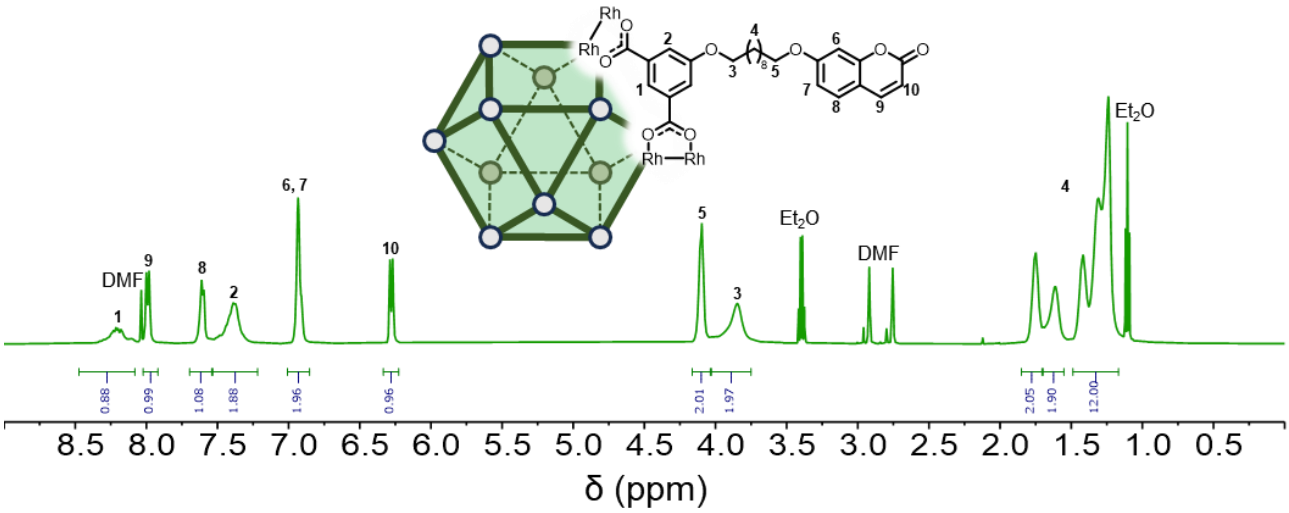

Figure S1. ^{1}H NMR spectrum (DMF-d_7, 500 MHz, 298 K) of C_{10}-Coumarin-RhMOP.

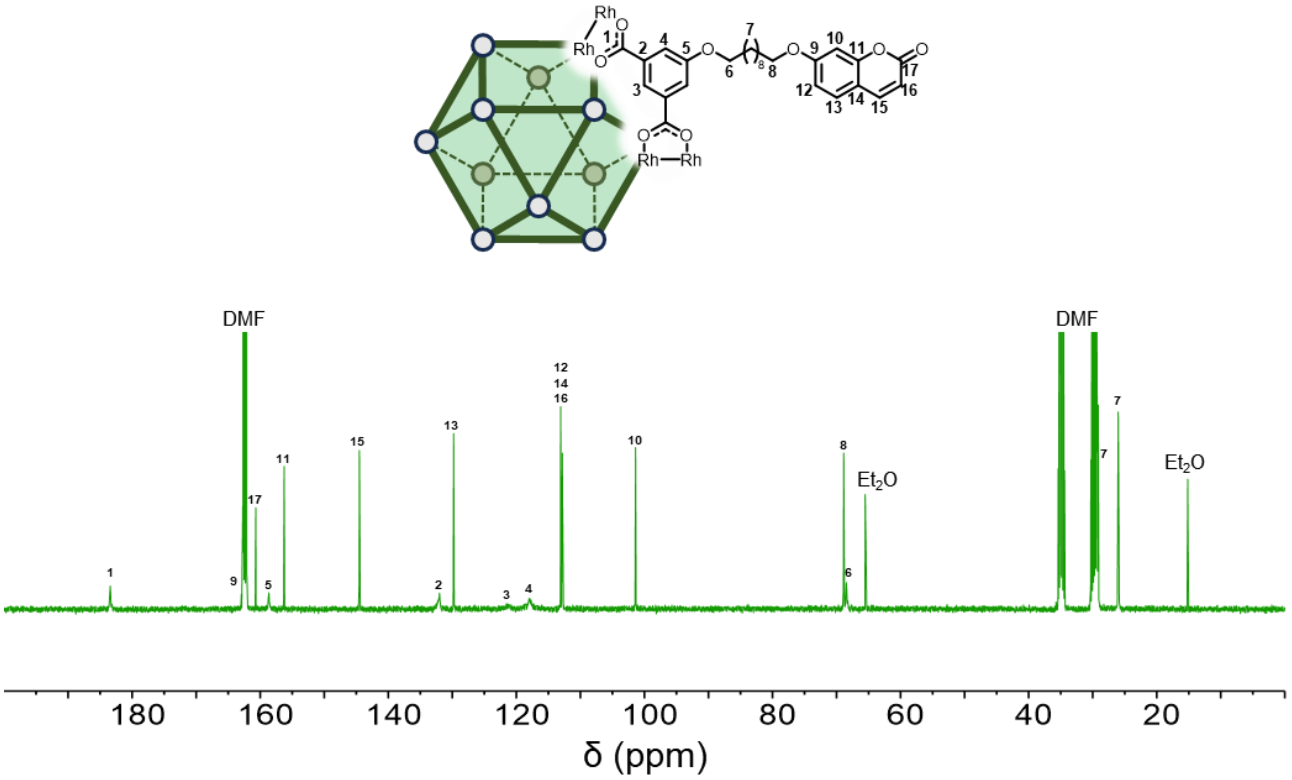

Figure S2. ^{13}C NMR spectrum (DMF-d_7, 125 MHz, 298 K) of C_{10}-Coumarin-RhMOP.

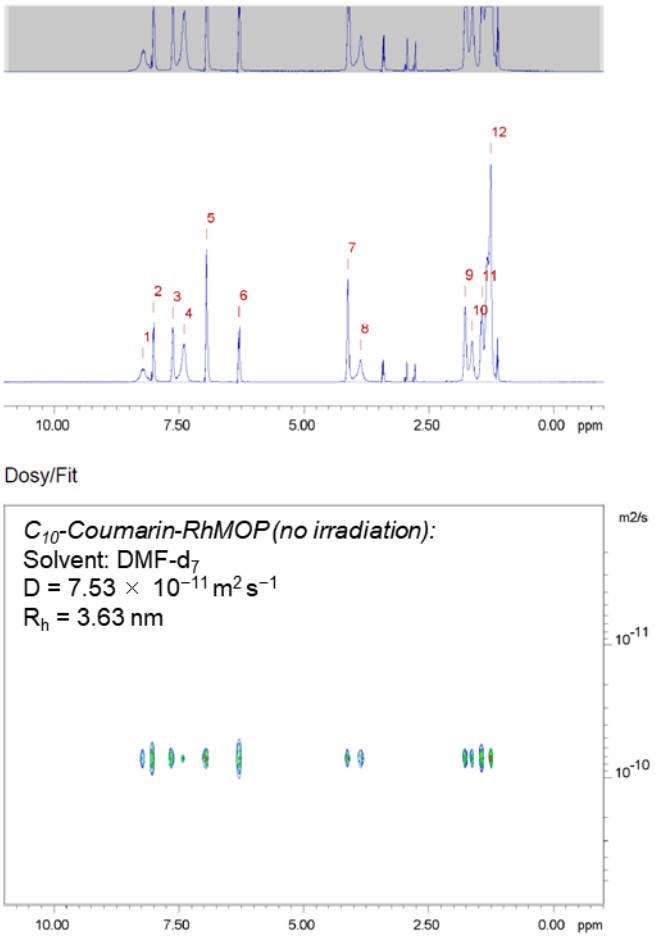

Figure S3. DOSY spectrum of C_{10}-Coumarin-RhMOP in DMF-d_7.

signal	ppm	D_s / m^2 s^{-1}	σ
1	8.223	7.47×10^{-11}	2.386×10^{-13}
2	8.012	7.57×10^{-11}	3.458×10^{-13}
3	7.629	7.58×10^{-11}	2.087×10^{-13}
4	7.400	7.53×10^{-11}	1.118×10^{-13}
5	6.953	7.57×10^{-11}	1.622×10^{-13}
6	6.299	7.47×10^{-11}	3.831×10^{-13}
7	4.118	7.53×10^{-11}	1.258×10^{-13}
8	3.864	7.59×10^{-11}	1.770×10^{-13}
9	1.773	7.50×10^{-11}	1.548×10^{-13}
10	1.630	7.54×10^{-11}	1.770×10^{-13}
11	1.437	7.50×10^{-11}	2.400×10^{-13}
12	1.260	7.53×10^{-11}	1.496×10^{-13}

Table S1. Peak positions, diffusion coefficients (D), and errors (σ) corresponding to the DOSY data in **Figure S3**.

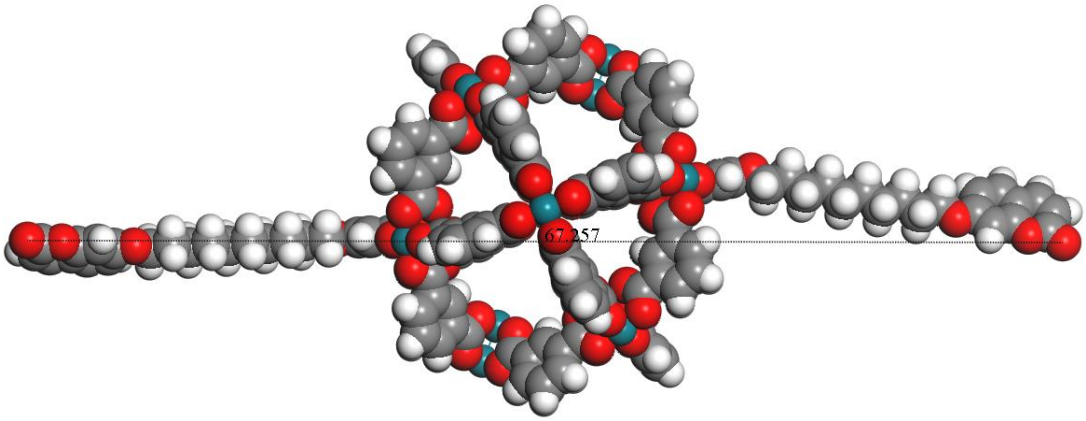

Figure S4. Geometry-optimized model of a cuboctahedral RhMOP with two C_{10}-Coumarin side chains extended outward on opposite sides of the cage, which are used to approximate a theoretical cage diameter for C_{10}-Coumarin-RhMOP (67.257 Å).

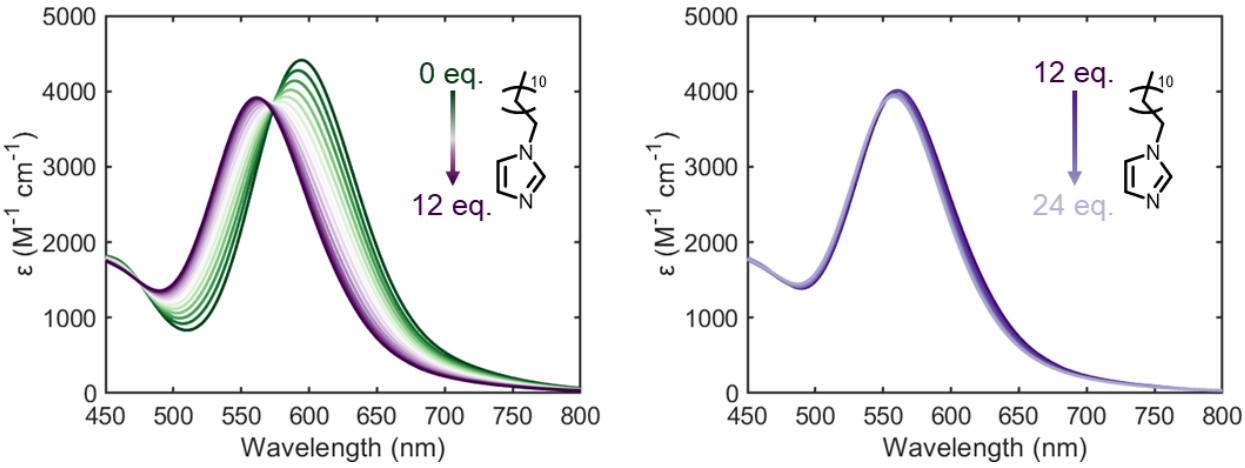

Figure S5. UV-Vis titration of C_{10}-Coumarin-RhMOP with up to 24 equivalents of diz. A shift in the π*→σ* band of the dirhodium paddlewheel from λ_{max} = 594 nm to 561 nm occurs upon addition of 12 equivalents of diz (left). Subsequent addition up to 24 equivalents of diz produces little change in the UV-Vis profile of the cage (right), suggesting that the cage is composed of 12 dirhodium paddlewheel complexes.

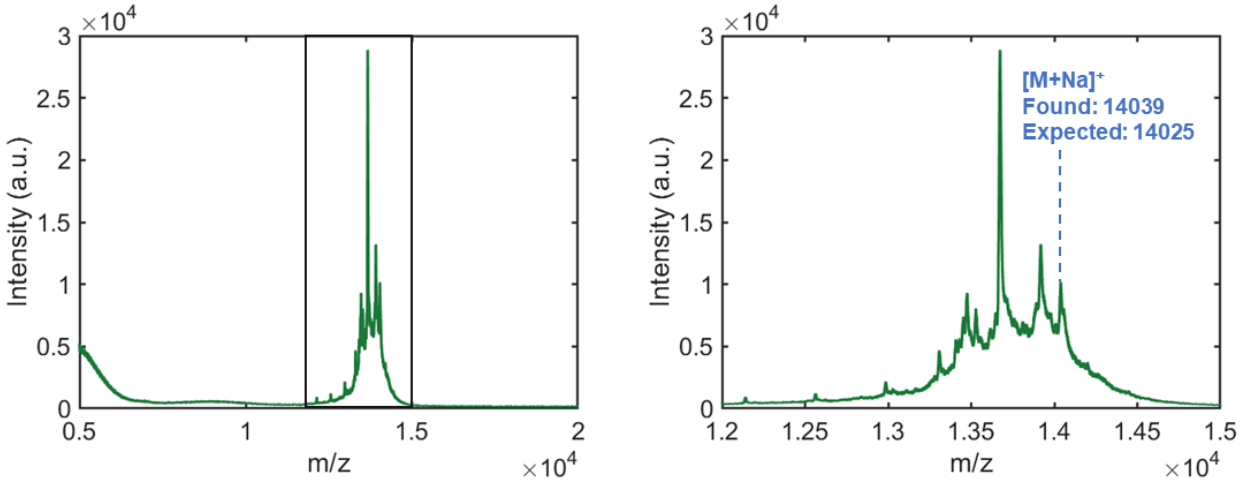

Figure S6. Expanded (left) and zoomed (right) MALDI mass spectra of C_{10}-Coumarin-RhMOP collected using a DCTB matrix and sodium trifluoroacetate as a cationizing agent. A peak at m/z = 14039 is clearly observed, which can be attributed to the $[M+Na]^+$ adduct of the cage (expected: m/z = 14025). Additional peaks with lower m/z values are also observed, which may correspond to decomposition byproducts formed upon irradiation of the strongly-absorbing C_{10}-Coumarin-RhMOP with the UV laser during sample ionization.

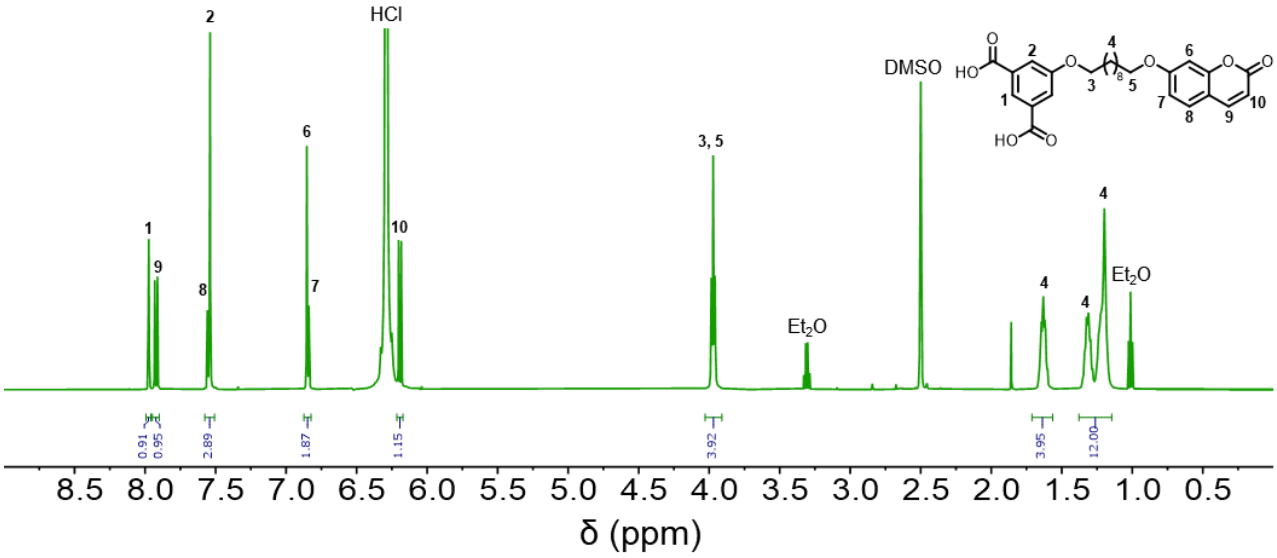

Figure S7. ^{1}H NMR spectrum (500 MHz, 298 K) of a sample of C_{10}-Coumarin-RhMOP decomposed by heating at 100 ºC in a mixture of DMSO-d_6, D_2O, and DCl for 1 h.

5.2. Structural Characterization Data for C_3-Coumarin-RhMOP

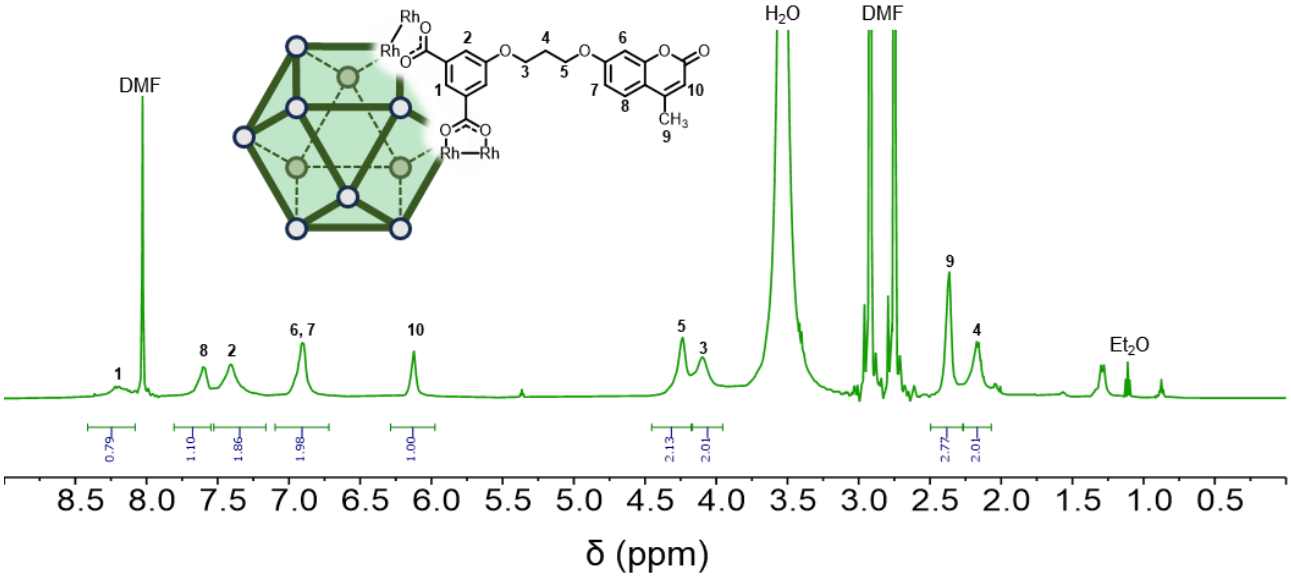

Figure S8. ^{1}H NMR spectrum (DMF-d_7, 500 MHz, 298 K) of C_3-Coumarin-RhMOP.

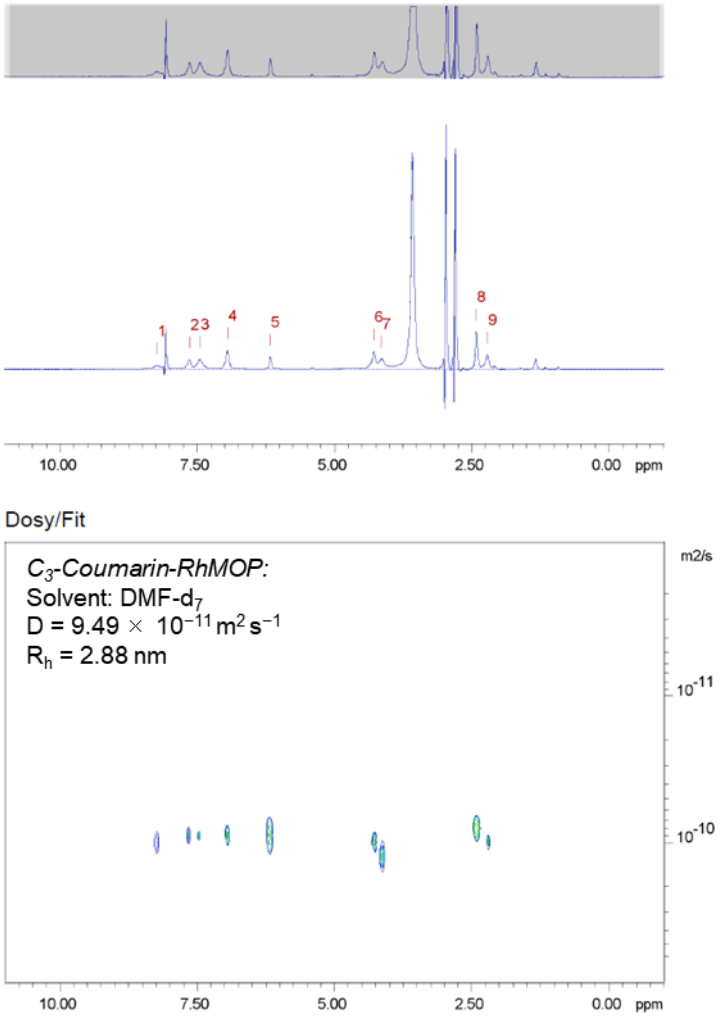

Figure S9. DOSY spectrum of C_3-Coumarin-RhMOP in DMF-d_7.

signal	ppm	D_s / m^2 s^{-1}	σ
1	8.229	1.02×10^{-10}	8.256×10^{-12}
2	7.640	8.87×10^{-11}	2.937×10^{-12}
3	7.446	9.04×10^{-11}	2.466×10^{-12}
4	6.943	8.65×10^{-11}	3.297×10^{-12}
5	6.165	8.88×10^{-11}	7.117×10^{-12}
6	4.280	9.91×10^{-11}	3.936×10^{-12}
7	4.137	1.22×10^{-10}	7.858×10^{-12}
8	2.411	7.97×10^{-11}	3.460×10^{-12}
9	2.208	9.68×10^{-11}	2.705×10^{-12}

Table S2. Peak positions, diffusion coefficients (D), and errors (σ) corresponding to the DOSY data in **Figure S9**.

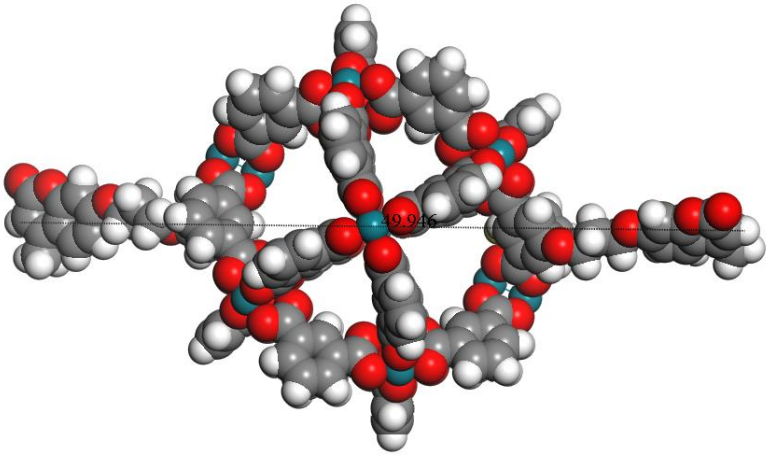

Figure S10. Geometry-optimized model of a cuboctahedral RhMOP with two C_3-Coumarin side chains extended outward on opposite sides of the cage, which are used to approximate a theoretical cage diameter for C_3-Coumarin-RhMOP (49.946 Å).

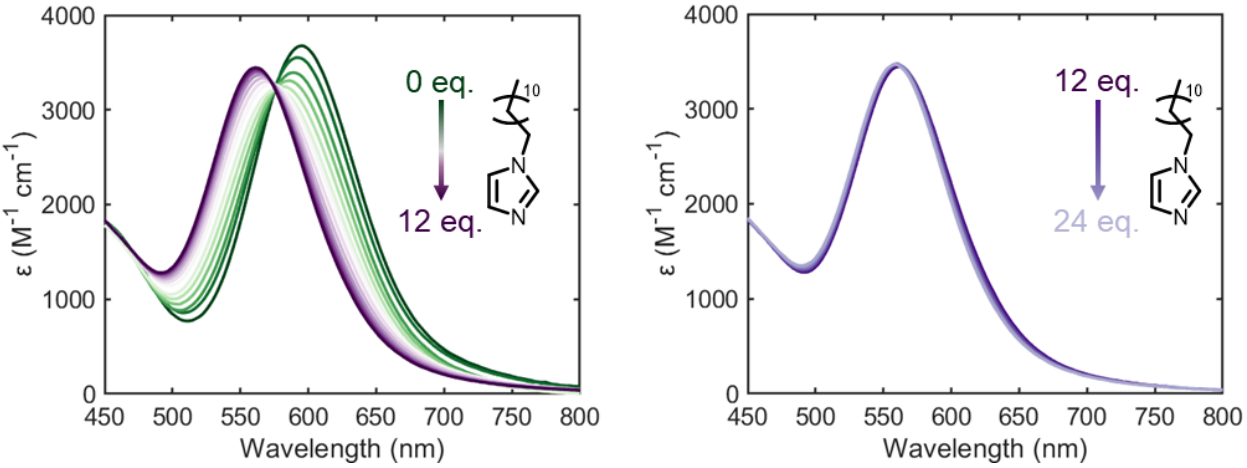

Figure S11. UV-Vis titration of C_3-Coumarin-RhMOP with up to 24 equivalents of diz. A shift in the π*→σ* band of the dirhodium paddlewheel from λ_{max} = 595 nm to 561 nm occurs upon addition of 12 equivalents of diz (left). Subsequent addition of up to 24 equivalents of diz produces little change in the UV-Vis profile of the cage (right), suggesting that the cage is composed of 12 dirhodium paddlewheel complexes.

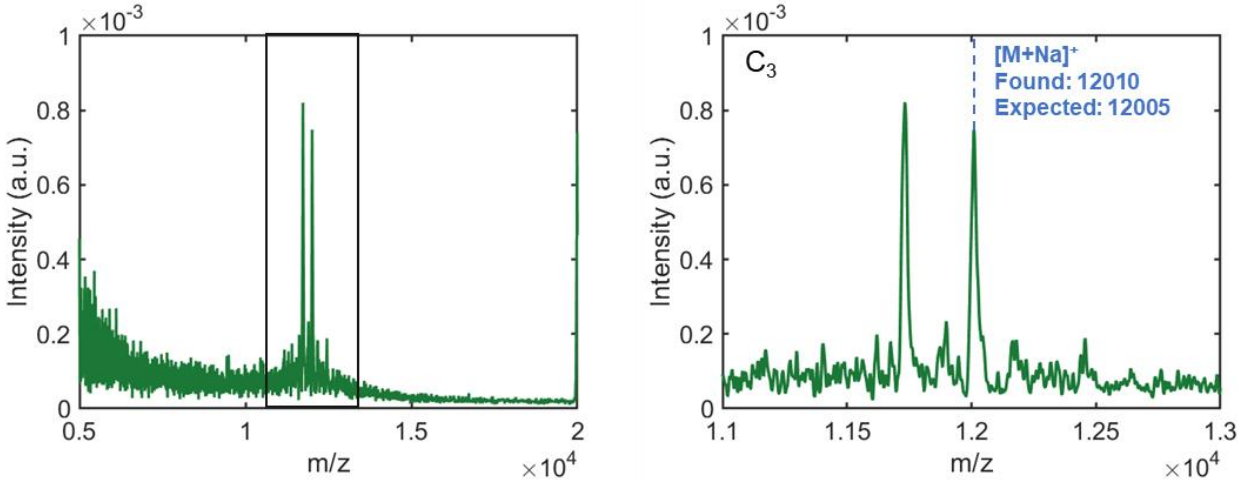

Figure S12. Expanded (left) and zoomed (right) MALDI mass spectra of C_3-Coumarin-RhMOP collected using a DCTB matrix and sodium trifluoroacetate as a cationizing agent. A peak at m/z = 12010 is clearly observed, which can be attributed to the $[M+Na]^+$ adduct of the cage (expected: m/z = 12005). One additional peak with a lower m/z value is also observed, which may correspond to a decomposition byproduct formed upon irradiation of the strongly-absorbing C_3-Coumarin-RhMOP with the UV laser during sample ionization.

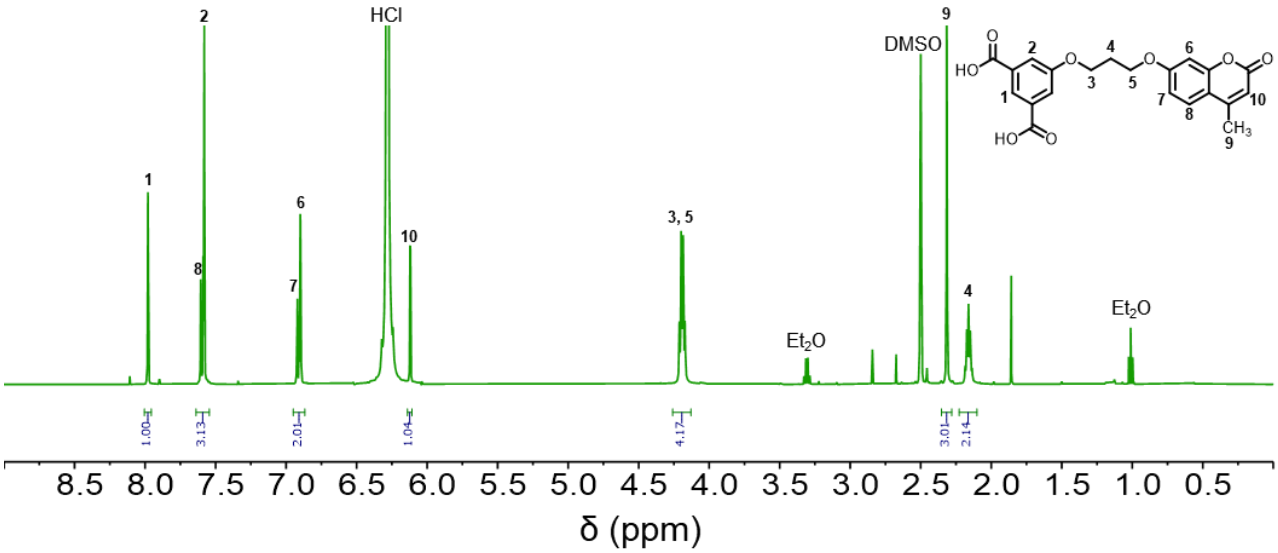

Figure S13. ^{1}H NMR spectrum (500 MHz, 298 K) of a sample of C_3-Coumarin-RhMOP decomposed by heating at 100 ºC in a mixture of DMSO-d_6, D_2O, and DCl for 1 h.

5.3. Structural Characterization Data for 12:12 C_{10}-Coumarin/OH-RhMOP

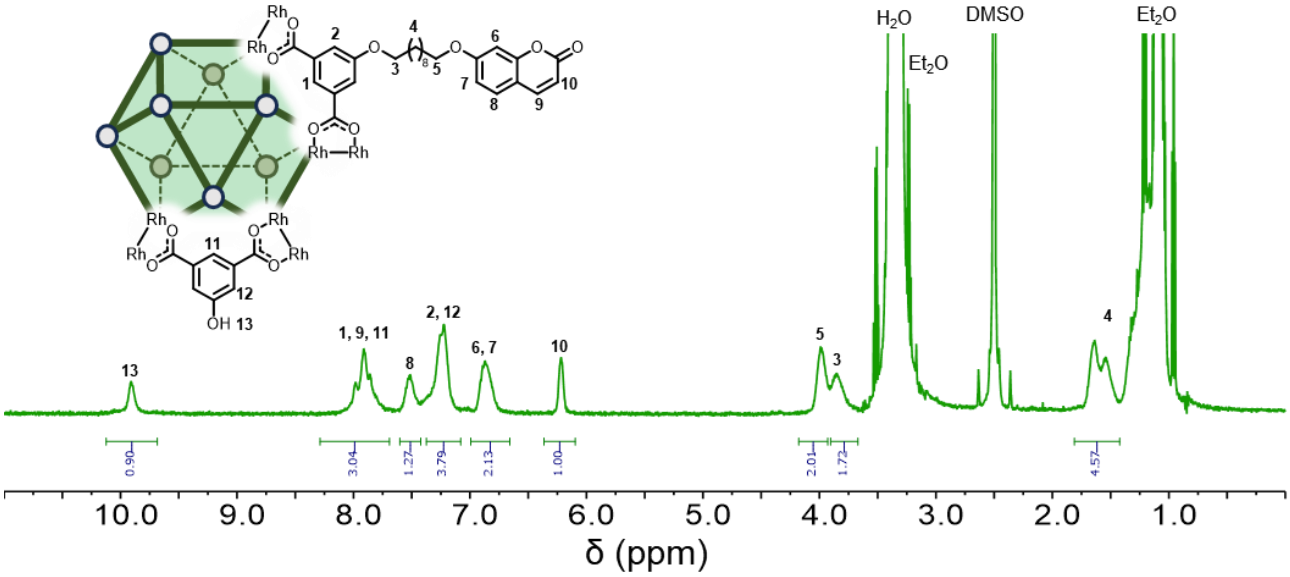

Figure S14. ^{1}H NMR spectrum (DMSO-d_6, 500 MHz, 298 K) of 12:12 C_{10}-Coumarin/OH-RhMOP.

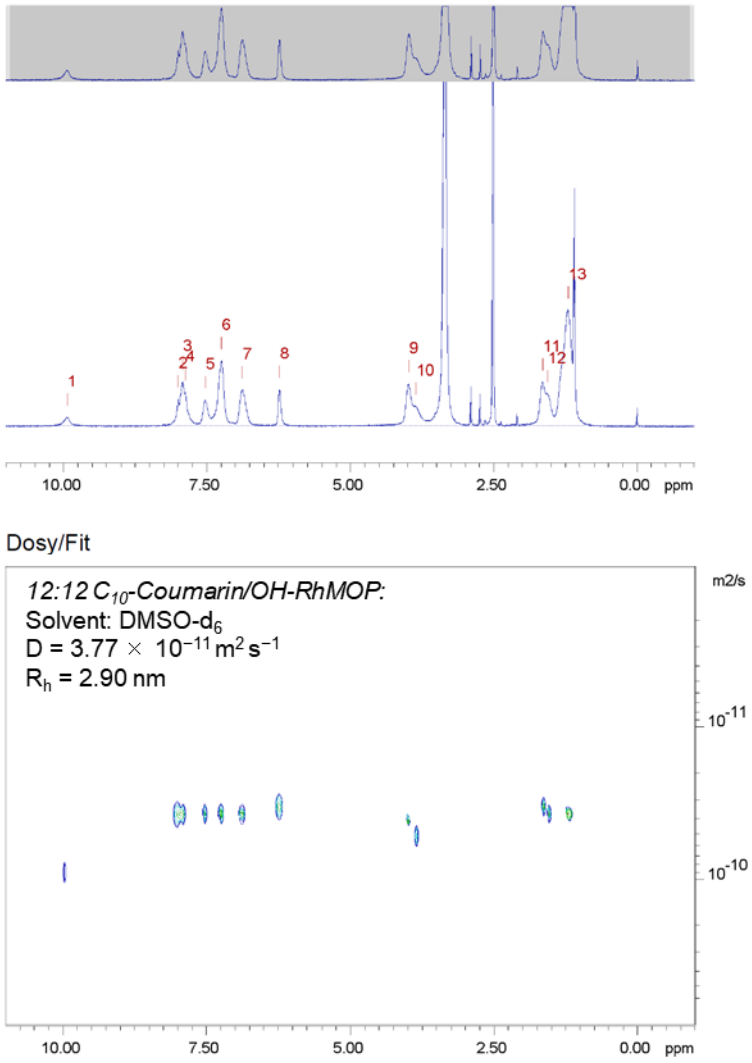

Figure S15. DOSY spectrum of 12:12 C_{10}-Coumarin/OH-RhMOP in DMSO-d_6. Note that signal 1 was excluded in the calculation of the cage's average diffusion coefficient ($D = 3.77 \times 10^{-11}$ m^2/s) because this peak corresponds to the exchangeable hydroxyl proton of the 5-hydroxyisophthalate residues.[7]

signal	ppm	D_s / m^2 s^{-1}	σ
1	9.933	8.77×10^{-11}	8.190×10^{-12}
2	8.000	3.75×10^{-11}	2.517×10^{-12}
3	7.918	3.60×10^{-11}	1.033×10^{-12}
4	7.874	3.71×10^{-11}	1.642×10^{-12}
5	7.525	3.60×10^{-11}	1.795×10^{-12}
6	7.244	3.87×10^{-11}	1.449×10^{-12}
7	6.874	3.54×10^{-11}	1.354×10^{-12}
8	6.222	3.37×10^{-11}	1.968×10^{-12}
9	3.984	3.99×10^{-11}	1.049×10^{-12}
10	3.851	5.16×10^{-11}	3.267×10^{-12}
11	1.643	3.38×10^{-11}	1.274×10^{-12}
12	1.554	3.58×10^{-11}	1.408×10^{-12}
13	1.199	3.70×10^{-11}	7.014×10^{-13}

Table S3. Peak positions, diffusion coefficients (D), and errors (σ) corresponding to the DOSY data in **Figure S15**.

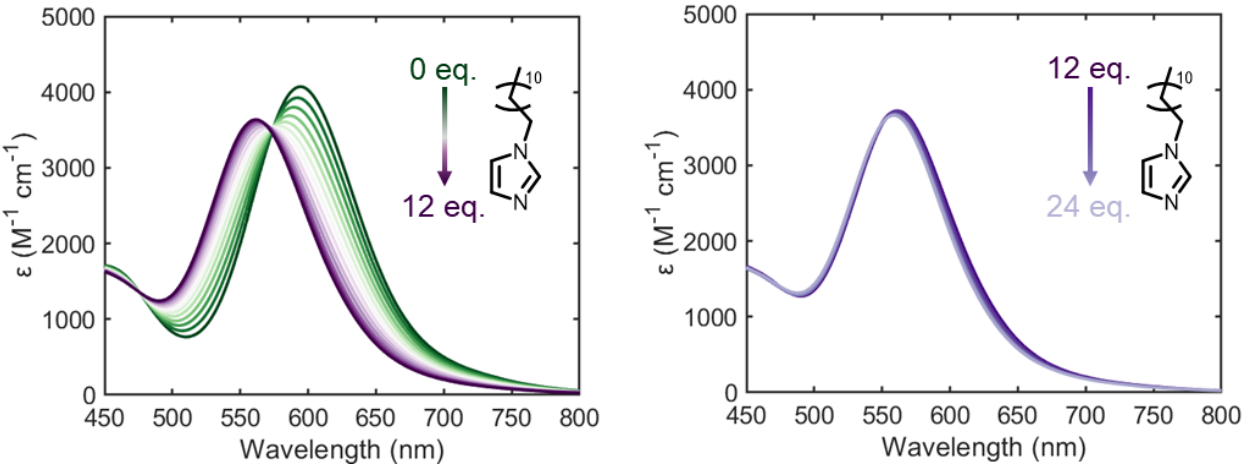

Figure S16. UV-Vis titration of 12:12 C_{10}-Coumarin/OH-RhMOP with up to 24 equivalents of diz. A shift in the π*→σ* band of the dirhodium paddlewheel from λ_{max} = 594 nm to 561 nm occurs upon addition of 12 equivalents of diz (left). Subsequent addition of up to 24 equivalents of diz produces little change in the UV-Vis profile of the cage (right), suggesting that the cage is composed of 12 dirhodium paddlewheel complexes.

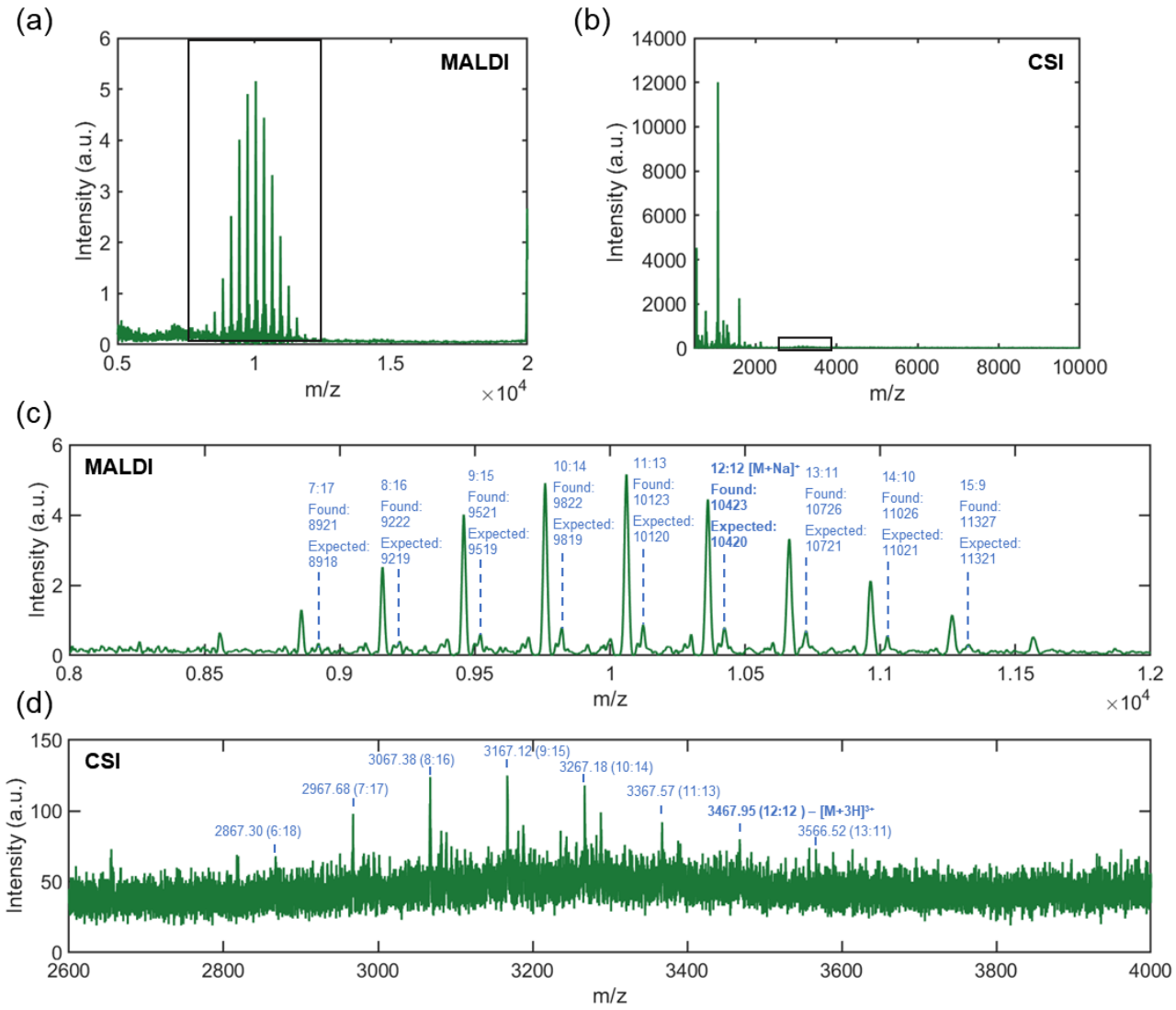

Figure S17. (a) Expanded and (c) zoomed-in MALDI mass spectra of 12:12 C_{10}-Coumarin/OH-RhMOP collected using a DCTB matrix and sodium trifluoroacetate as a cationizing agent. A peak at m/z = 10423 is clearly observed, which can be attributed to the $[M+Na]^+$ adduct of the 12:12 mixed ligand cage (expected: m/z = 10420). Additional peaks are also observed at m/z ~ 10423 ± 300n (where n = integers), which correspond to the $[M+Na]^+$ adducts of cages with other C_{10}-Coumarin-bdc : 5-hydroxyisophthalate ratios. Several other unassignable peaks also observed, which may correspond to decomposition byproducts formed upon irradiation of the strongly-absorbing 12:12 C_{10}-Coumarin/OH-RhMOP with the UV laser during sample ionization. (b) Expanded and (d) zoomed-in CSI mass spectra of 12:12 C_{10}-Coumarin/OH-RhMOP reveal a signal at m/z = 3467.95, which corresponds to the $[M+3H]^{3+}$ adduct of the 12:12 mixed ligand cage (expected: m/z = 3466.76). Additional signals were also observed at m/z ~ 3467 ± 100n (where n = integers), which correspond to $[M+3H]^{3+}$ adducts of cages with other C_{10}-Coumarin-bdc : 5-hydroxyisophthalate ratios.

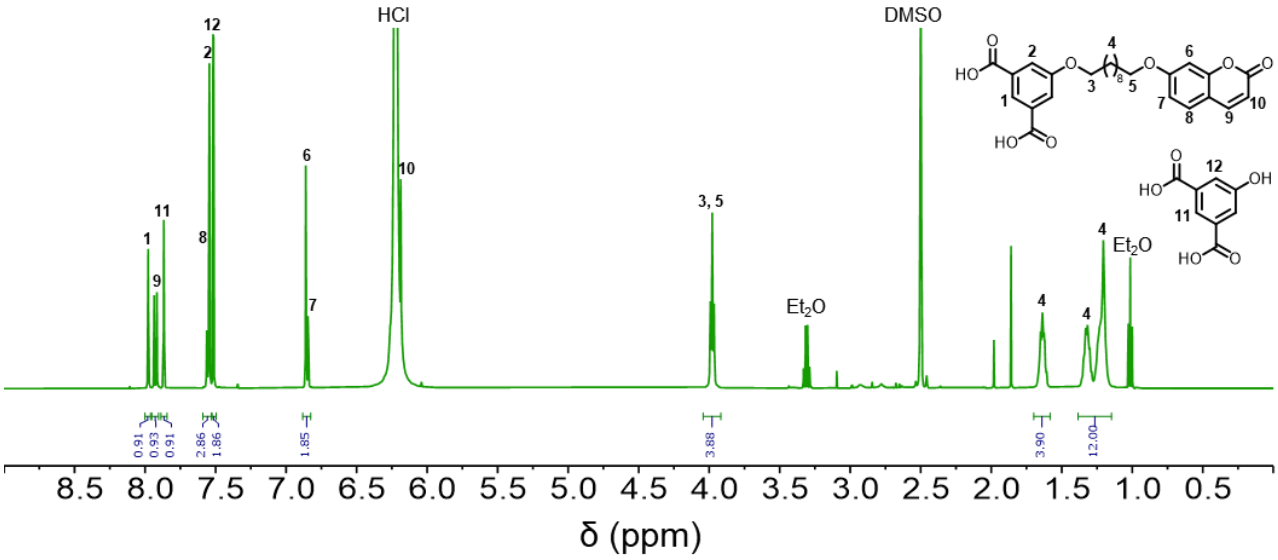

Figure S18. ^{1}H NMR spectrum (500 MHz, 298 K) of a sample of 12:12 C_{10}-Coumarin/OH-RhMOP decomposed by heating at 100 ºC in a mixture of DMSO-d_6, D_2O, and DCl for 1 h. Relative integrations of peaks corresponding to C_{10}-Coumarin-bdcH_2 and 5-hydroxyisopthalic acid indicate that the sample is composed of a 1:1 mixture of the two ligands.

5.4. Solution-state C_{10}-Coumarin-bdcH_2 Photodimerization Data

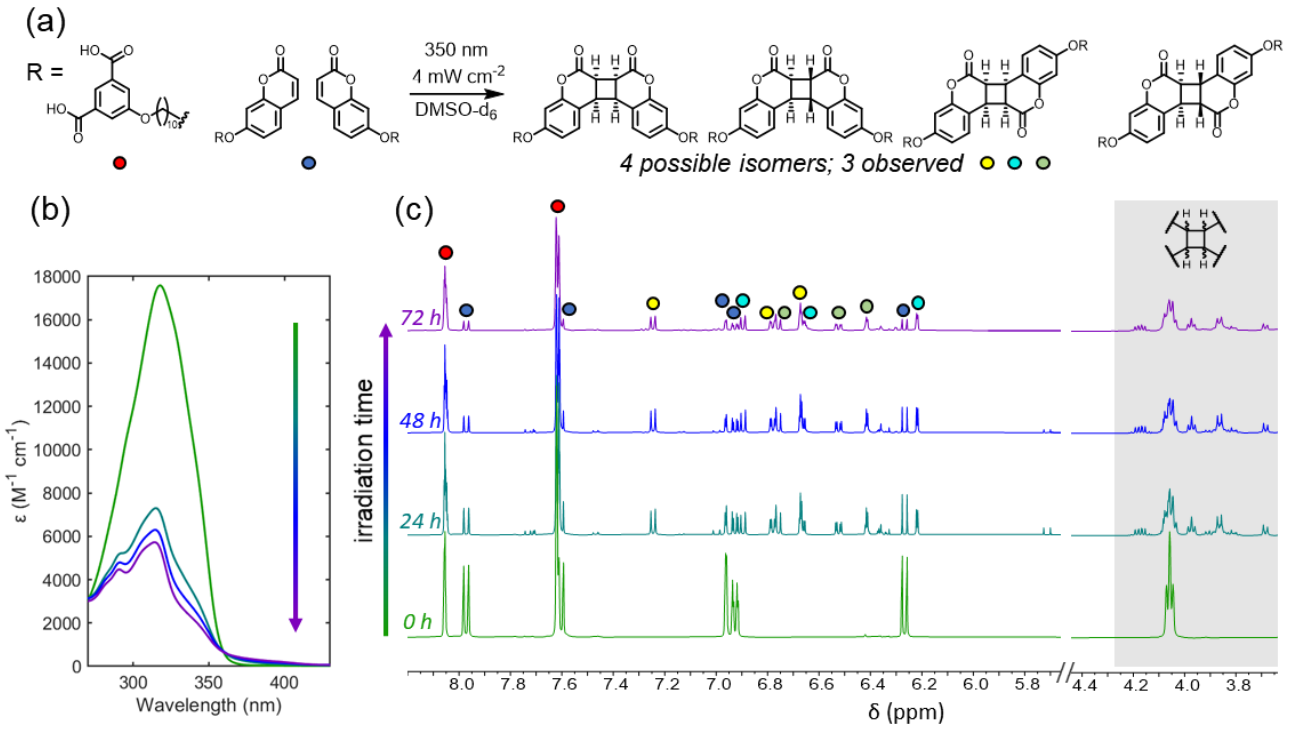

Figure S19. Spectroscopic characterization data for the solution-state C_{10}-Coumarin-bdcH_2 photodimerization experiment. (a) Reaction scheme for the photodimerization of C_{10}-Coumarin-bdcH_2 upon irradiation with 350 nm light. Coumarin dimerization reactions can produce up to four spectroscopically distinct isomers, with isomer ratios determined by the choice of solvent, coumarin structure, and reaction concentration. In this case, only three isomers were observed. (b) UV-Vis spectra of a 20 mM DMSO-d_6 solution of C_{10}-Coumarin-bdcH_2 after irradiation for 0 h (green), 24 h (teal), 48 h (blue) and 72 h (purple) at 350 nm (4 mW/cm^2). The strong coumarin absorbance feature at 320 nm decreases throughout the irradiation process, corresponding to an overall dimerization yield of 80% at 72 h. (c) ^{1}H NMR spectra (DMSO-d_6, 500 MHz, 298 K) of the same C_{10}-Coumarin-bdcH_2 solution collected after irradiation for 0 h (green), 24 h (teal), 48 h (blue) and 72 h (purple) at 350 nm. New peaks emerge between 7.4 and 6.2 ppm, corresponding to the aromatic signals of three coumarin dimer isomers (labeled with yellow, light blue, and green circles). Note that the exact stereochemical configuration corresponding to each correlated set of coumarin dimer signals cannot be verified through these methods. Signals corresponding to monomeric coumarin residues (dark blue circles) decrease upon irradiation, consistent with their consumption during the photodimerization reaction. New cyclobutane signals also emerge between 4.3 and 3.6 ppm, corroborating the formation of coumarin dimer isomers. The relative integrations of coumarin dimer signals and coumarin monomer signals after 72 h of irradiation time reveal a dimerization yield of 83%, which is in excellent agreement with the UV-Vis data.

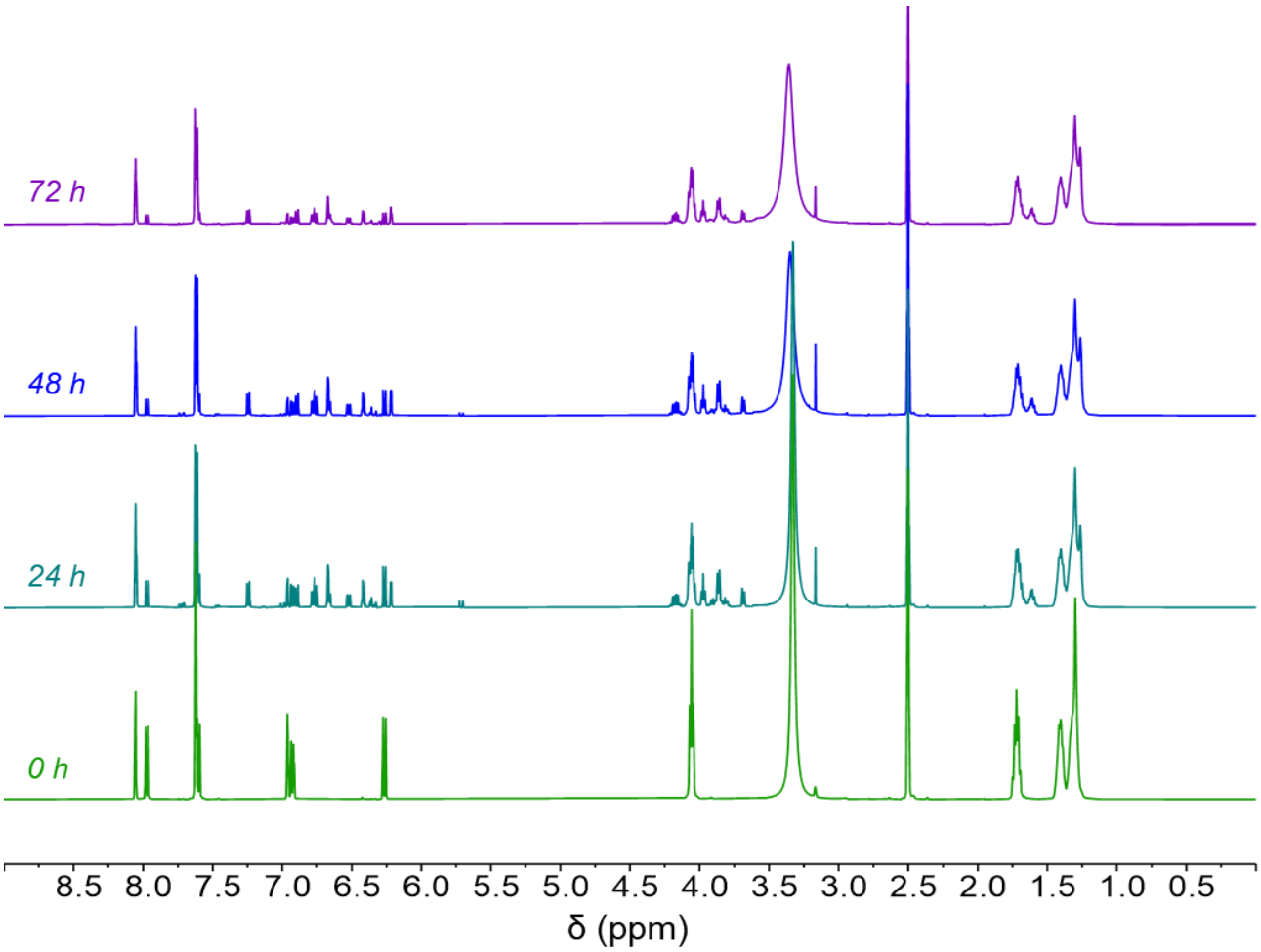

Figure S20. Expanded versions of the ^{1}H NMR spectra (DMSO-d_6, 500 MHz, 298 K) of C_{10}-Coumarin-bdcH_2 presented in **Figure S19**.

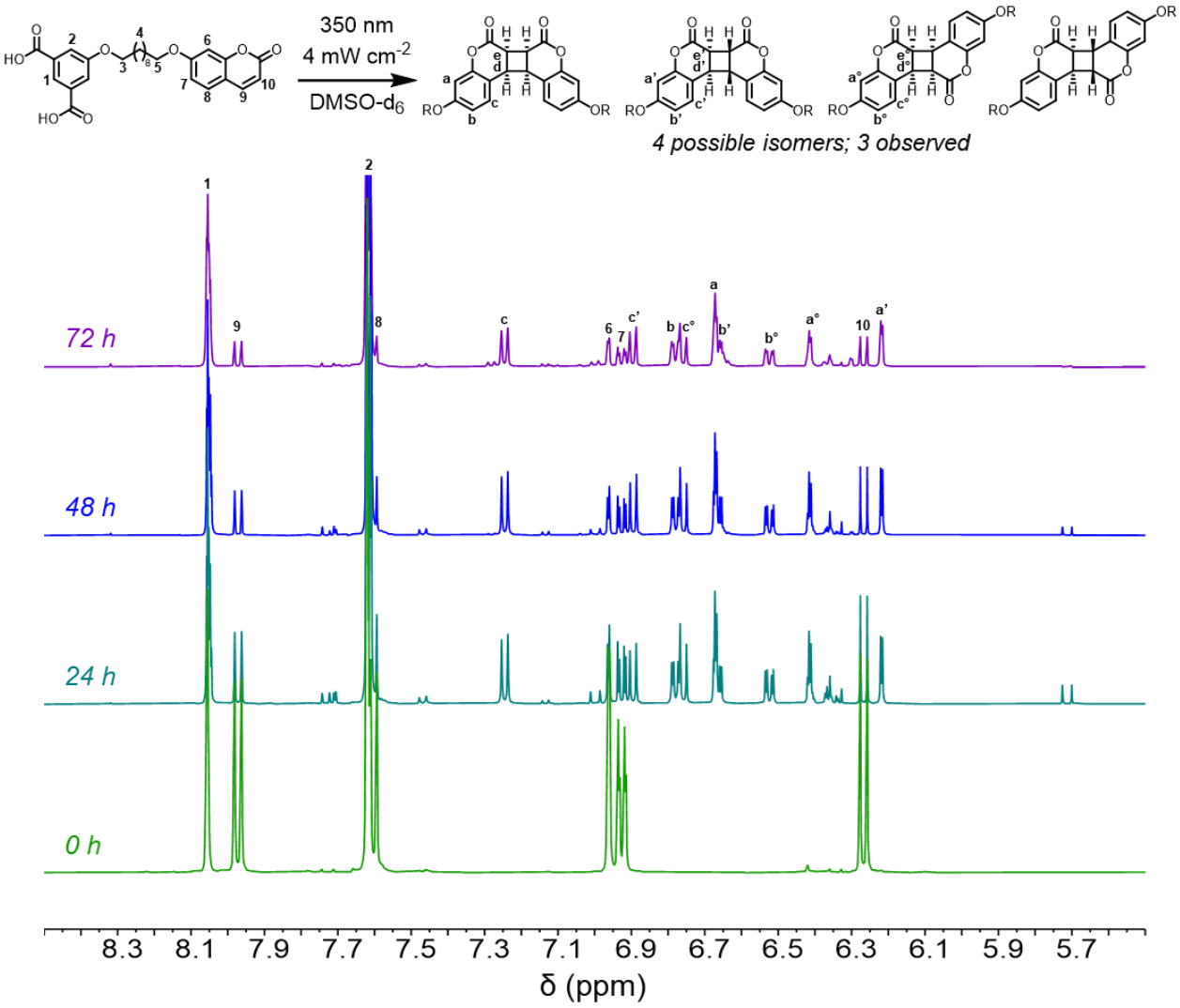

Figure S21. Zoomed-in version of the ^{1}H NMR spectra (DMSO-d_6, 500 MHz, 298 K) of C_{10}-Coumarin-bdcH_2 presented in **Figure S19** showcasing the aromatic region. Numbers and letters are used to assign peaks to specific protons of the of C_{10}-Coumarin-bdcH_2 monomer and dimer isomers, respectively. Note that the absolute stereochemical configuration of the isomer corresponding to each set of peaks is not known, and the sets of letters are arbitrarily assigned to a particular dimer isomer structure.

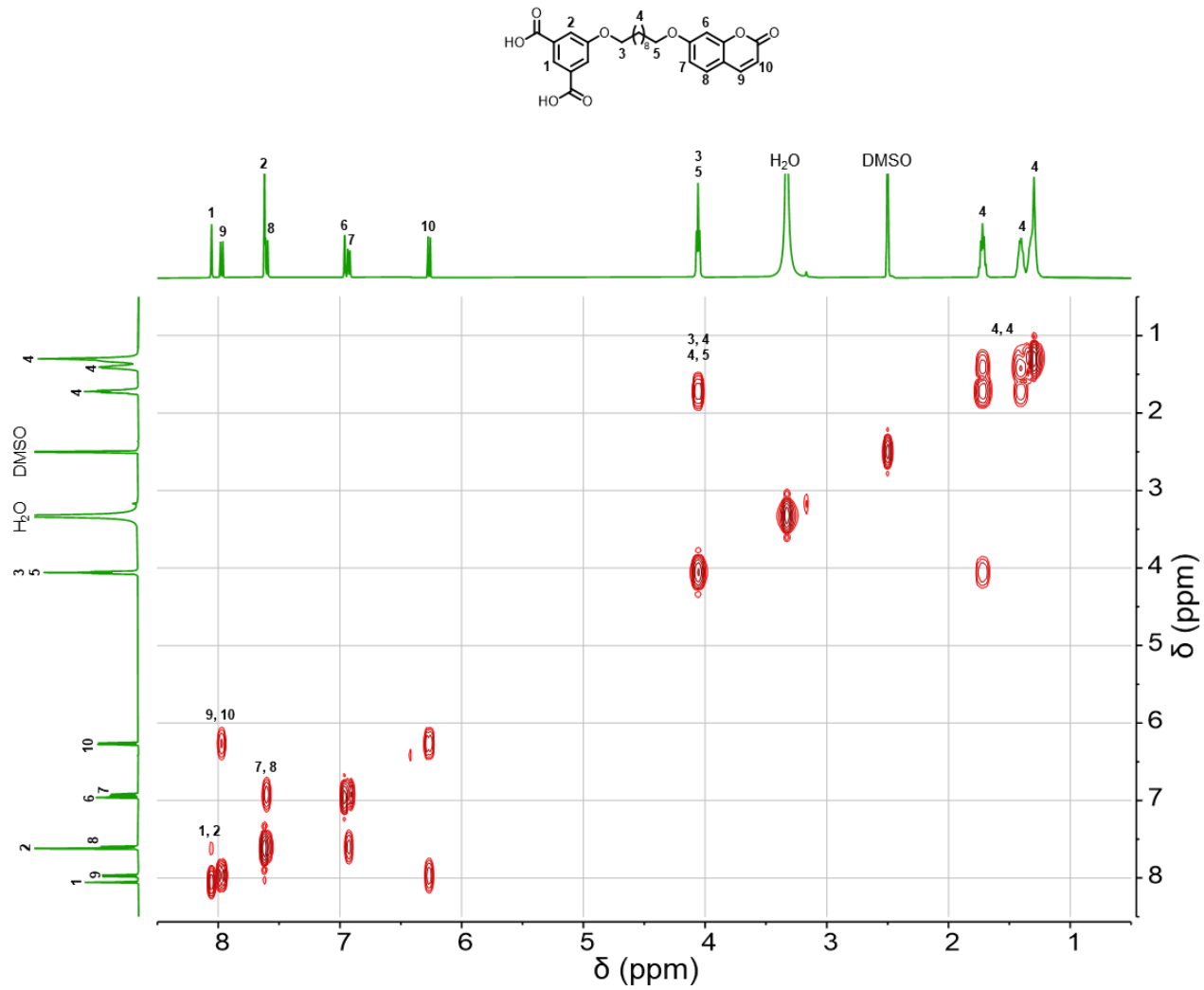

Figure S22. COSY spectrum of the 20 mM DMSO-d_6 solution of C_{10}-Coumarin-bdcH_2 prior to irradiation. Correlations are assigned according to the chemical structure above the spectrum.

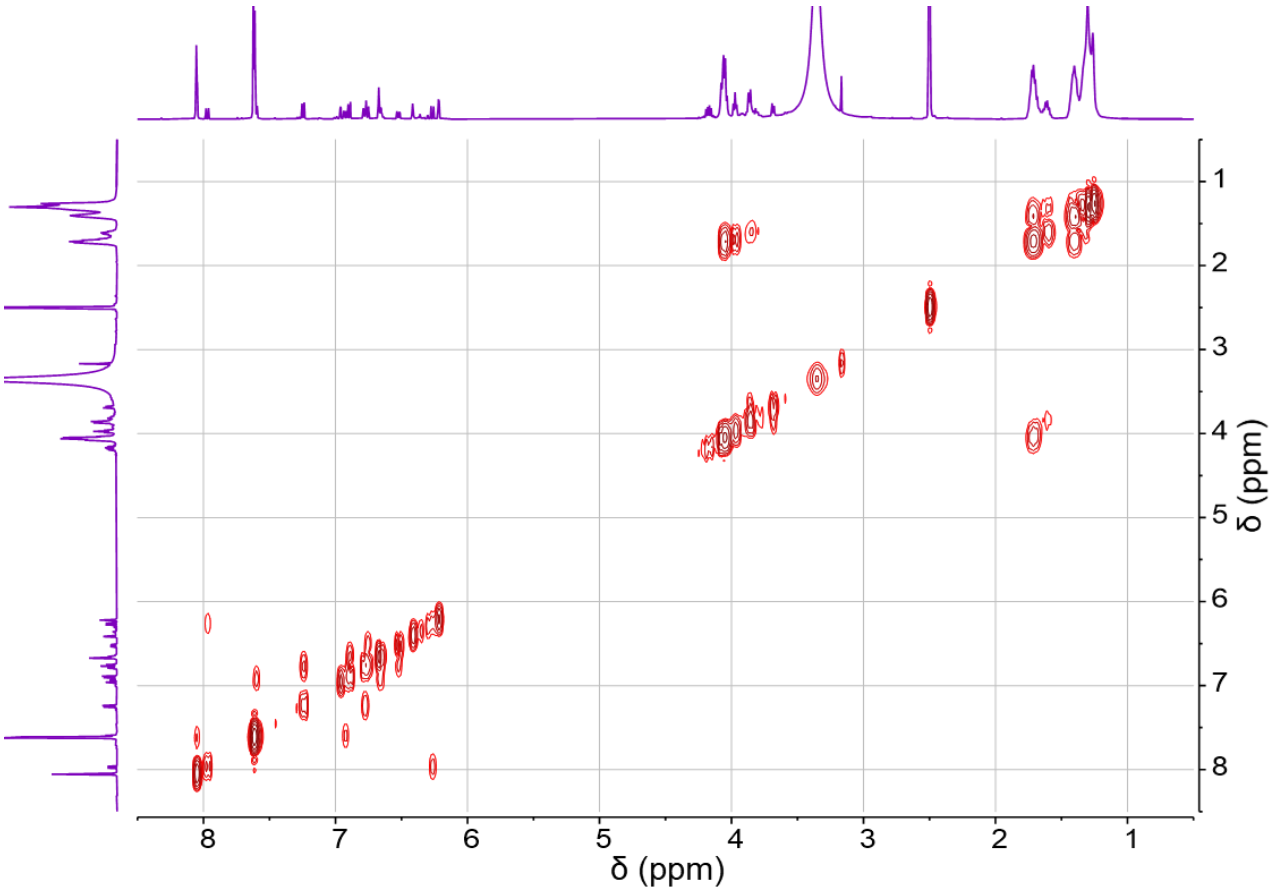

Figure S23. Zoomed-out COSY spectrum of the 20 mM DMSO-d_6 solution of C_{10}-Coumarin-bdcH_2 after irradiation at 350 nm (4 mW/cm^2) for 72 h.

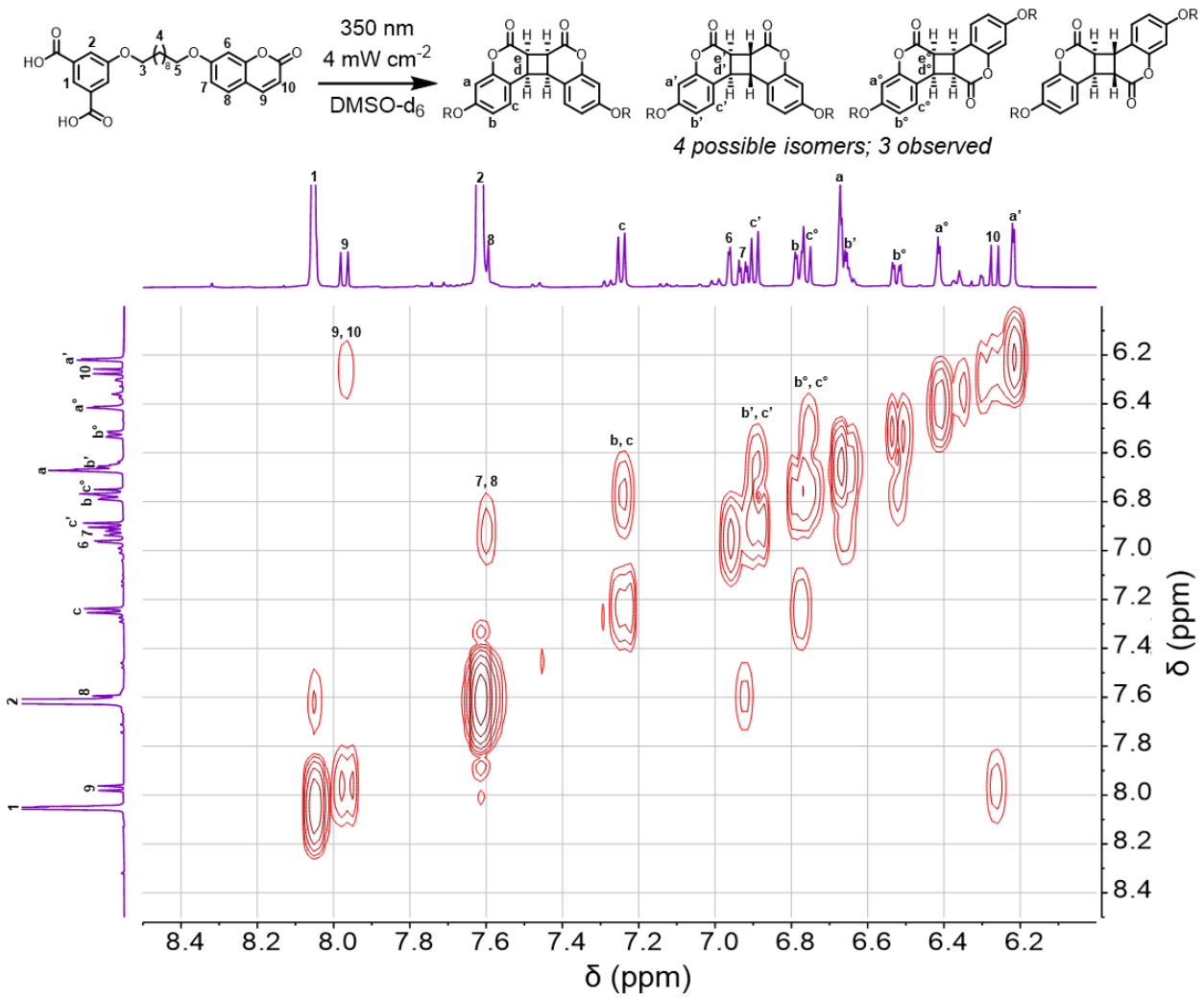

Figure S24. Zoomed-in COSY spectrum of the 20 mM DMSO-d_6 solution of C_{10}-Coumarin-bdcH_2 after irradiation at 350 nm (4 mW/cm^2) for 72 h showcasing the aromatic region. Correlations are assigned according to the reaction scheme above the spectrum. Expected correlations between proton signals corresponding to three coumarin dimer isomers are observed.

5.5. Solution-state C_{10}-Coumarin-RhMOP Photodimerization Data

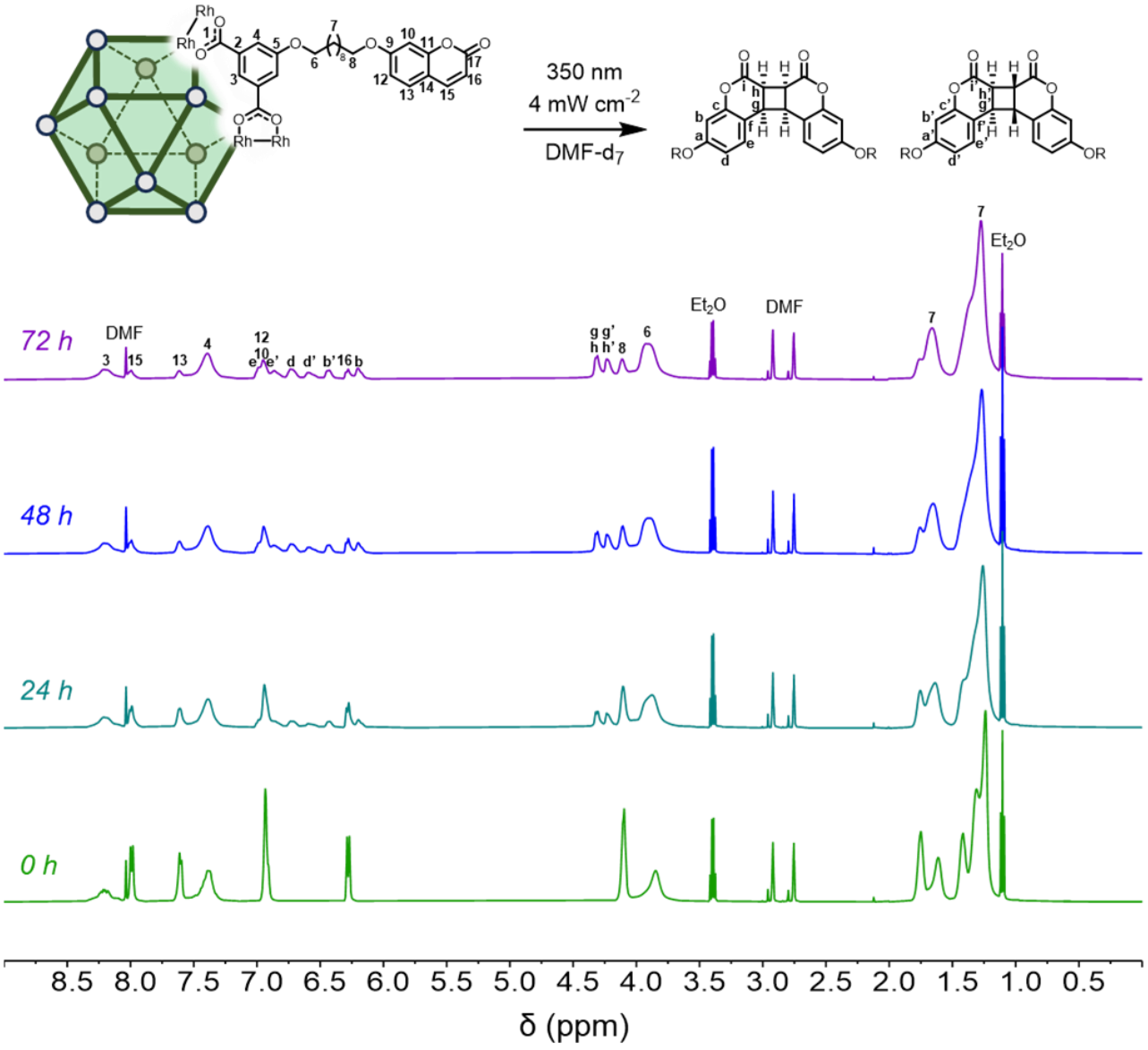

Figure S25. Expanded versions of the ^{1}H NMR spectra (DMF-d_7, 500 MHz, 298 K) of C_{10}-Coumarin-RhMOP presented in **Figure 3b**. Peaks are labeled according to the reaction scheme provided above the spectra. Note that the exact stereochemical configuration corresponding to each correlated set of coumarin dimer signals cannot be verified through these methods.

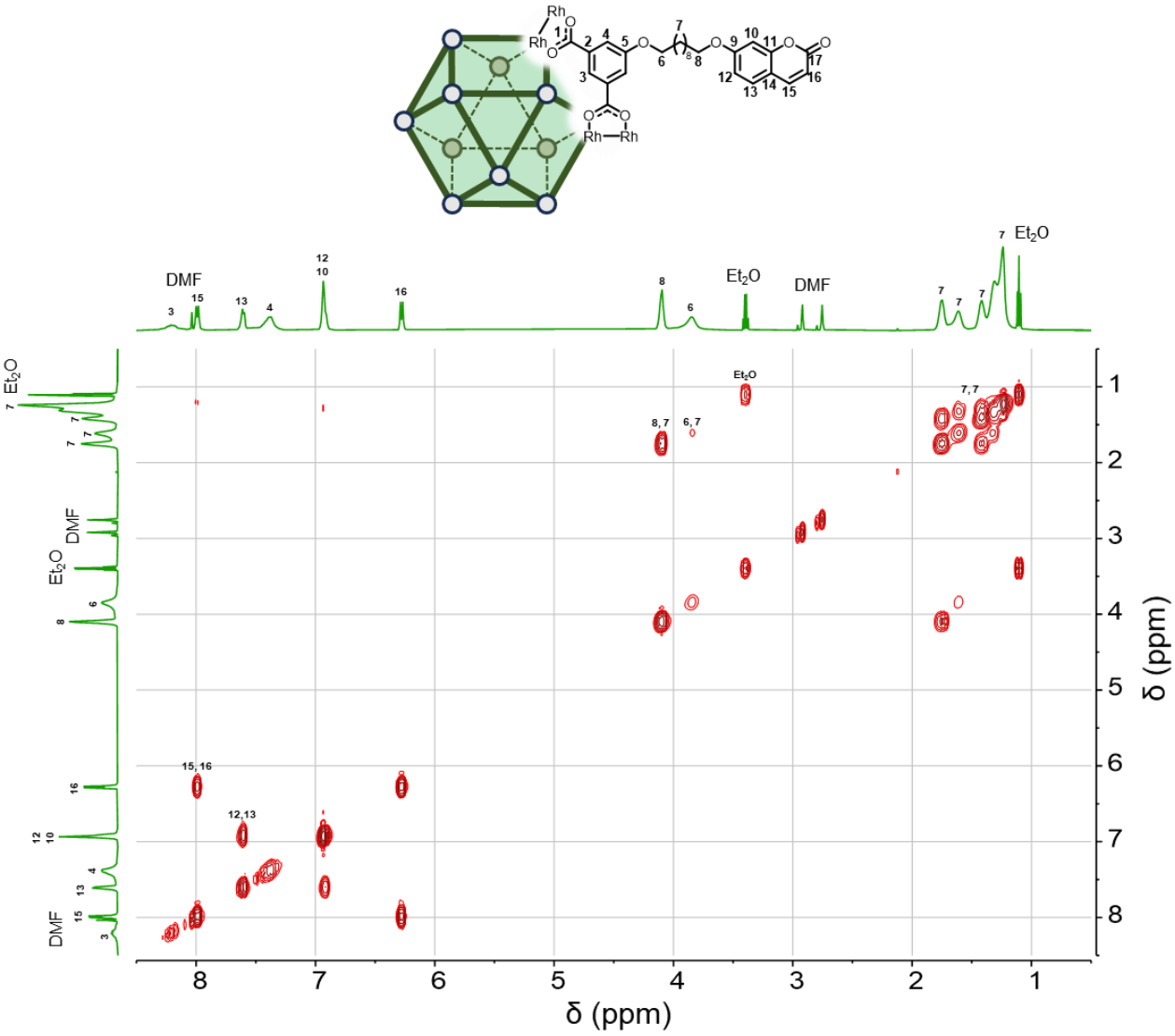

Figure S26. COSY spectrum of the 5 mM DMF-d_7 solution of C_{10}-Coumarin-RhMOP prior to irradiation. Correlations are assigned according to the MOP chemical structure above the spectrum.

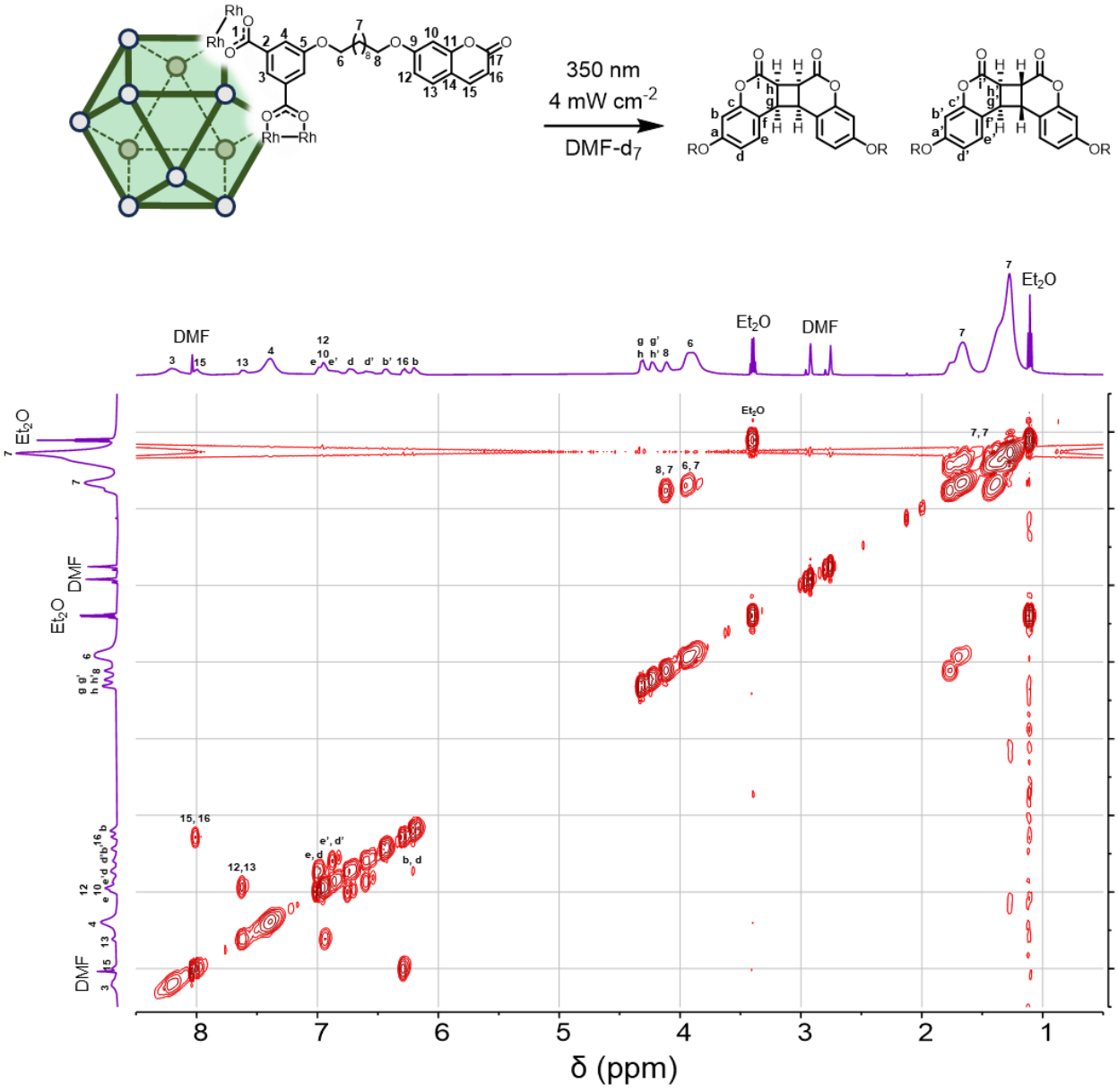

Figure S27. COSY spectrum of the 5 mM DMF-d_7 solution of C_{10}-Coumarin-RhMOP after irradiation at 350 nm (4 mW/cm^2) for 72 h. Correlations are assigned according to the reaction scheme above the spectrum. Expected correlations between proton signals corresponding to two coumarin dimer isomers are observed.

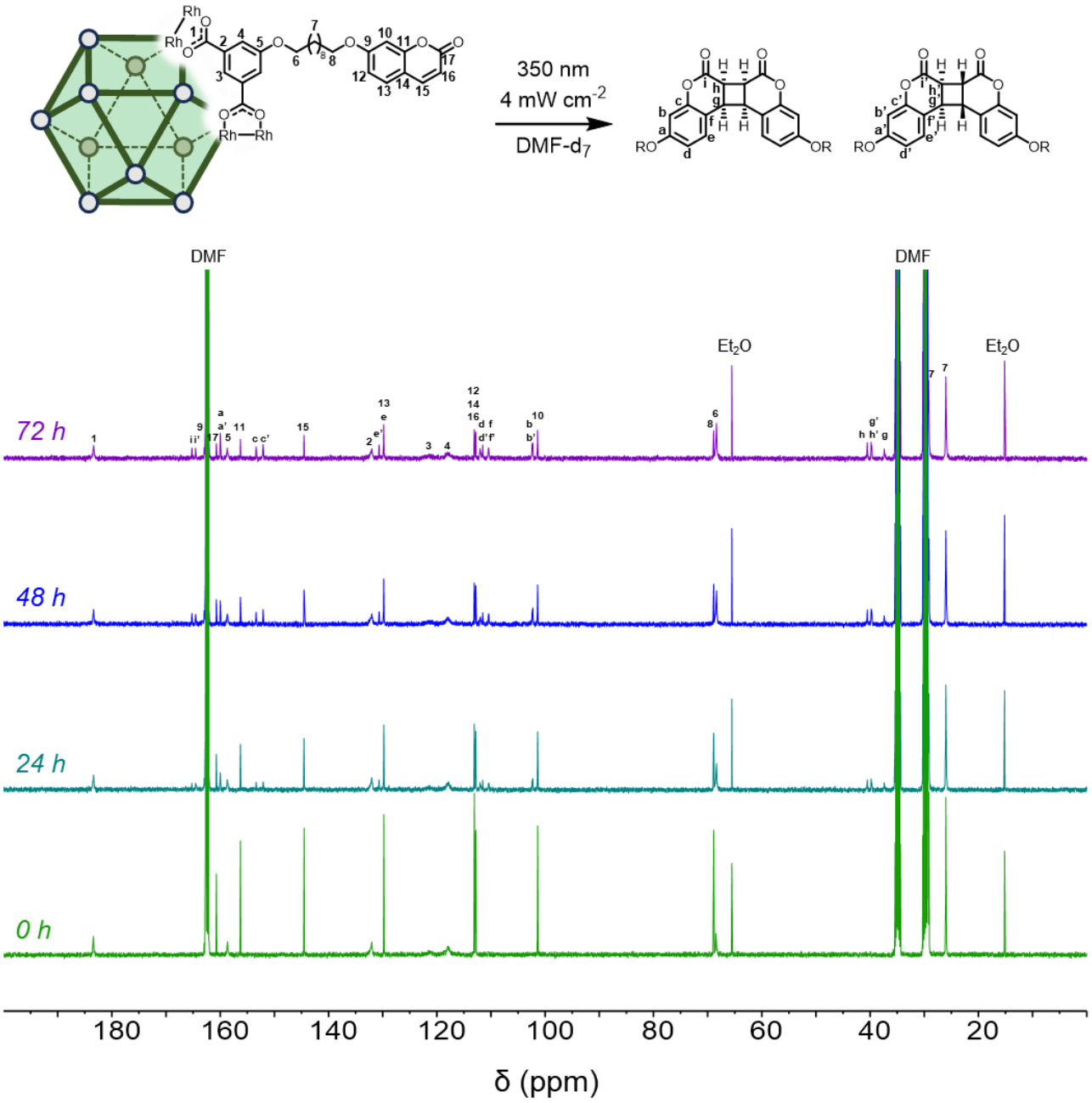

Figure S28. ^{13}C NMR spectra (DMF-d_7, 125 MHz, 298 K) of the 5 mM DMF-d_7 solution of C_{10}-Coumarin-RhMOP after irradiation at 350 nm (4 mW/cm^2) for 0 h (green), 24 h (teal), 48 h (blue), and 72 h (purple). Peaks are labeled according to the reaction scheme provided above the spectra.

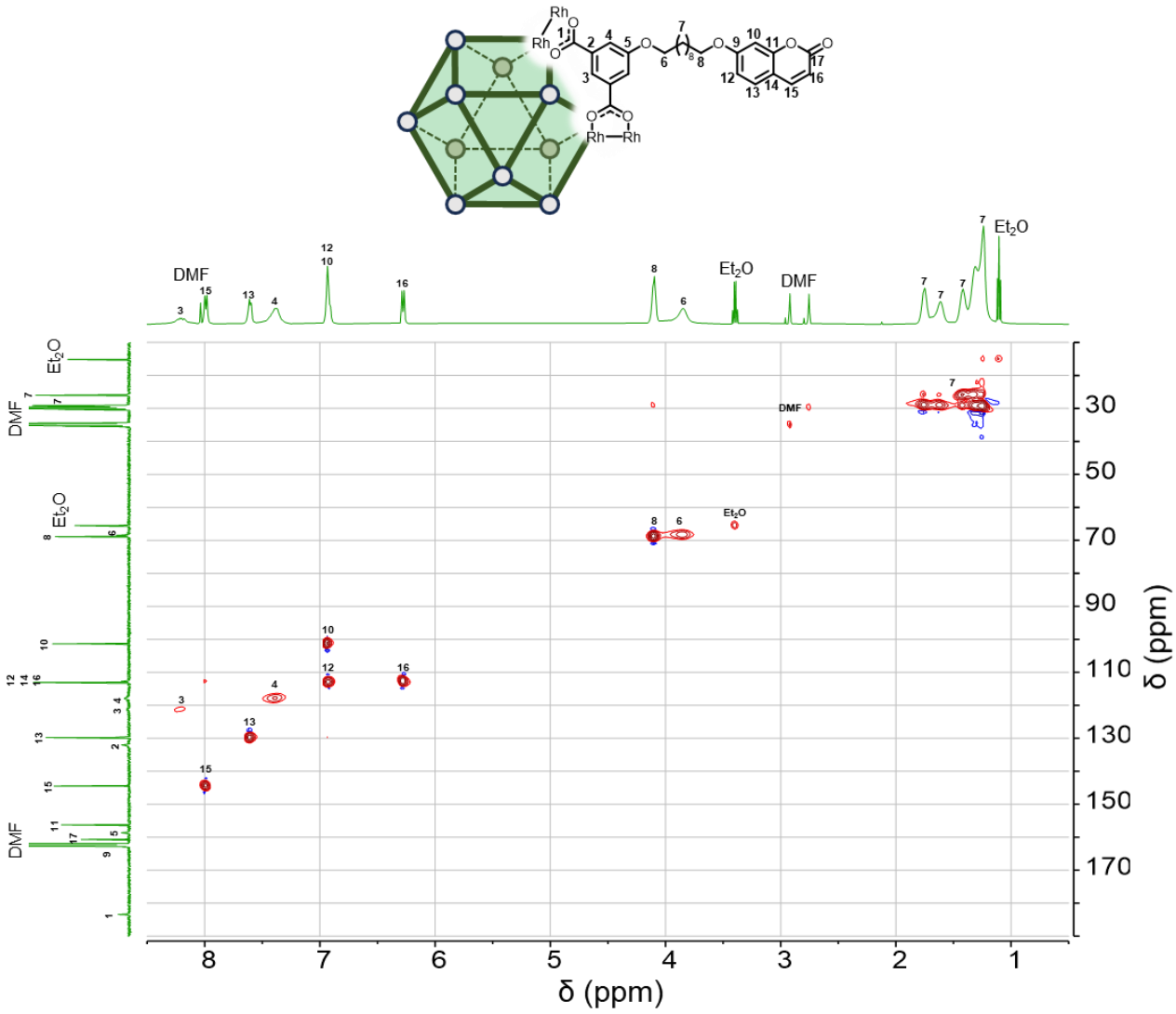

Figure S29. HSQC spectrum of the 5 mM DMF-d_7 solution of C_{10}-Coumarin-RhMOP prior to irradiation. Correlations are assigned according to the MOP chemical structure above the spectrum.

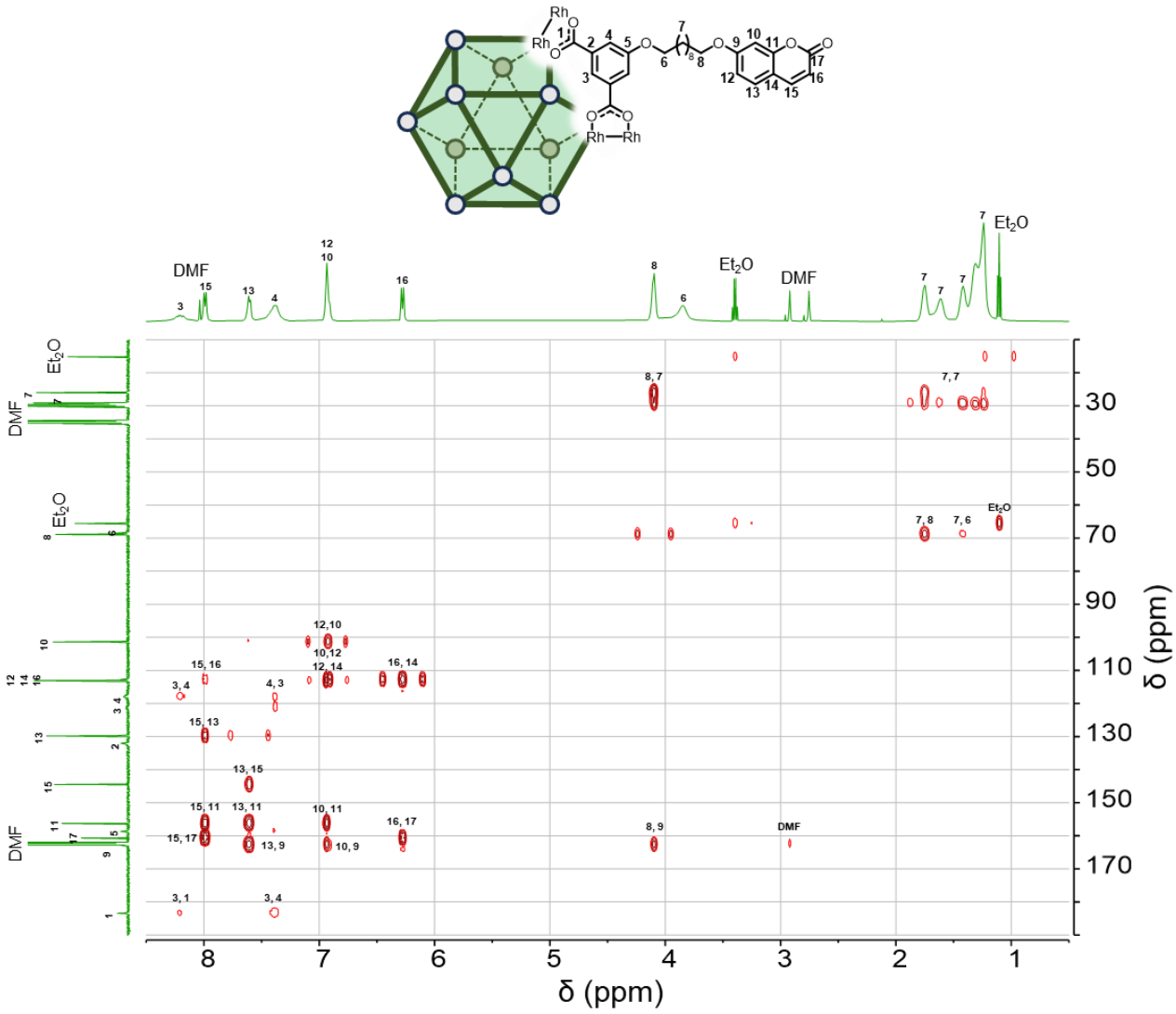

Figure S30. HMBC spectrum of the 5 mM DMF-d_7 solution of C_{10}-Coumarin-RhMOP prior to irradiation. Correlations are assigned according to the MOP chemical structure above the spectrum.

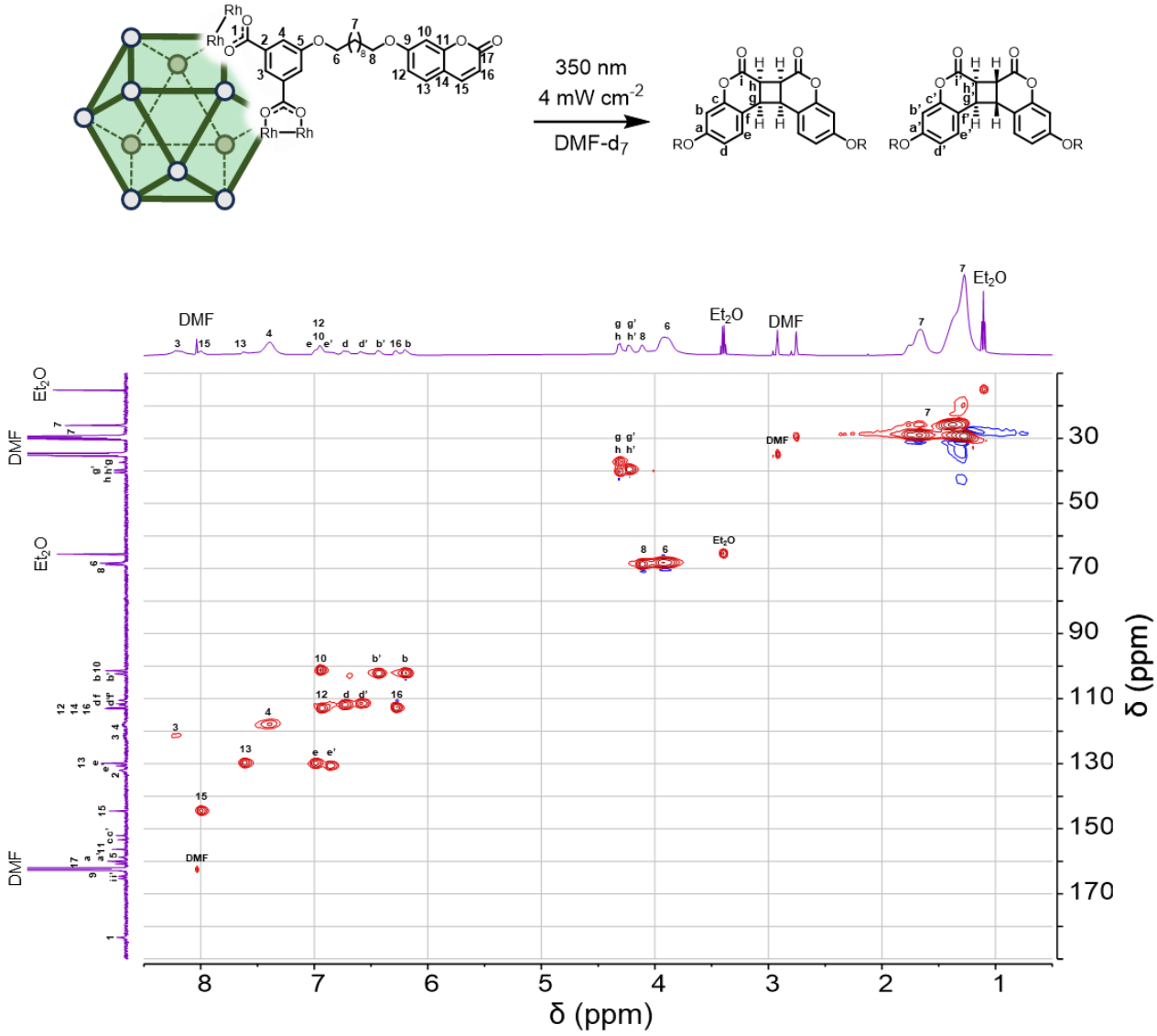

Figure S31. HSQC spectrum of the 5 mM DMF-d_7 solution of C_{10}-Coumarin-RhMOP after irradiation at 350 nm (4 mW/cm^2) for 72 h. Correlations are assigned according to the reaction scheme above the spectrum. Expected correlations between proton and carbon signals corresponding to two coumarin dimer isomers are observed.

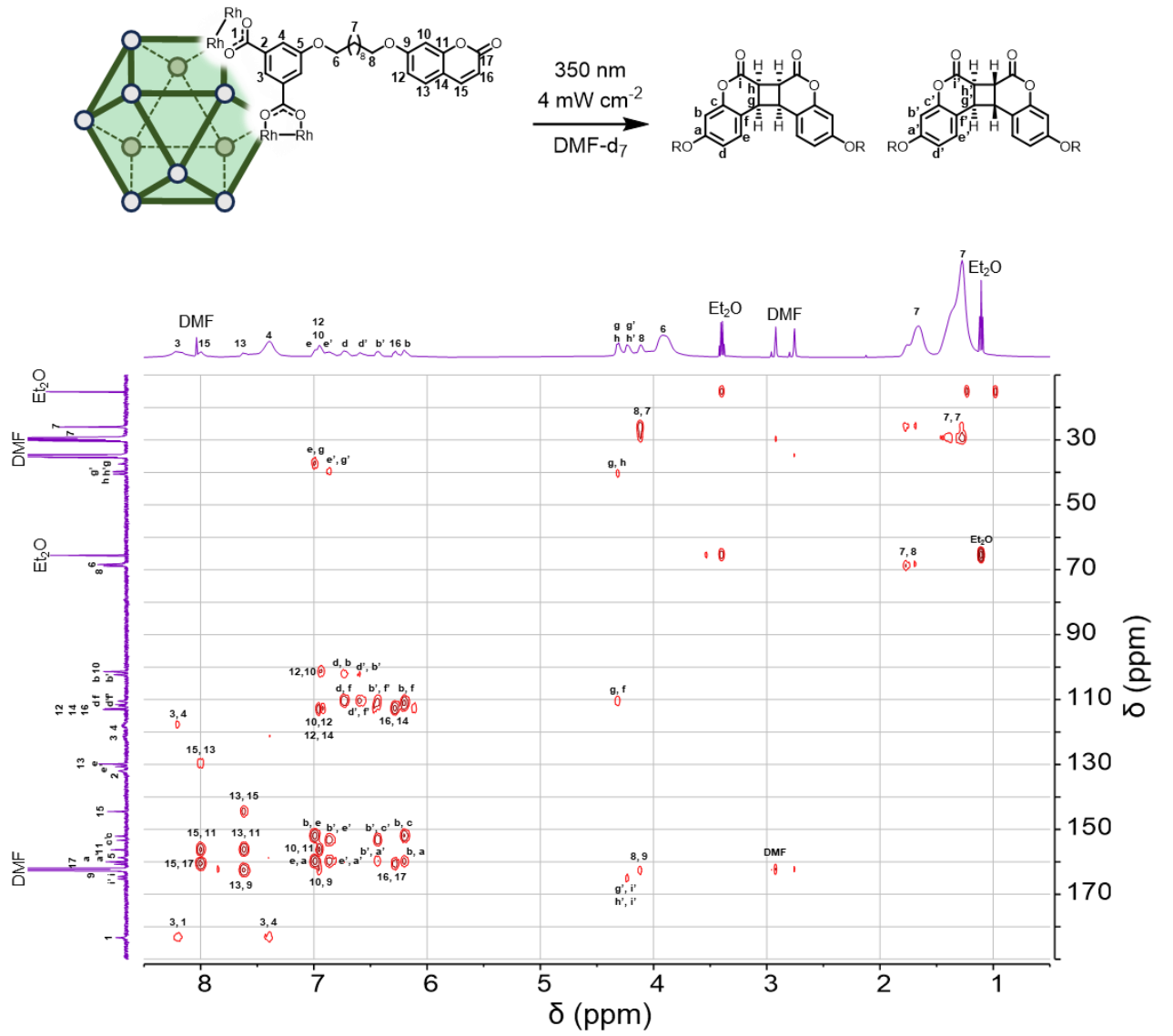

Figure S32. HMBC spectrum of the 5 mM DMF-d_7 solution of C_{10}-Coumarin-RhMOP after irradiation at 350 nm (4 mW/cm^2) for 72 h. Correlations are assigned according to the reaction scheme above the spectrum. Expected correlations between proton and carbon signals corresponding to two coumarin dimer isomers are observed.

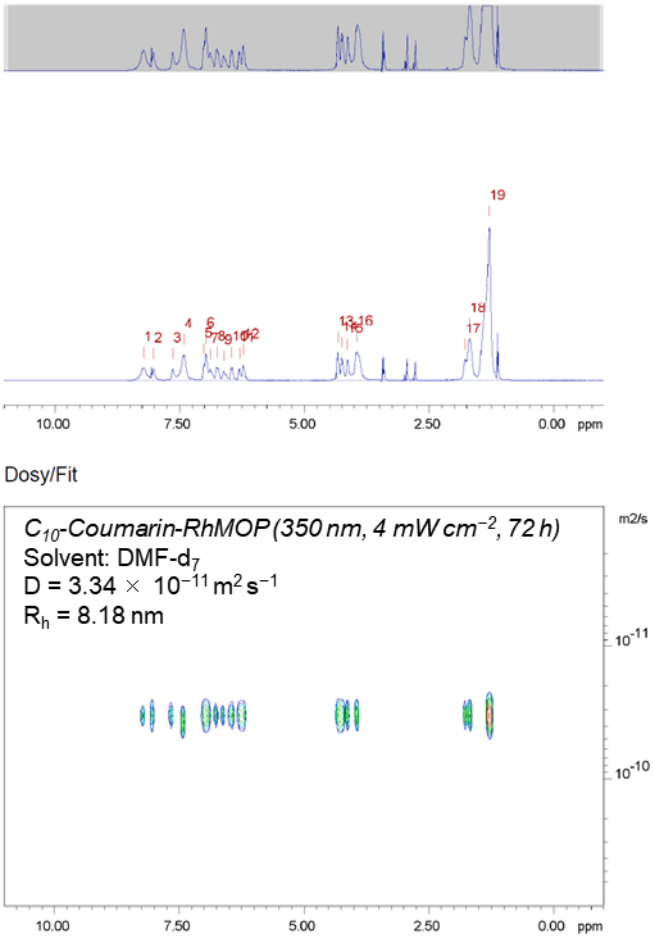

Figure S33. DOSY spectrum of the 5 mM DMF-d_7 solution of C_{10}-Coumarin-RhMOP after irradiation at 350 nm (4 mW/cm^2) for 72 h.

signal	ppm	D_s / m^2 s^{-1}	σ
1	8.218	3.22×10^{-11}	4.405×10^{-13}
2	8.016	3.50×10^{-11}	7.633×10^{-13}
3	7.633	3.29×10^{-11}	5.271×10^{-13}
4	7.411	3.63×10^{-11}	6.225×10^{-13}
5	7.009	3.32×10^{-11}	6.079×10^{-13}
6	6.969	3.28×10^{-11}	5.115×10^{-13}
7	6.882	3.30×10^{-11}	5.795×10^{-13}
8	6.746	3.19×10^{-11}	4.734×10^{-13}
9	6.608	3.27×10^{-11}	5.092×10^{-13}
10	6.452	3.24×10^{-11}	5.157×10^{-13}
11	6.298	3.21×10^{-11}	5.355×10^{-13}
12	6.218	3.29×10^{-11}	5.545×10^{-13}
13	4.326	3.50×10^{-11}	6.325×10^{-13}
14	4.245	3.38×10^{-11}	5.702×10^{-13}
15	4.133	3.30×10^{-11}	5.635×10^{-13}
16	3.942	3.51×10^{-11}	6.212×10^{-13}
17	1.778	3.20×10^{-11}	5.046×10^{-13}
18	1.682	3.44×10^{-11}	5.647×10^{-13}
19	1.295	3.40×10^{-11}	6.248×10^{-13}

Table S4. Peak positions, diffusion coefficients (D), and errors (σ) corresponding to the DOSY data in **Figure S33**.

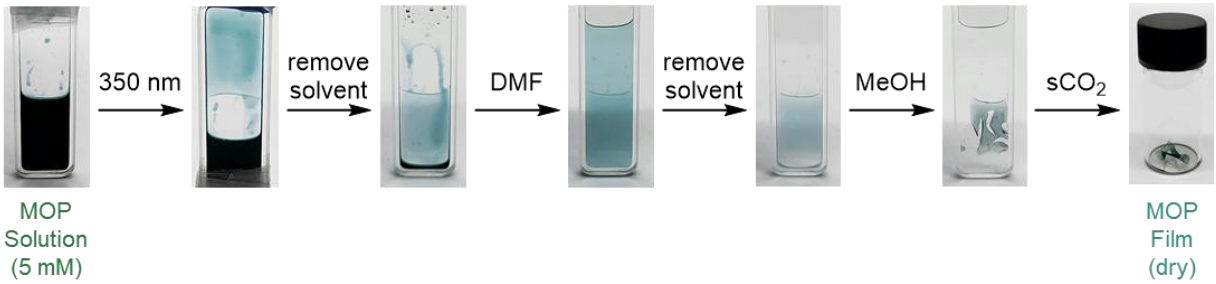

Figure S34. Photographs demonstrating the preparation of a C_{10}-Coumarin-RhMOP thin film via direct photoirradiation (350 nm, 10 mW/cm^2, 12 h) of a 20 mM DMF solution of C_{10}-Coumarin-RhMOP.

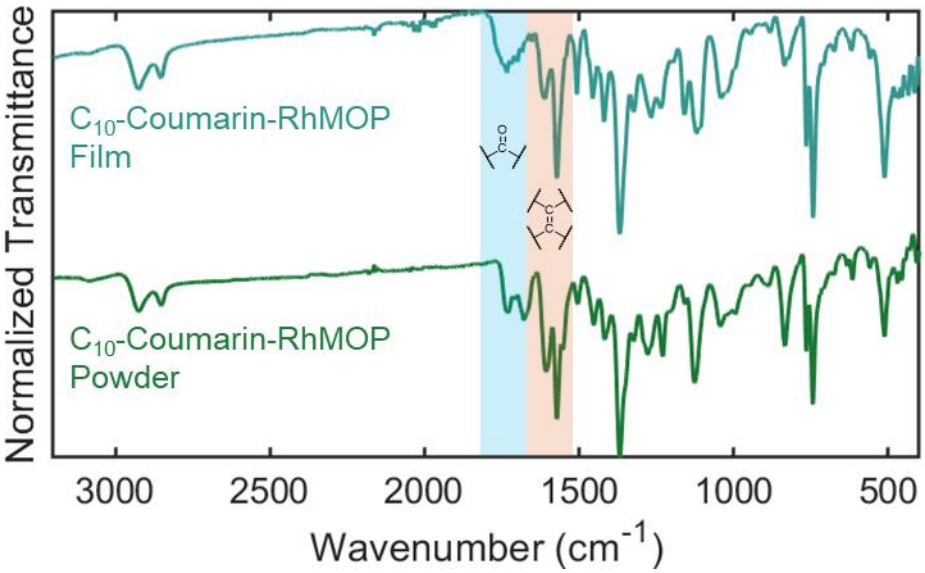

Figure S35. IR spectra of pristine C_{10}-Coumarin-RhMOP powder and a C_{10}-Coumarin-RhMOP thin film prepared via direct photoirradiation (350 nm, 10 mW/cm^2, 12 h) of a 20 mM DMF solution of the cage. The film exhibits a broadened C=O stretch (blue) and weakened C=C stretch (red) relative to the pristine powder, consistent with the formation of cyclobutane-based coumarin dimers upon photoirradiation.

5.6. UV-Vis Control Experiments and Photodimerization Quantum Yield Data

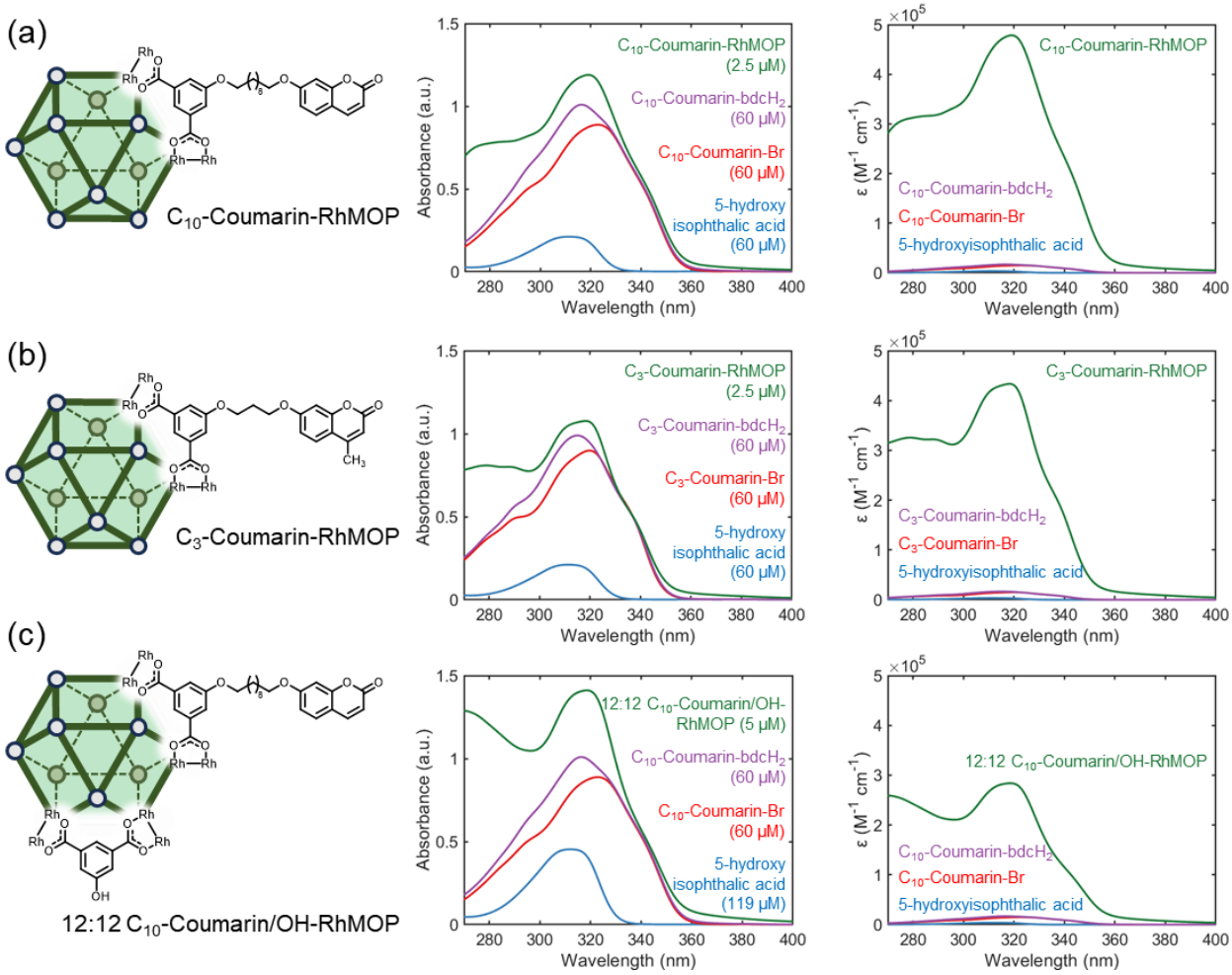

Figure S36. UV-Vis spectra of (a) C_{10}-Coumarin-RhMOP, (b) C_3-Coumarin-RhMOP, and (c) 12:12 C_{10}-Coumarin/OH-RhMOP, as well as representative constituent molecules (Coumarin-bdcH_2, Coumarin-Br, and 5-hydroxyisophthalic acid) at concentrations equivalent to those of the Coumarin-RhMOP solutions. Plots are provided as a function of both absorbance (left) and extinction coefficient (right). These data were used to calculate the absorbance contribution of the coumarin side chains themselves to the overall MOP absorbance at 320 nm (see sections **3.2.2** and **4.1** for details).

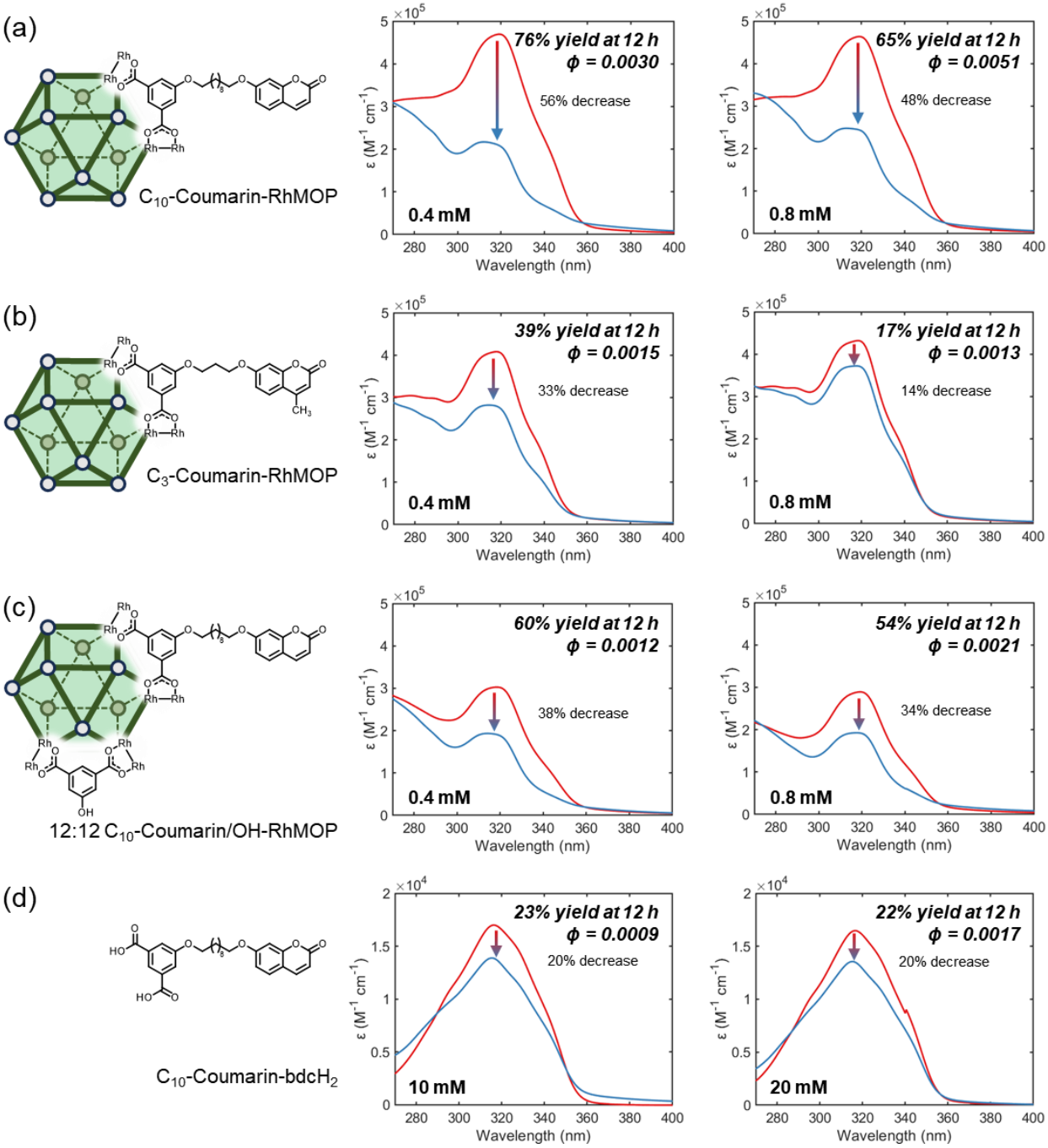

Figure S37. (a-c) UV-Vis spectra of (left) 0.4 mM and (right) 0.8 mM DMF solutions of (a) C_{10}-Coumarin-RhMOP, (b) C_3-Coumarin-RhMOP, and (c) 12:12 C_{10}-Coumarin/OH-RhMOP before (red) and after (blue) irradiation at 350 nm (10 mW/cm^2) for 12 h. (d) UV-Vis spectra of (left) 10 mM and (right) 20 mM DMF solutions of C_{10}-Coumarin-bdcH_2 before (red) and after (blue) irradiation at 350 nm (10 mW/cm^2) for 12 h. These data were used to calculate quantum yields for the photodimerization of free C_{10}-Coumarin-bdcH_2, as well as coumarin side chains attached to the surface of each cage (see sections **3.3.3** and **4.2** for details).

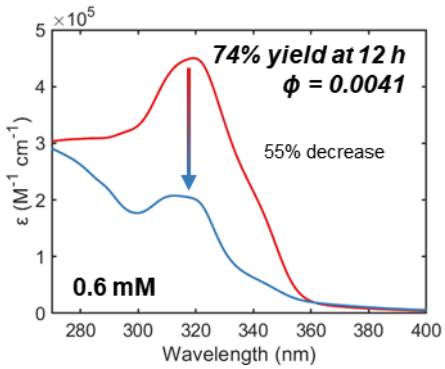

Figure S38. UV-Vis spectra of a 0.6 mM DMF solution of C_{10}-Coumarin-RhMOP before (red) and after (blue) irradiation at 350 nm (10 mW/cm^2) for 12 h. These data were used to calculate a quantum yield for the photodimerization of coumarin side chains on the surface of the cage (see sections **3.3.3** and **4.2** for details).

5.7. C_{10}-Coumarin-RhMOP Gel and Aerogel Characterization Data

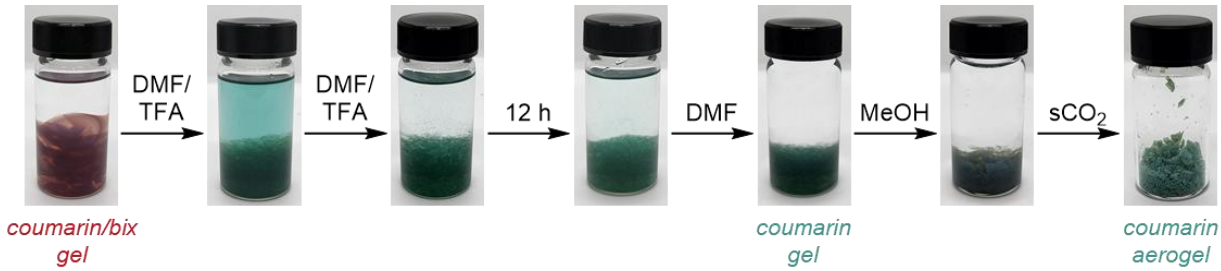

Figure S39. Photographs of each step of the coumarin gel workup procedure.

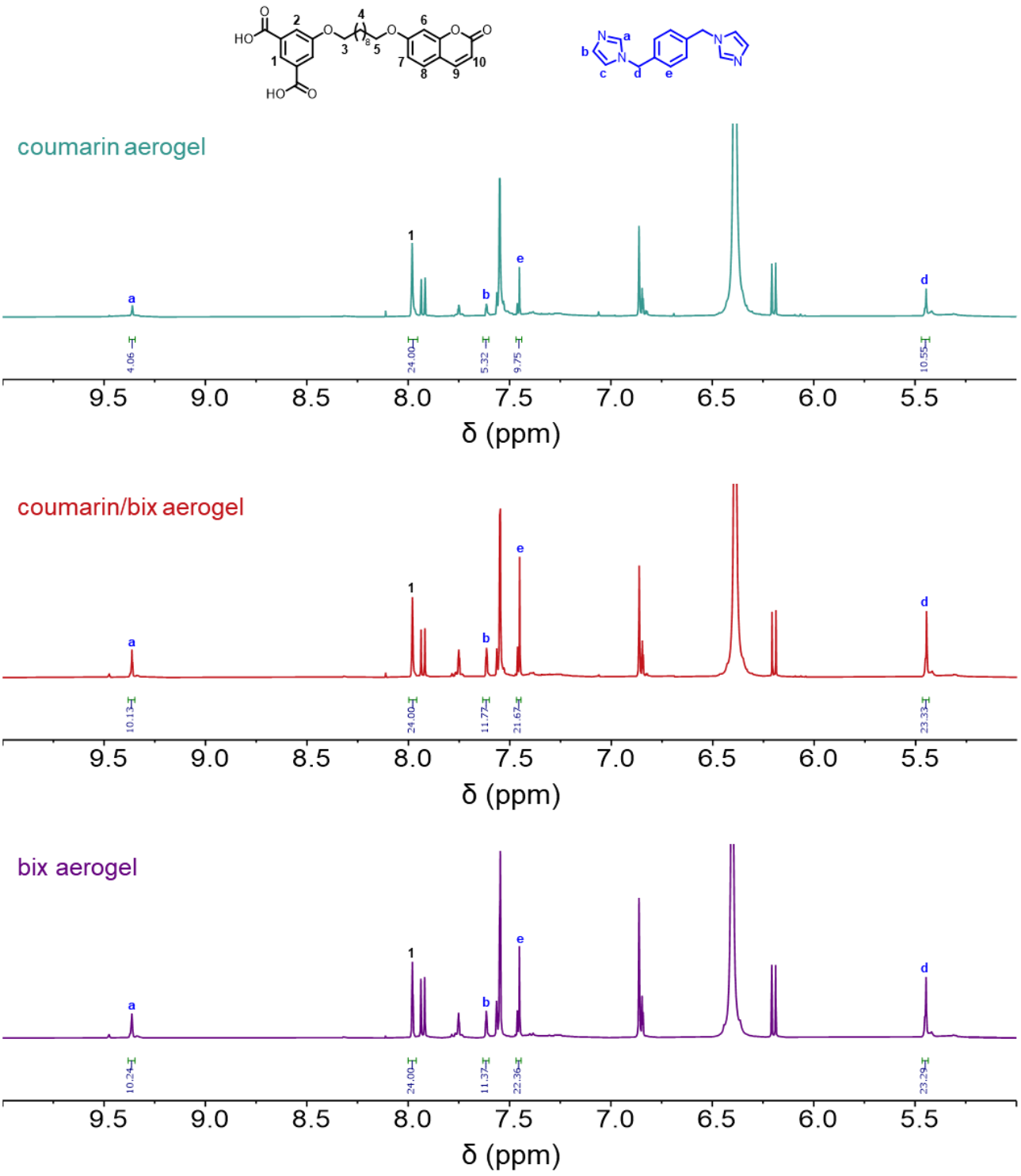

Figure S40. ^{1}H NMR spectra (500 MHz, 298 K) of bix aerogel, coumarin/bix aerogel, and coumarin aerogel samples decomposed by heating at 100 ºC in a mixture of DMSO-d_6, D_2O, and DCl for 1 h. Relative integrations of peaks corresponding to C_{10}-Coumarin-bdcH_2 and bix reveal the MOP:bix ratio for each material (see section **4.3** for details).

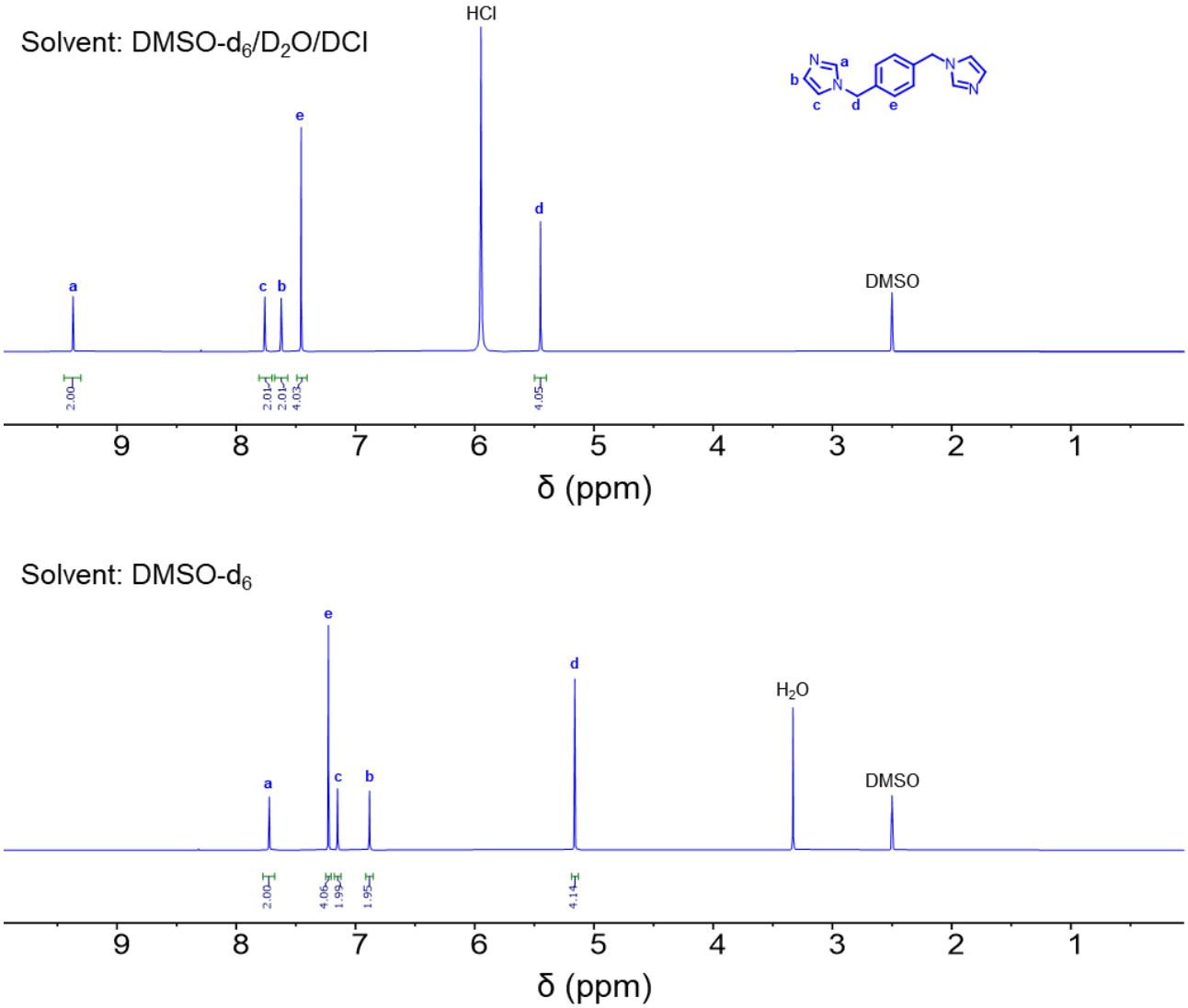

Figure S41. Assigned ^{1}H NMR spectra (500 MHz, 298 K) of bix in DMSO-d_6 (bottom) and a mixture of 600 µL DMSO-d_6 and 50 µL 35% DCl in D_2O (top).

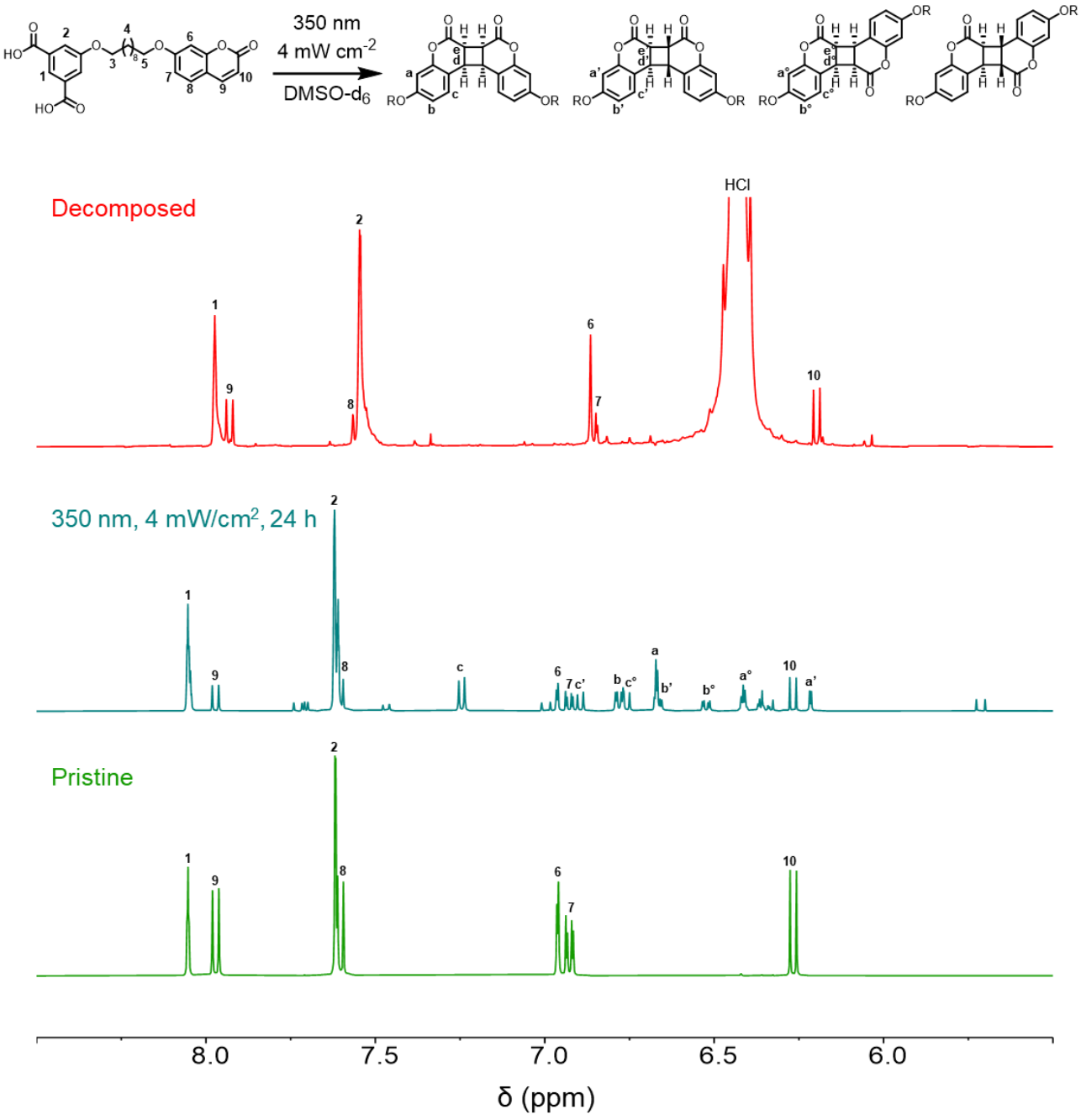

Figure S42. ^{1}H NMR spectra (500 MHz, 298 K) of a 10 mM DMSO-d_6 solution of C_{10}-Coumarin-bdcH_2 before (green) and after (teal) irradiation at 350 nm (4 mW/cm^2) for 24 h, resulting in the formation of cyclobutane-based coumarin dimers. A 600 µL aliquot of the dimer solution was mixed with 50 µL of 35% DCl in D_2O, then heated at 100 ºC for 1 h and remeasured (red), revealing the near-complete disappearance of all coumarin dimer signals. These experiments indicate that the MOP decomposition protocol employed in this work also results in the degradation of the coumarin dimers.

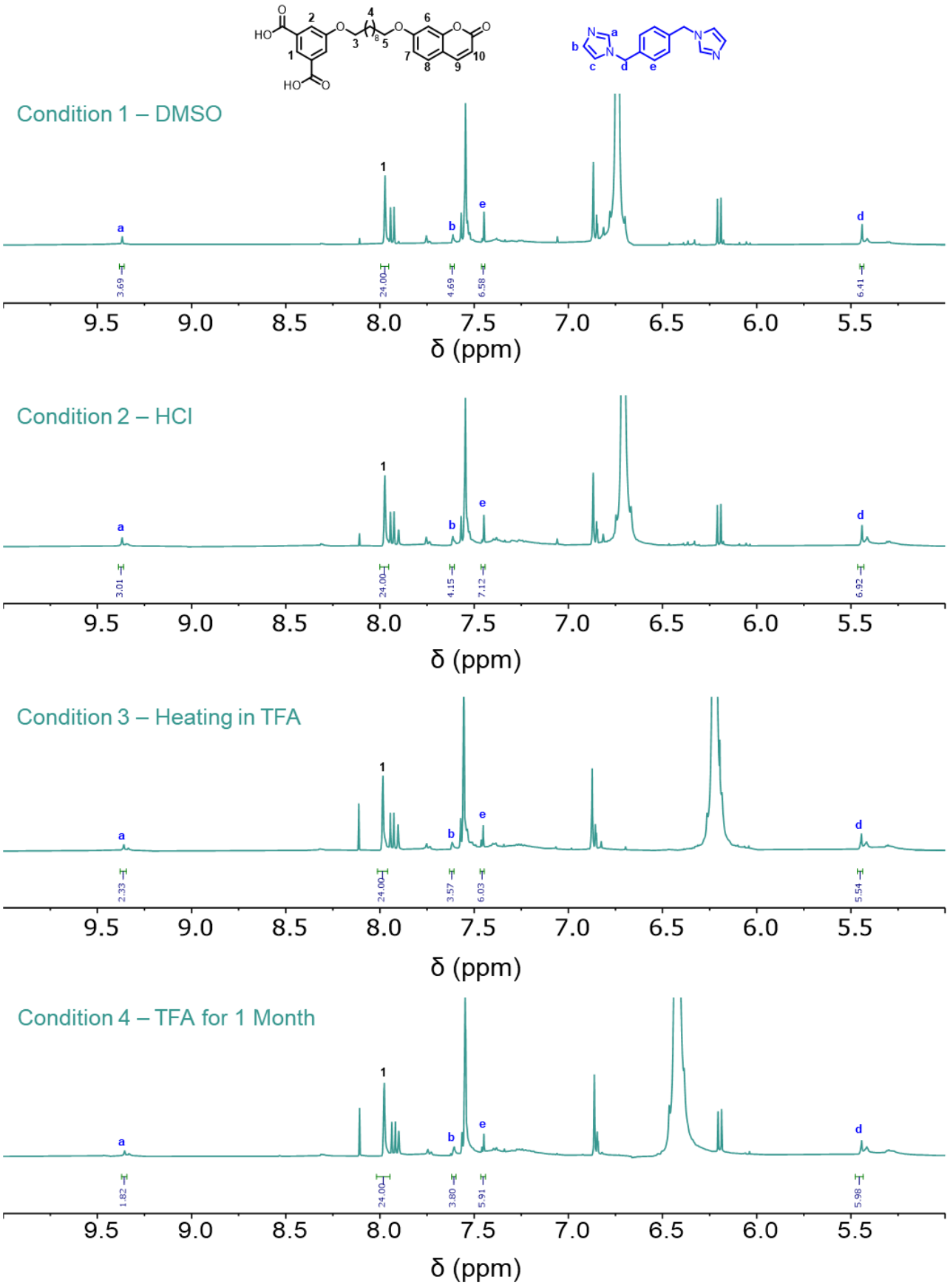

Figure S43. [1]H NMR spectra (500 MHz, 298 K) of degraded coumarin gel and aerogel samples prepared via the harsh bix dissociation conditions described in section **2.3.8**. In each case, signals corresponding to bix were still observed.

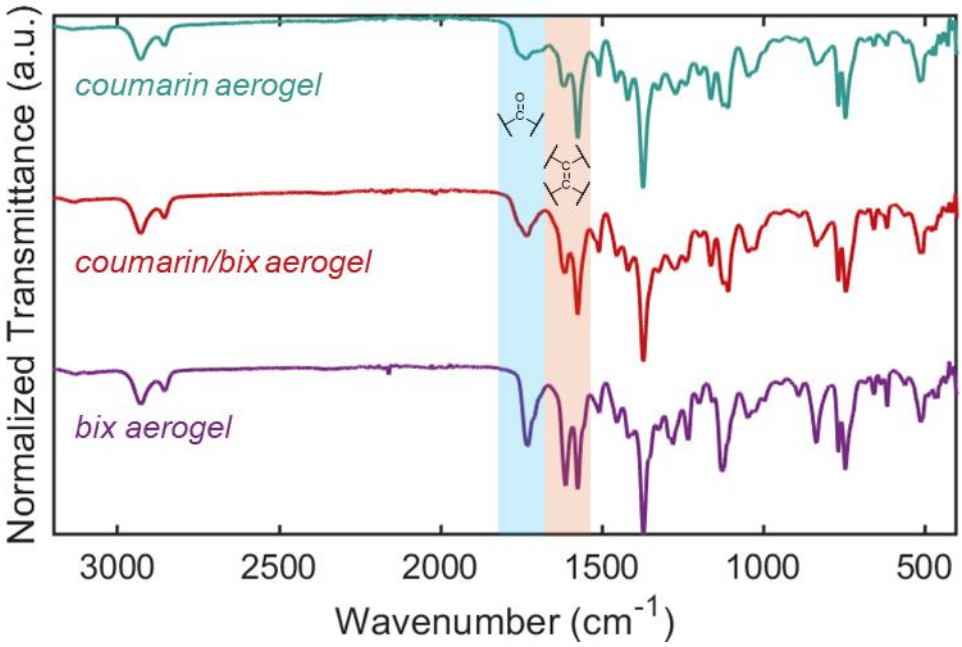

Figure S44. IR spectra of bix aerogel (purple), coumarin/bix aerogel (red), and coumarin aerogel (teal). Both coumarin/bix and coumarin aerogels exhibit broadened C=O stretches (blue) and weakened C=C stretches (red) relative to bix gel, indicating that cyclobutane-based coumarin dimers are formed upon irradiation.

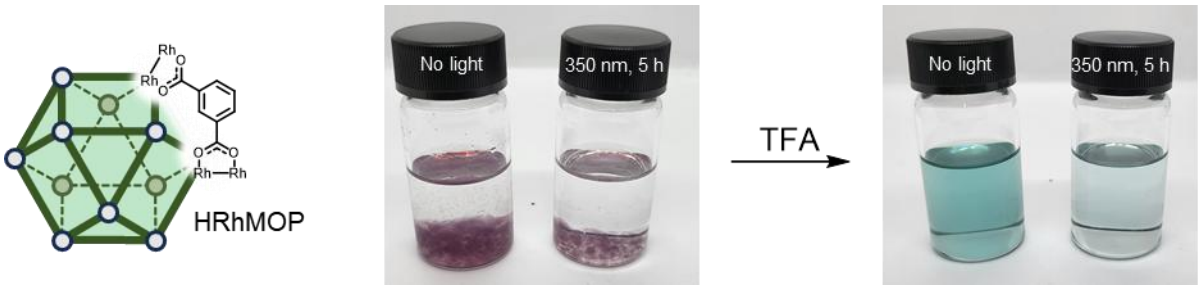

Figure S45. Samples of pristine HRhMOP/bix gel (no light) and the same gel after irradiation at 350 nm (4 mW/cm^2) for 5 h were treated with TFA, after which both materials immediately dissolved.

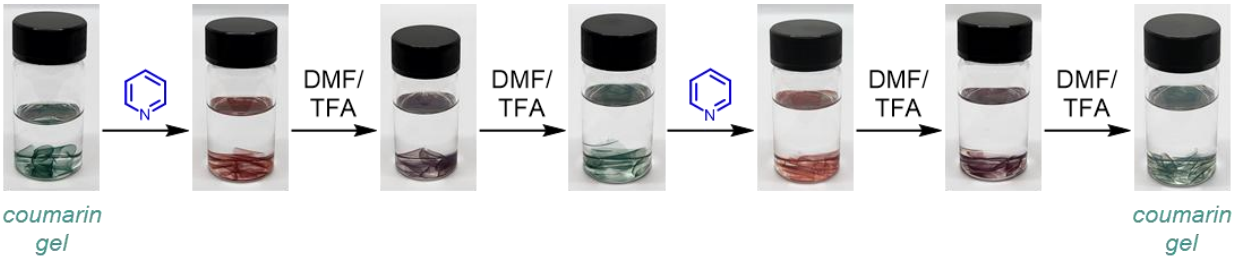

Figure S46. Addition of pyridine (blue) to a sample of coumarin gel, followed by washes with a mixture of DMF (10 mL) and TFA (1 mL), facilitates of the reversible functionalization of the gel's open metal sites, as indicated by the reversible change in color from green to red.

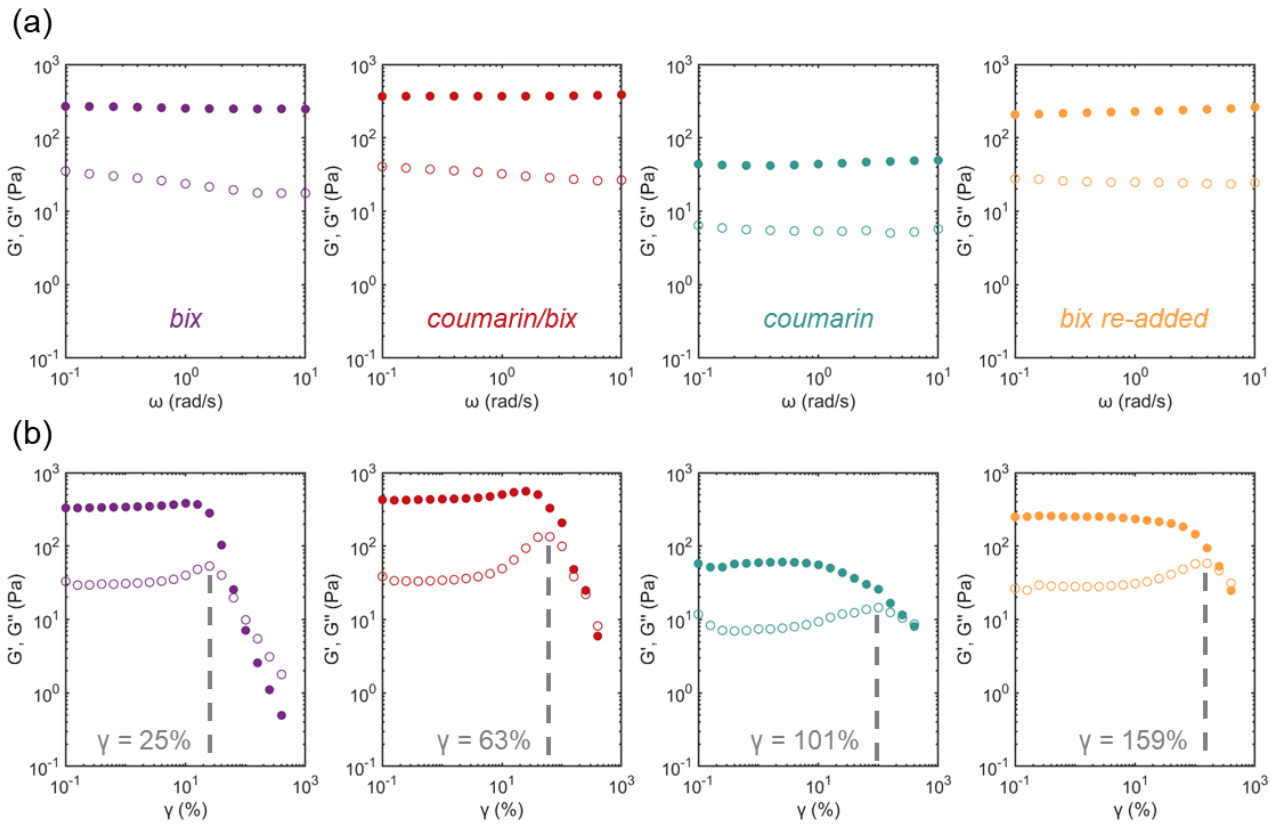

Figure S47. (a) Frequency sweep measurements for bix, coumarin/bix, coumarin, and bix-readded gels in DMF after compression reveal an increase in their storage and loss moduli relative to the pristine, uncompressed samples (**Figure 5a**). In all cases, the storage moduli are frequency independent and approximately one order of magnitude larger than the loss moduli, indicating that the networks were not fractured during compression. (b) Strain amplitude sweep measurements for the four gels reveal the onset of fracture for each gel, as indicated by the grey line in each plot. After the measurements, the gels were each found to exhibit a rough surface texture, with some visible cracks or tears along their edges, though the core of each circular gel disc appeared to remain largely intact.

5.8. ^{1}H NMR Spectra of Reported Compounds

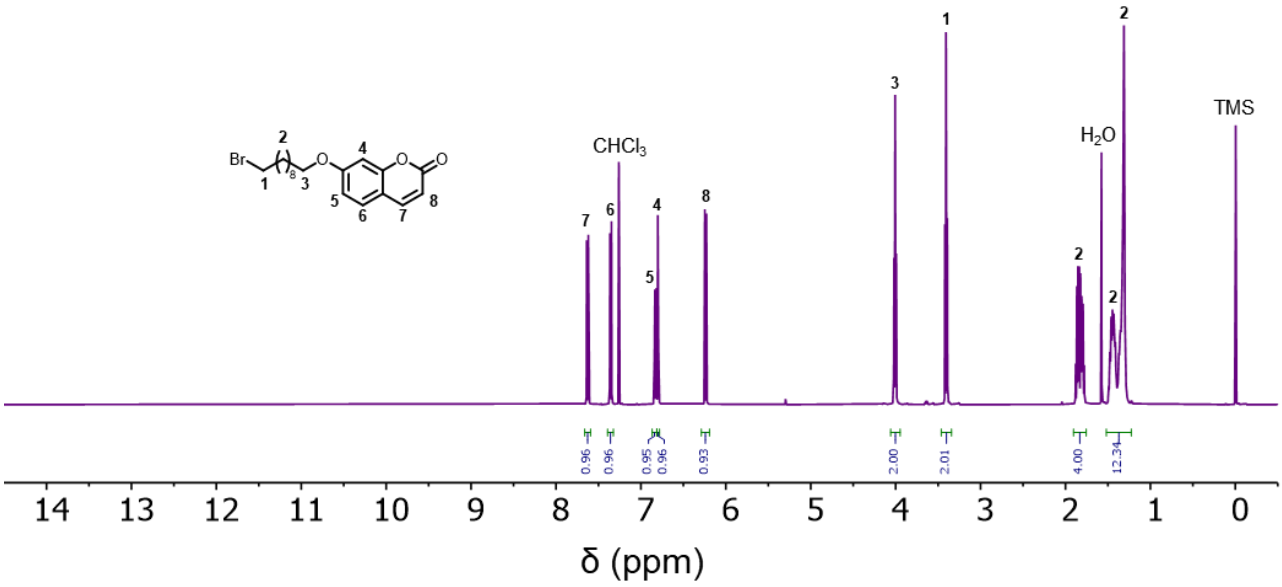

Figure S48. ^{1}H NMR spectrum ($CDCl_3$, 500 MHz, 298 K) of compound **1**.

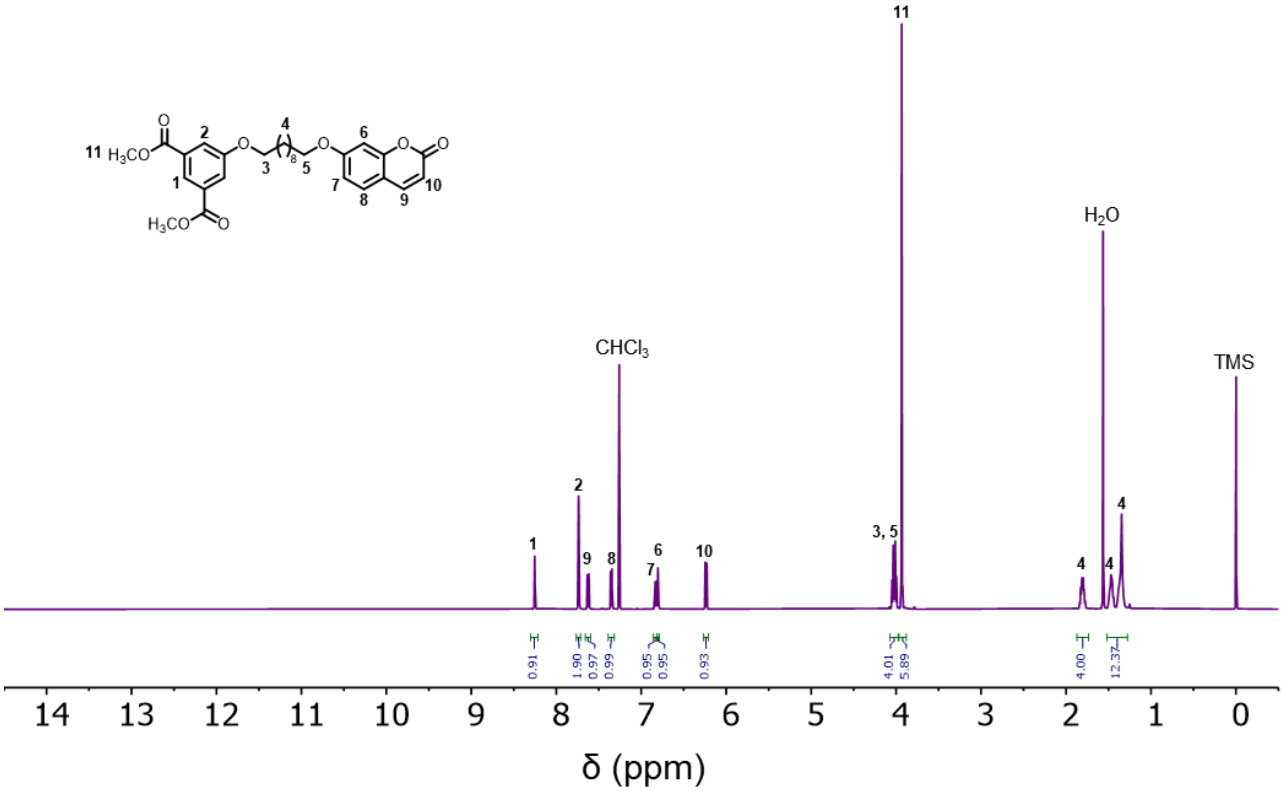

Figure S49. ^{1}H NMR spectrum ($CDCl_3$, 500 MHz, 298 K) of compound **2**.

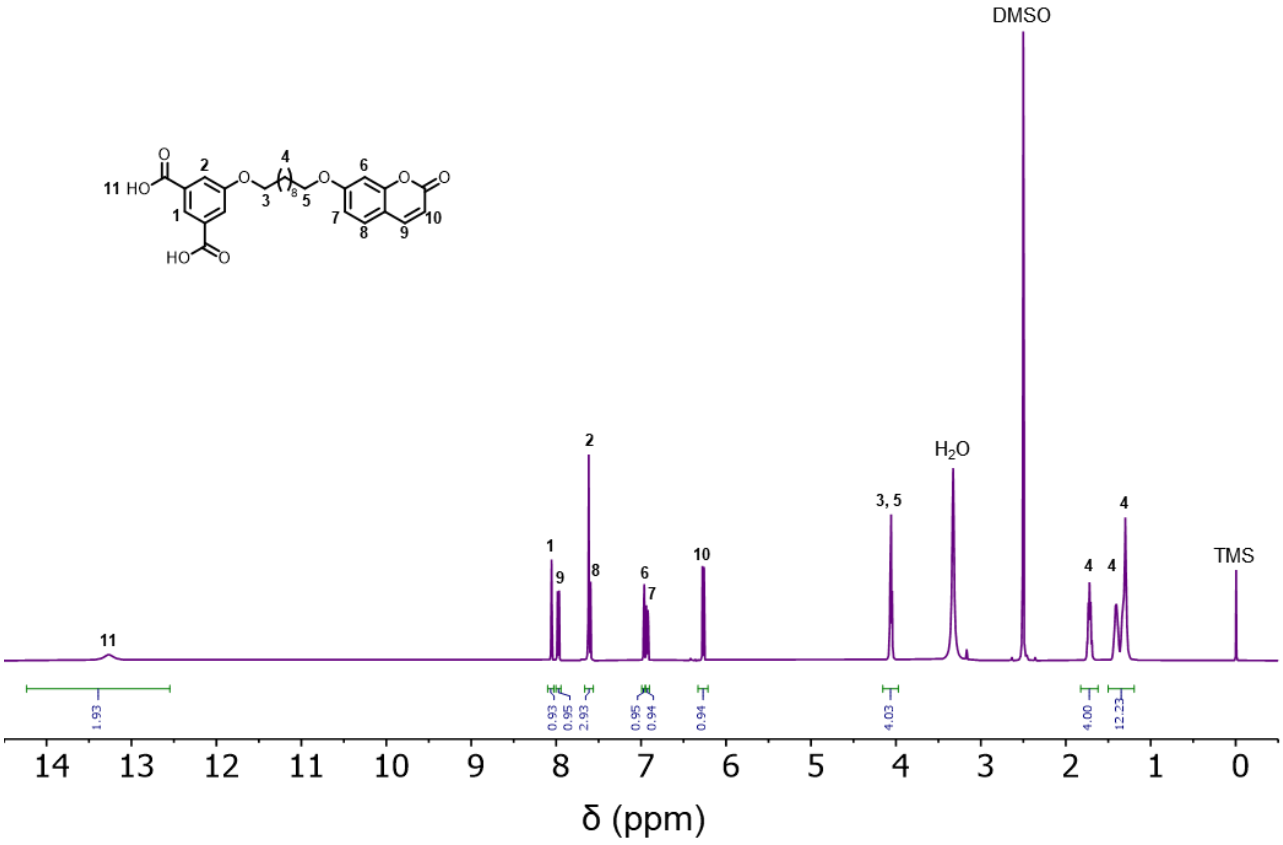

Figure S50. ^{1}H NMR spectrum (DMSO-d_6, 500 MHz, 298 K) of compound **3** (C_{10}-Coumarin-bdcH_2).

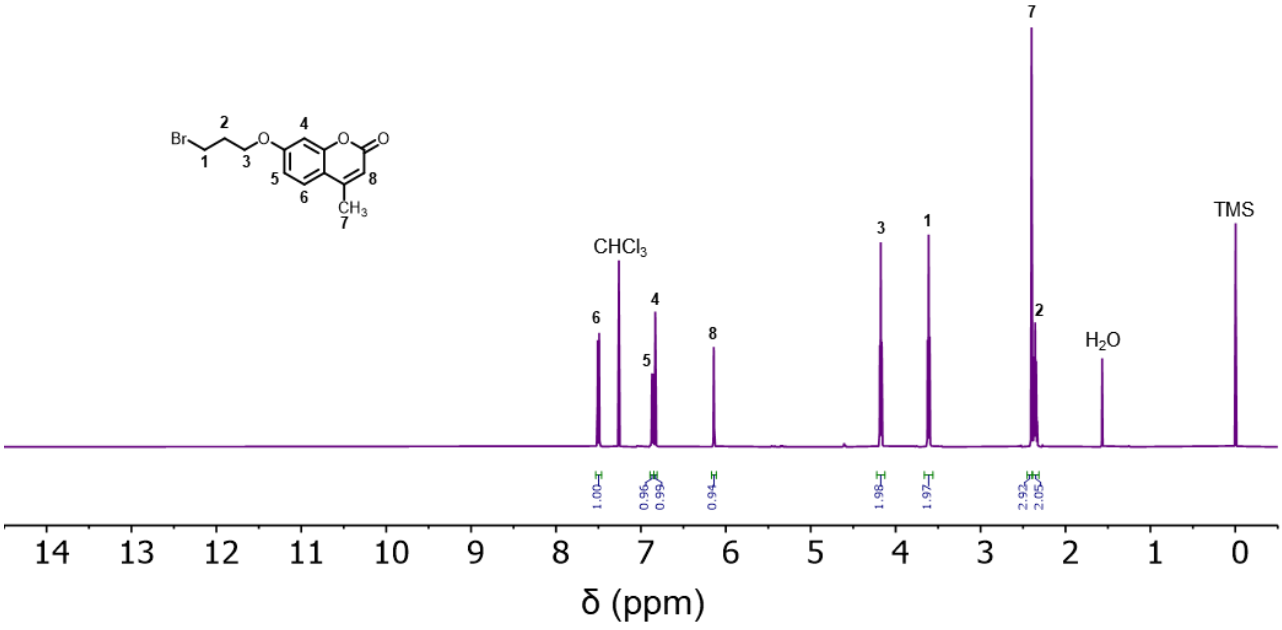

Figure S51. ^{1}H NMR spectrum ($CDCl_3$, 500 MHz, 298 K) of compound **4**.

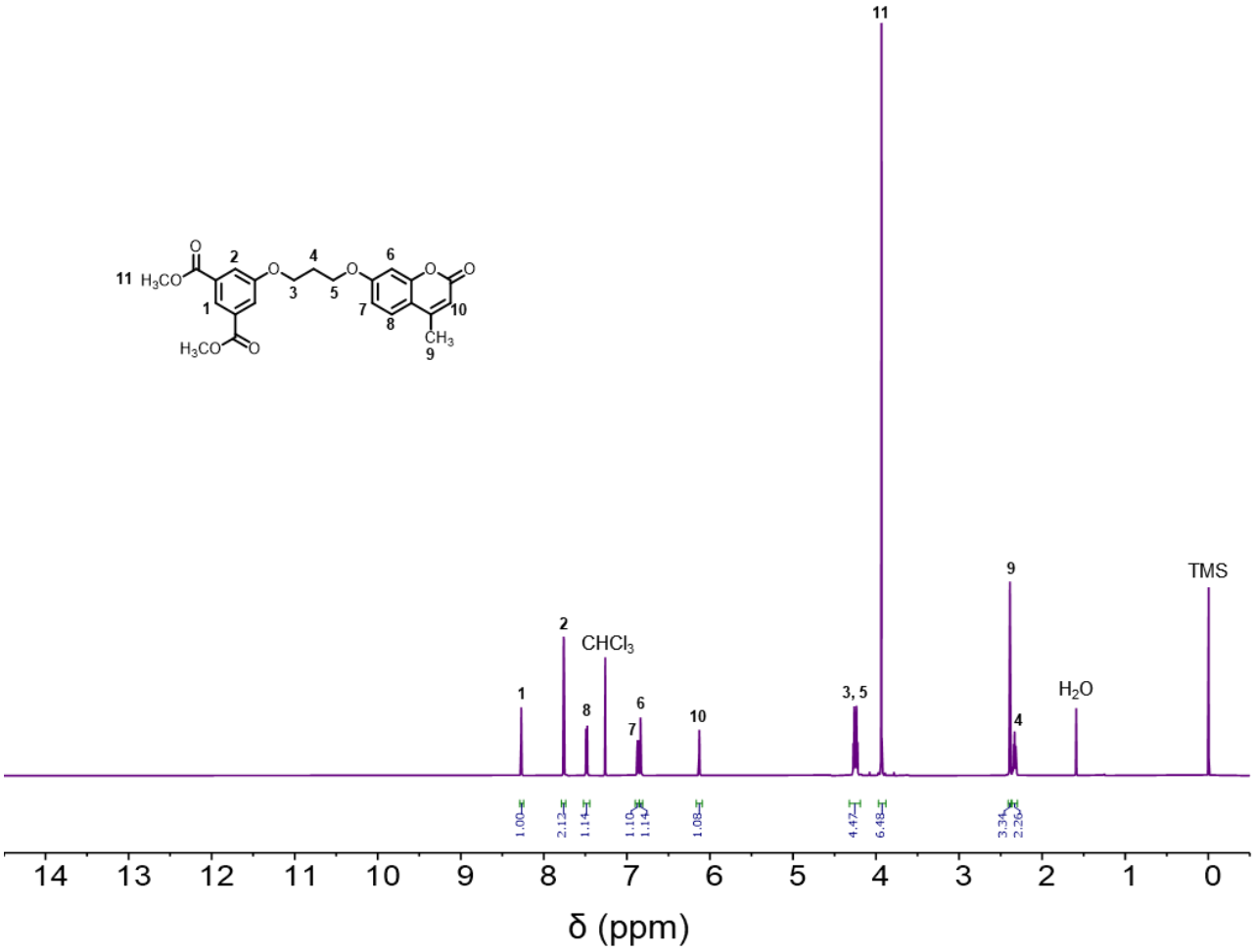

Figure S52. ^{1}H NMR spectrum ($CDCl_3$, 500 MHz, 298 K) of compound **5**.

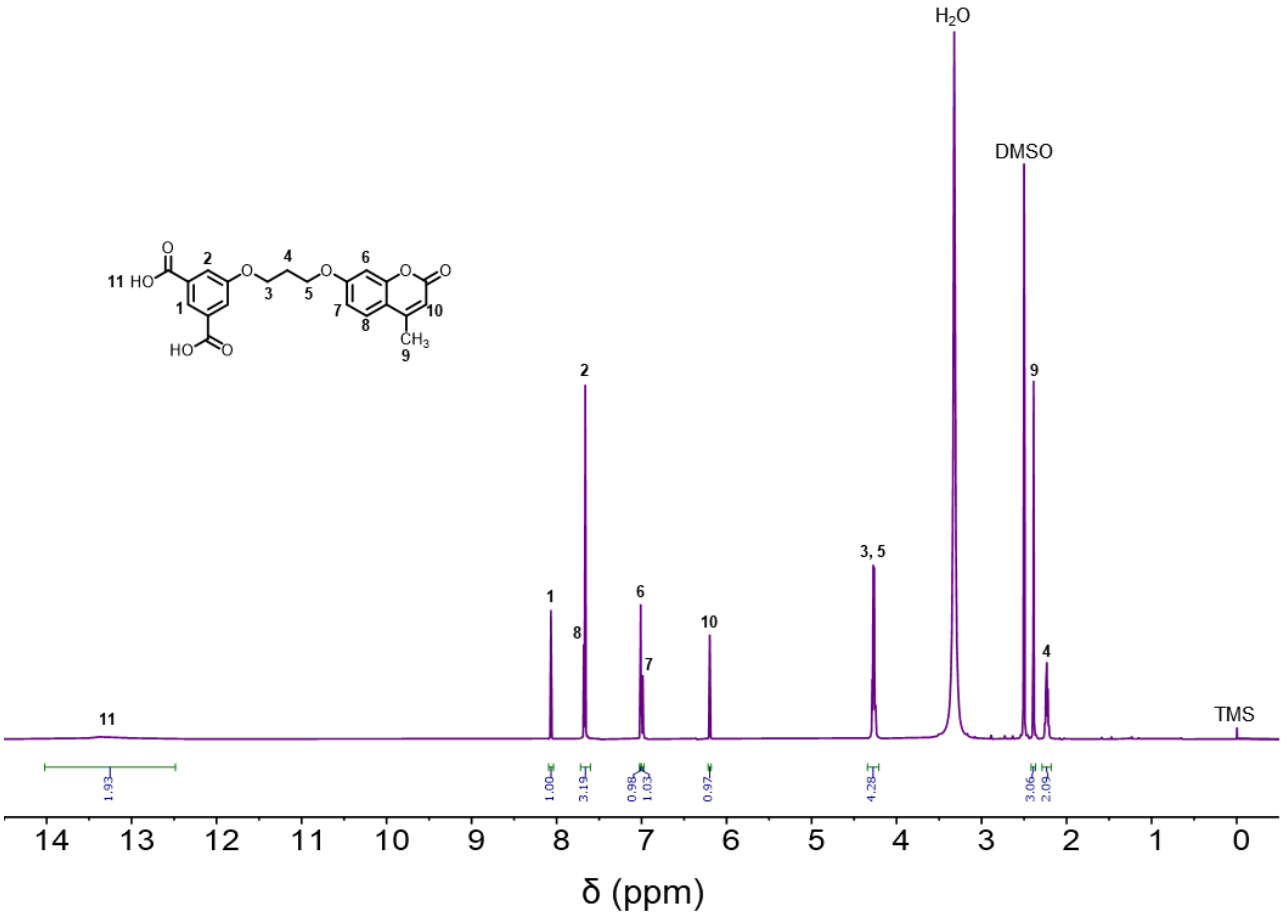

Figure S53. ^{1}H NMR spectrum (DMSO-d_6, 500 MHz, 298 K) of compound **6** (C_3-Coumarin-bdcH_2).

5.9. ^{13}C NMR Spectra of Reported Compounds

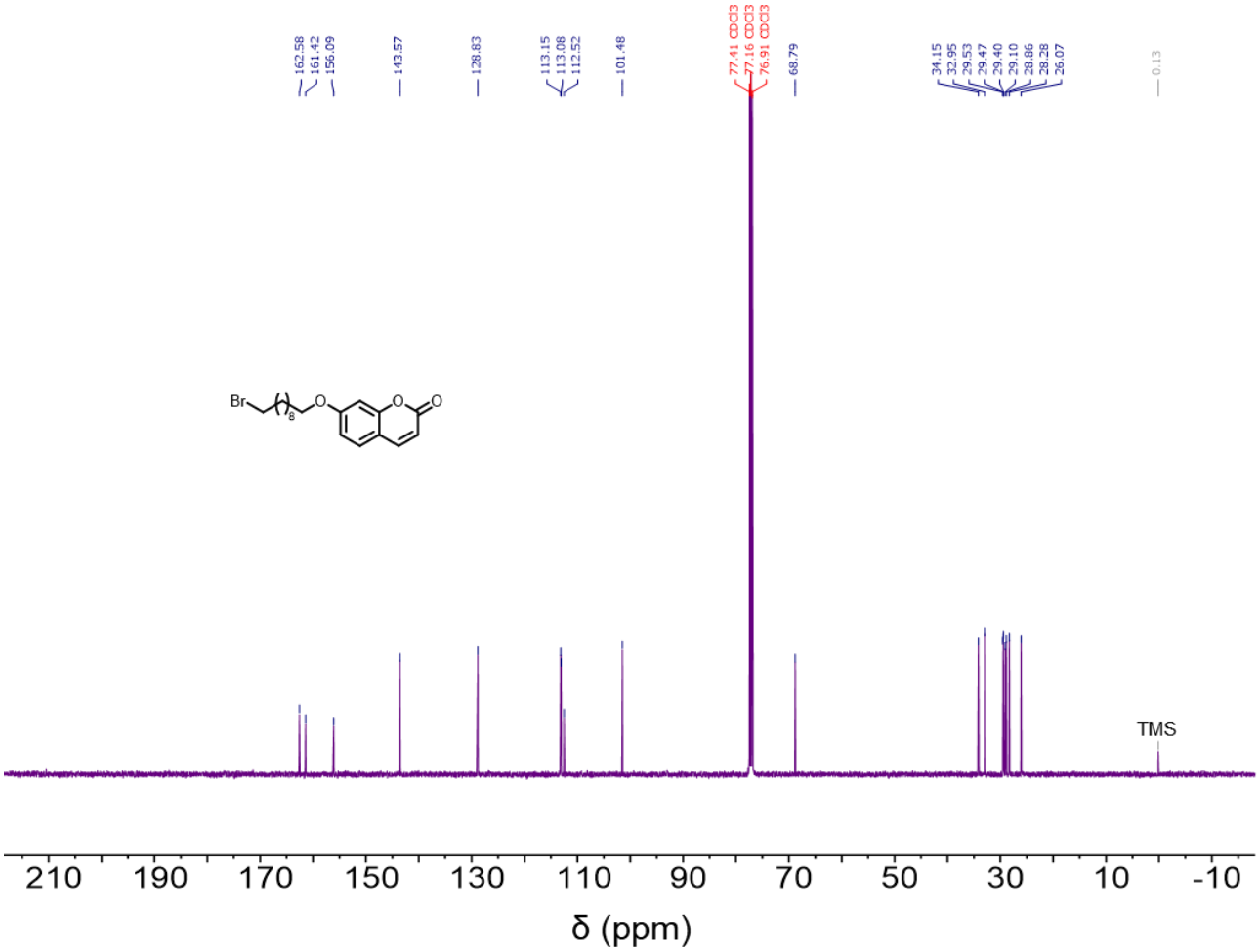

Figure S54. ^{13}C NMR spectrum ($CDCl_3$, 125 MHz, 298 K) of compound **1**.

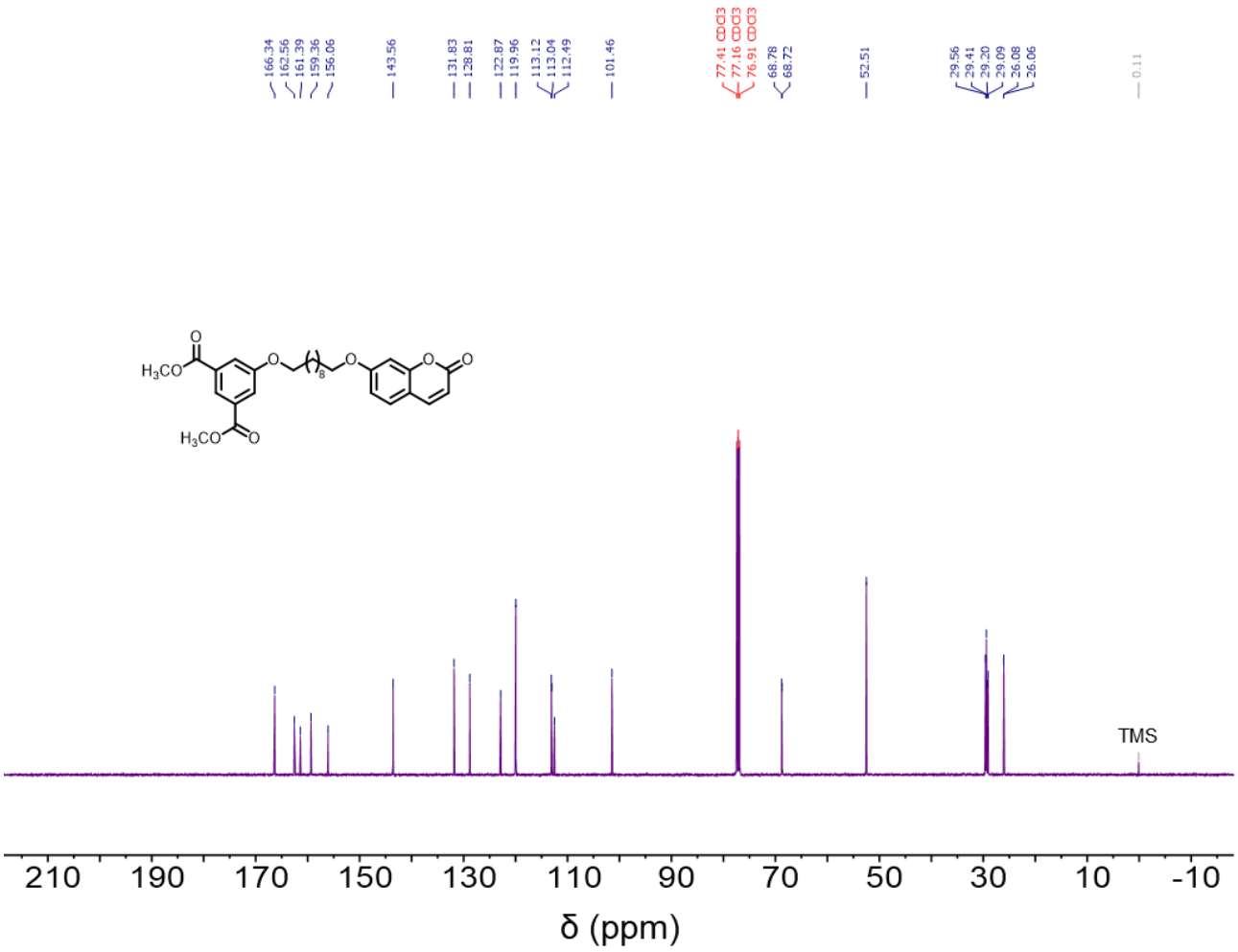

Figure S55. ^{13}C NMR spectrum ($CDCl_3$, 125 MHz, 298 K) of compound **2**.

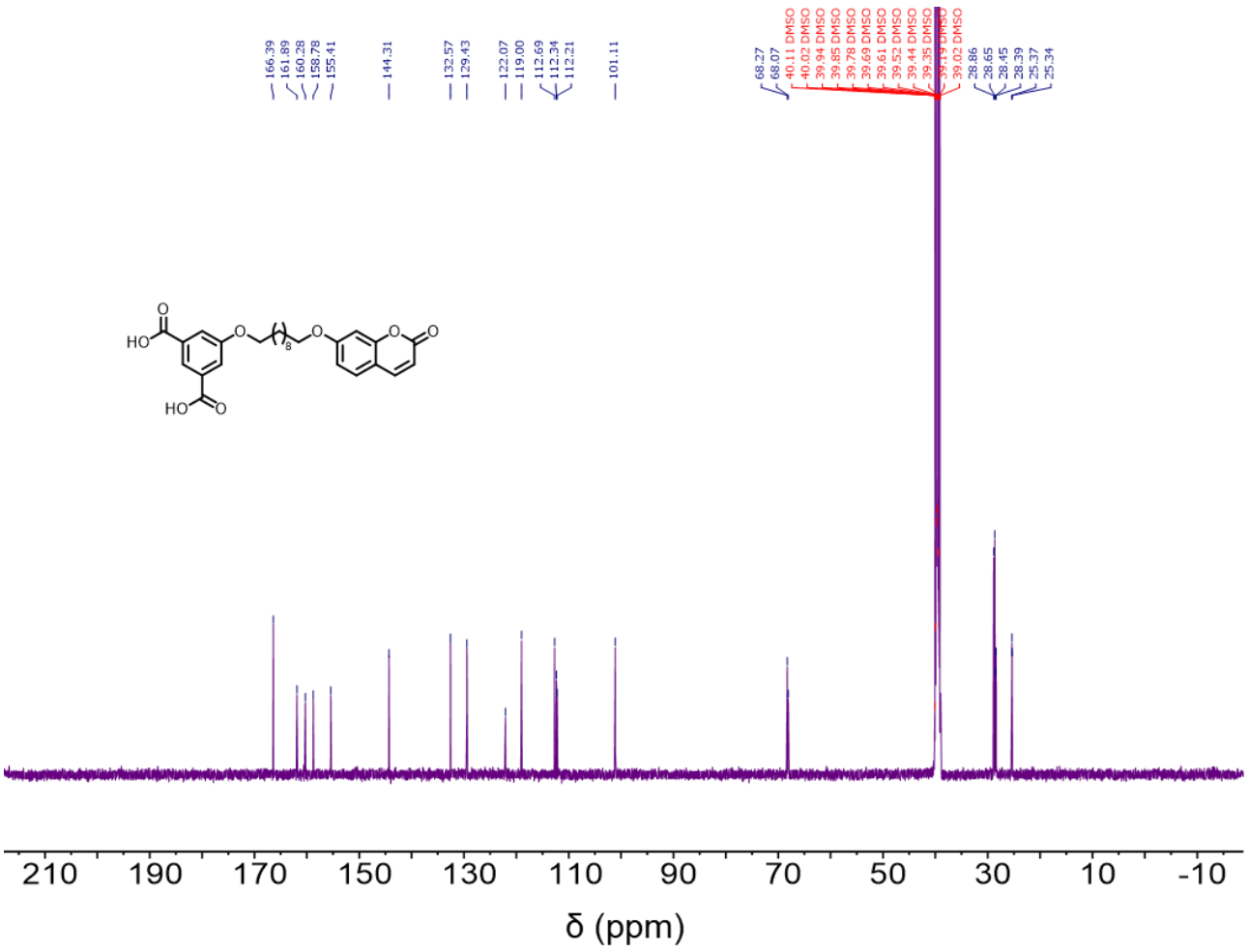

Figure S56. ^{13}C NMR spectrum (DMSO-d_6, 125 MHz, 298 K) of compound **3** (C_{10}-Coumarin-bdcH_2).

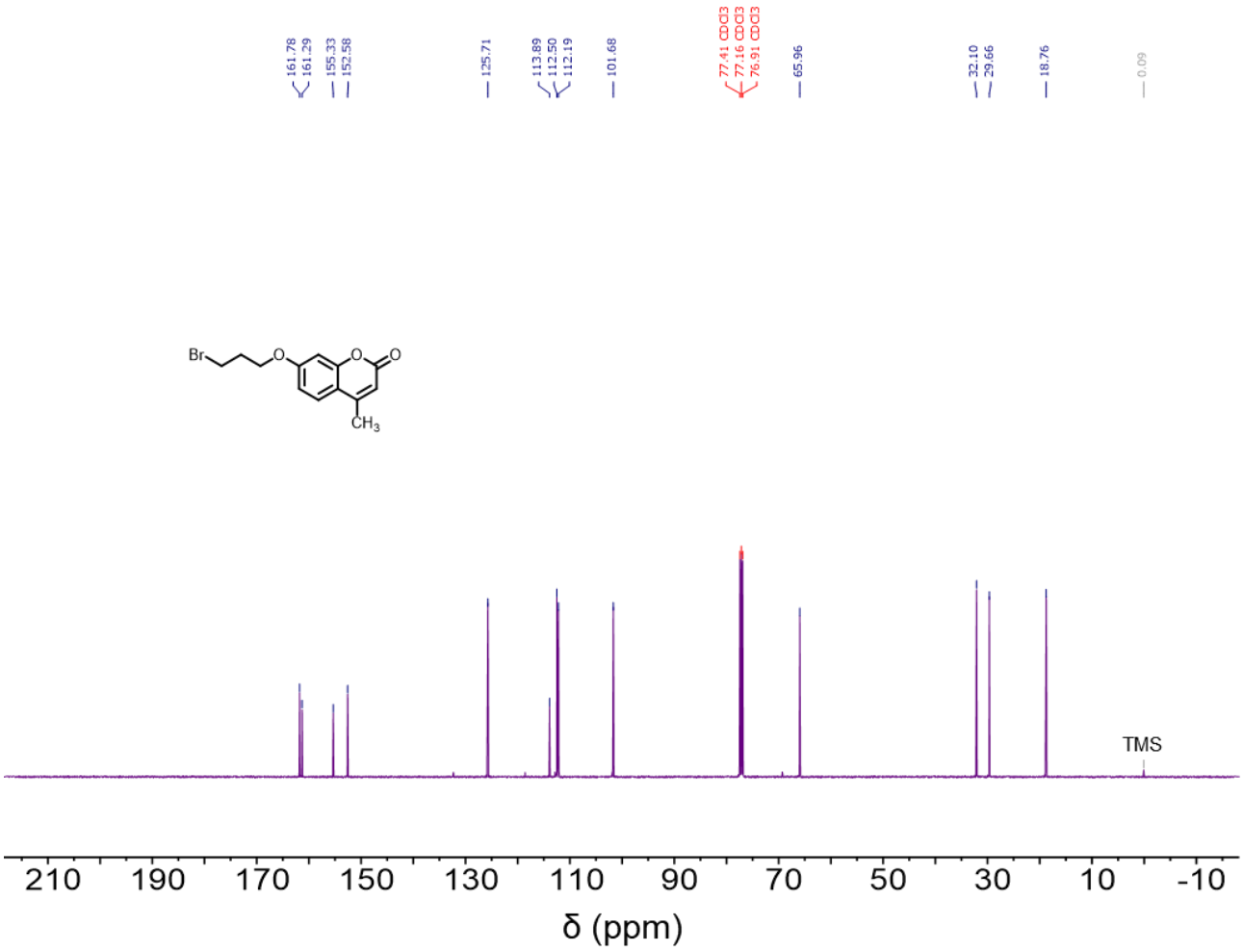

Figure S57. ^{13}C NMR spectrum ($CDCl_3$, 125 MHz, 298 K) of compound **4**.

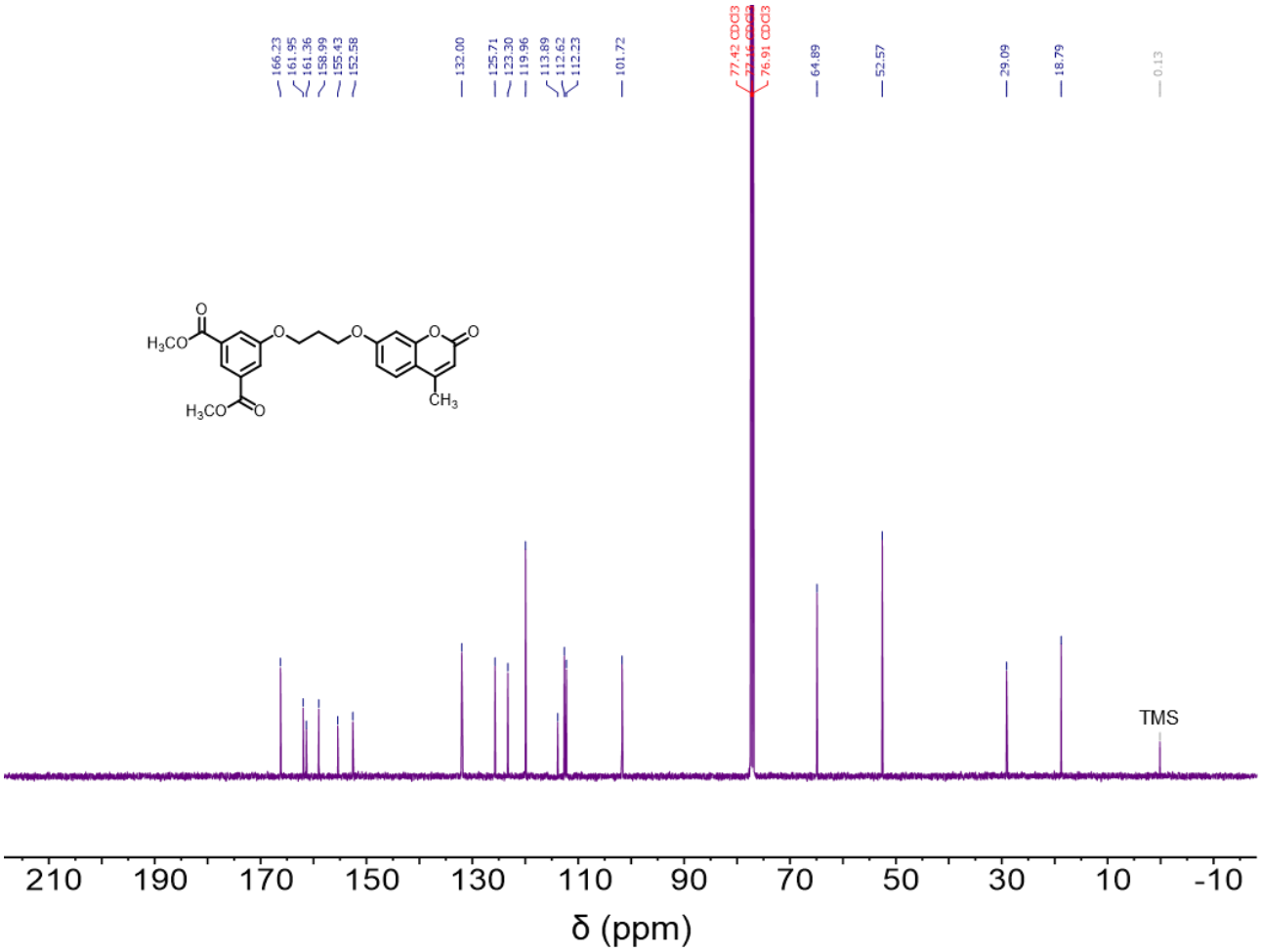

Figure S58. ^{13}C NMR spectrum ($CDCl_3$, 125 MHz, 298 K) of compound **5**.

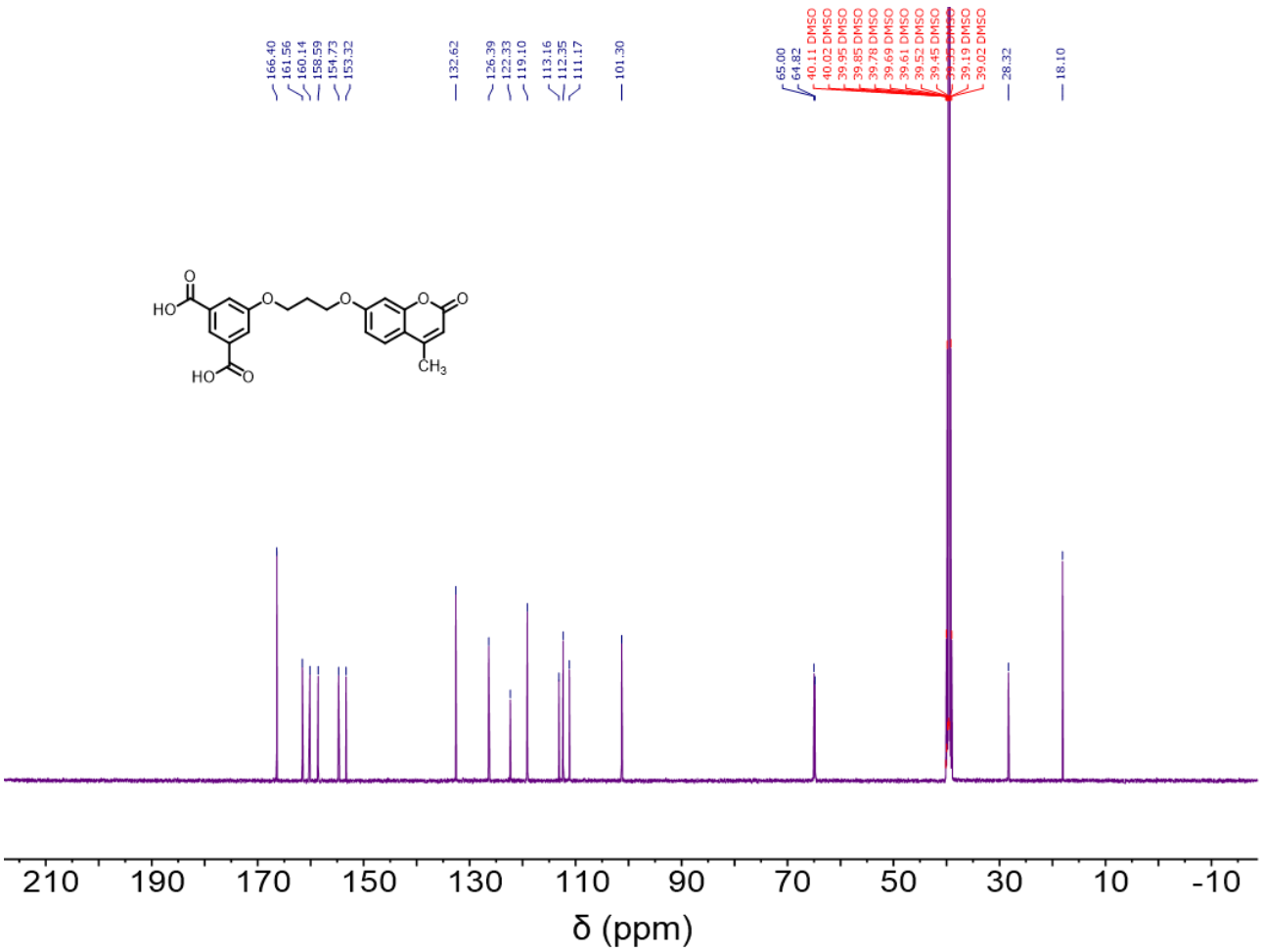

Figure S59. ^{13}C NMR spectrum (DMSO-d_6, 125 MHz, 298 K) of compound **6** (C_3-Coumarin-bdcH_2).

5.10. High-Resolution Mass Spectrometry Data for Reported Compounds

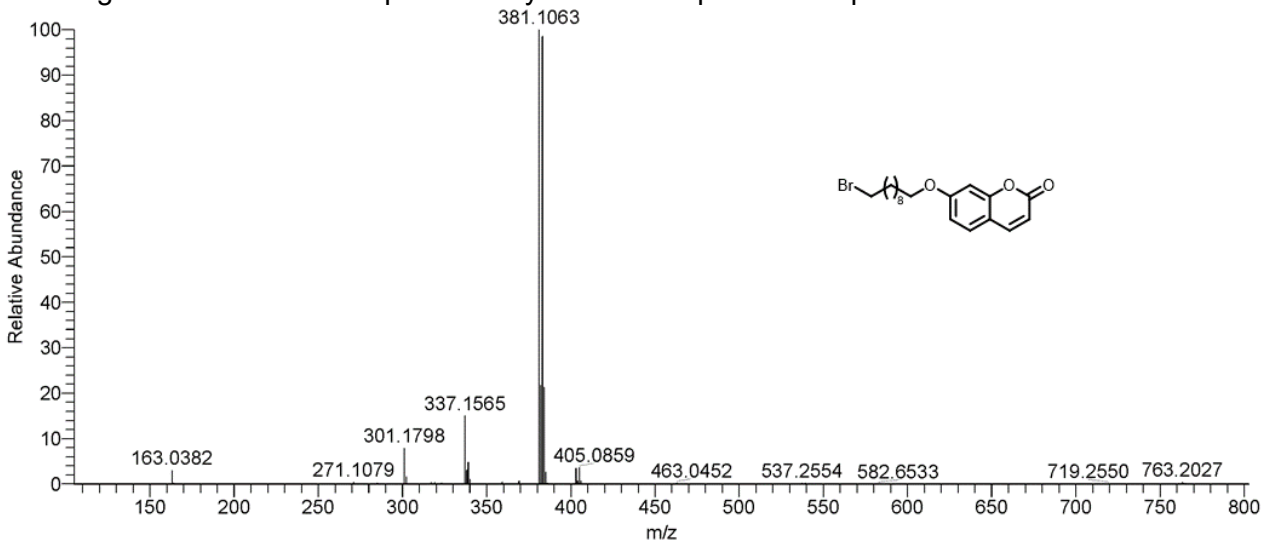

Figure S60. HRMS (APCI, positive mode) data for compound **1**. A clear signal corresponding to the $[M+H]^+$ adduct of the targeted compound is observed (calculated: 381.1060; found: 381.1063).

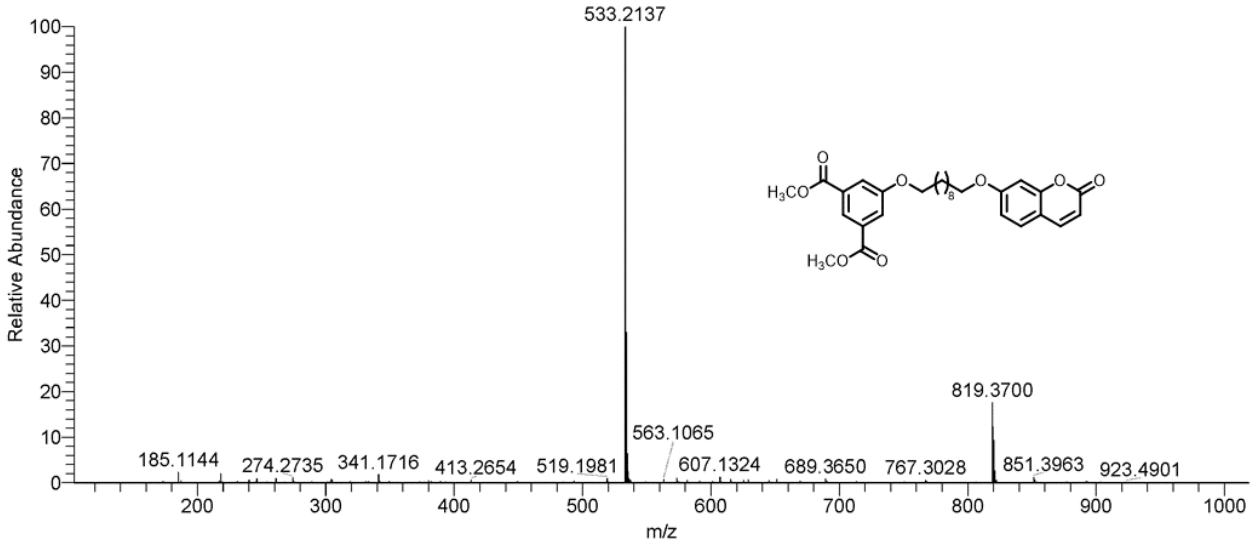

Figure S61. HRMS (ESI, positive mode) data for compound **2**. A clear signal corresponding to the $[M+Na]^+$ adduct of the targeted compound is observed (calculated: 533.2146; found: 533.2137).

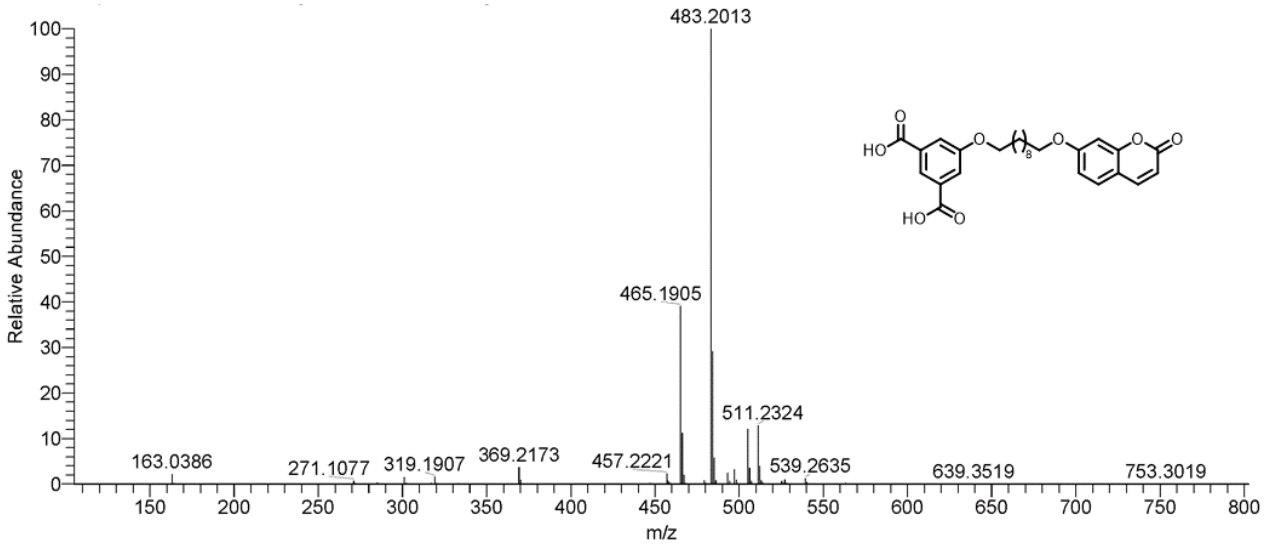

Figure S62. HRMS (APCI, positive mode) data for compound **3** (C_{10}-Coumarin-bdcH_2). A clear signal corresponding to the $[M+H]^+$ adduct of the targeted compound is observed (calculated: 483.2013; found: 483.2013).

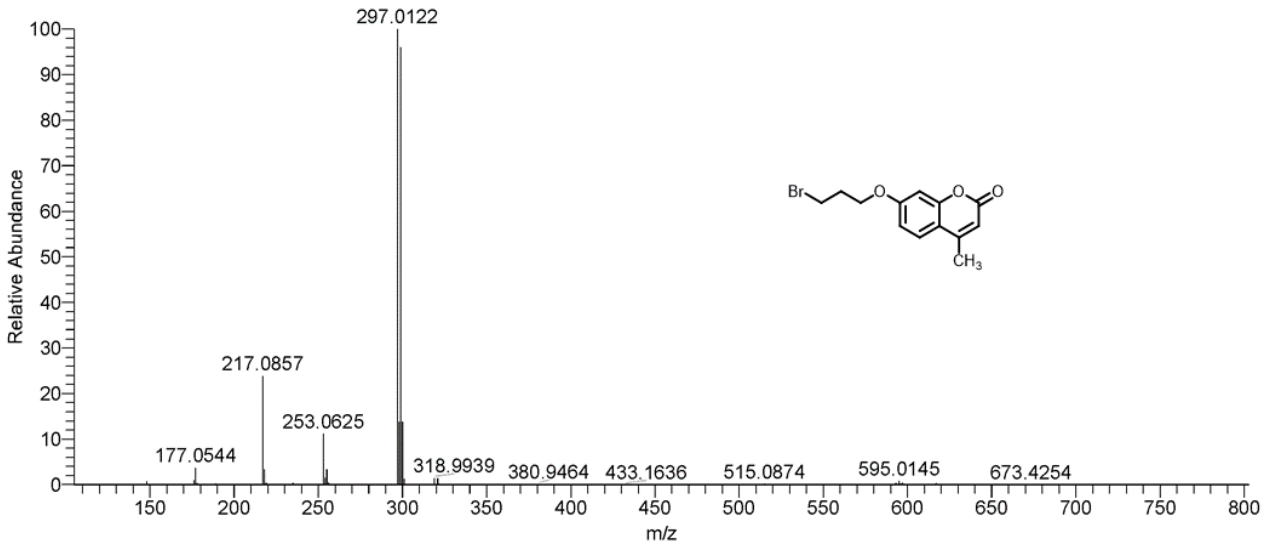

Figure S63. HRMS (APCI, positive mode) data for compound **4**. A clear signal corresponding to the $[M+H]^+$ adduct of the targeted compound is observed (calculated: 297.0121; found: 297.0122).

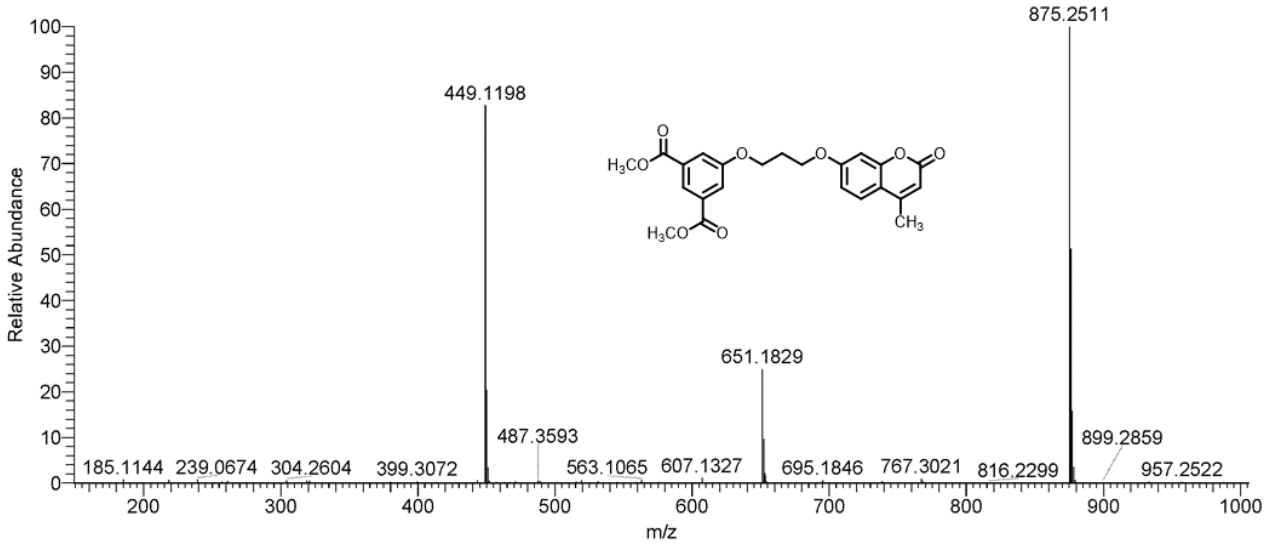

Figure S64. HRMS (ESI, positive mode) data for compound **5**. A clear signal corresponding to the $[M+Na]^+$ adduct of the targeted compound is observed (calculated: 449.1207; found: 449.1198).

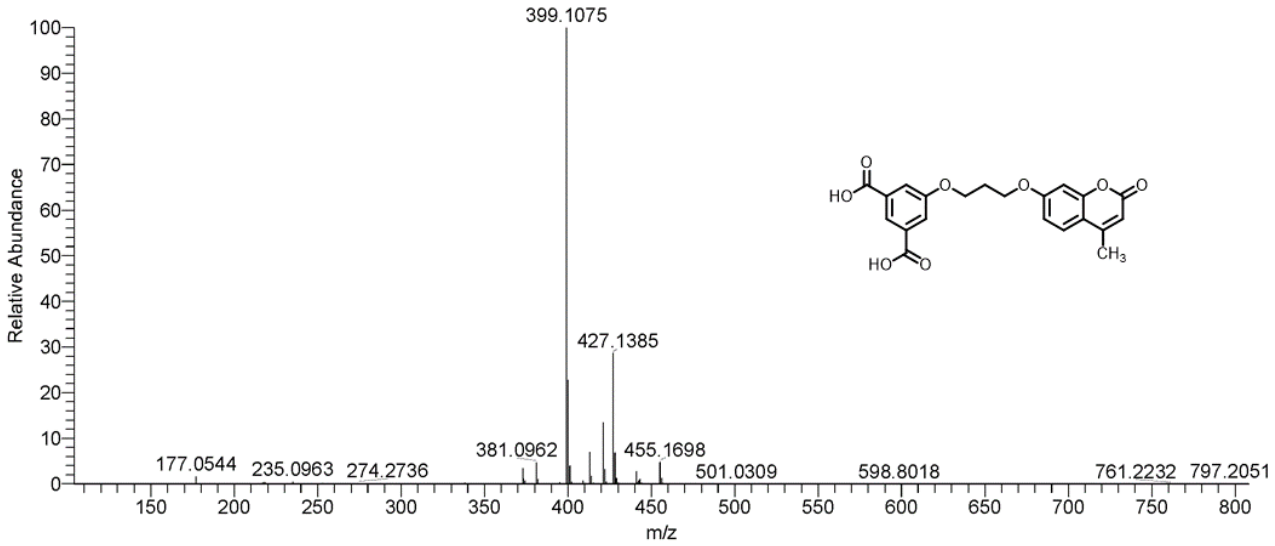

Figure S65. HRMS (APCI, positive mode) data for compound **6** (C_3-Coumarin-bdcH_2). A clear signal corresponding to the $[M+H]^+$ adduct of the targeted compound is observed (calculated: 399.1074; found: 399.1075).

5.11. BETSI Analysis of Aerogel Nitrogen Adsorption Isotherms

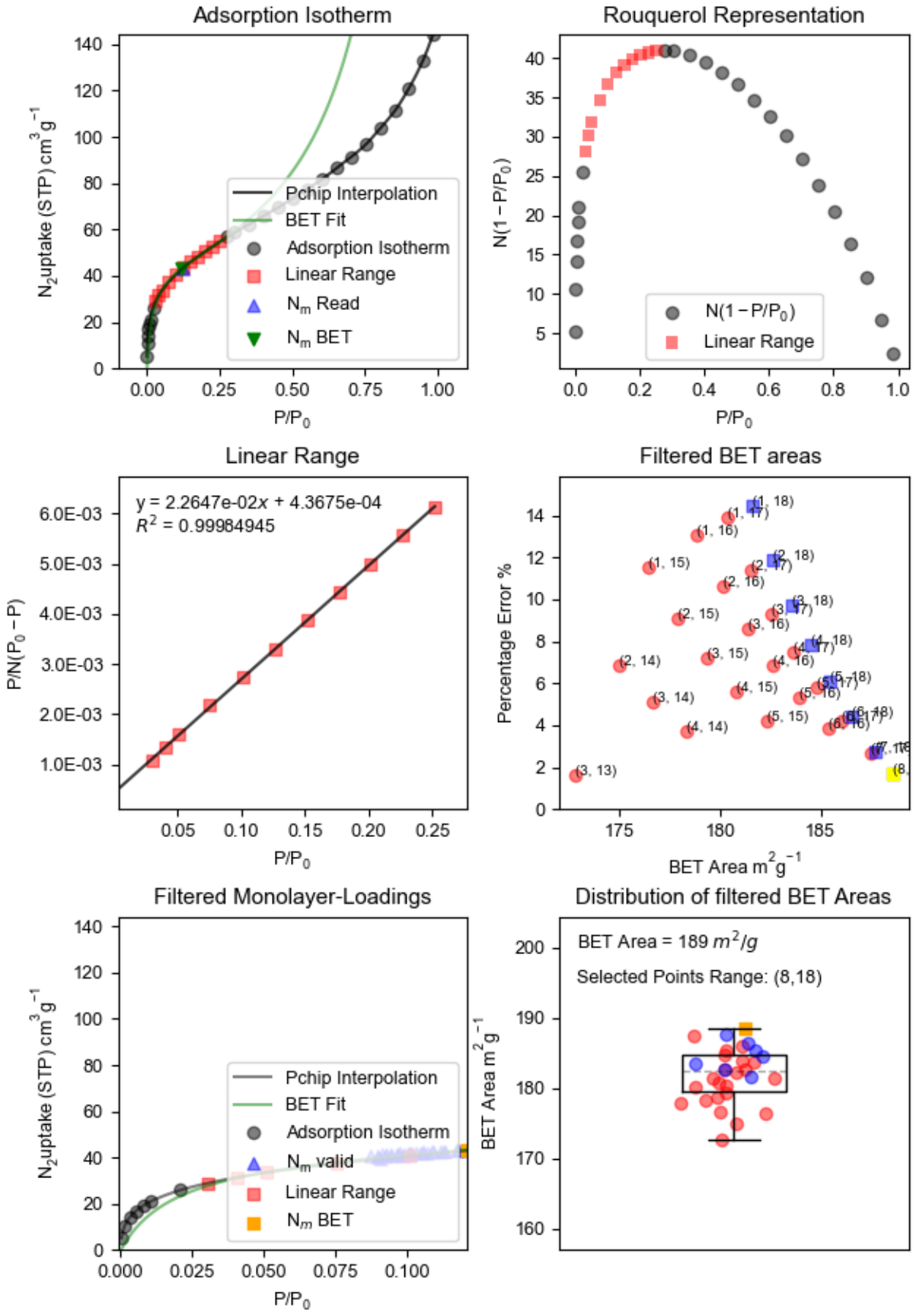

Figure S66. BETSI analysis of the bix aerogel N_2 adsorption isotherm presented in **Figure 5b**.

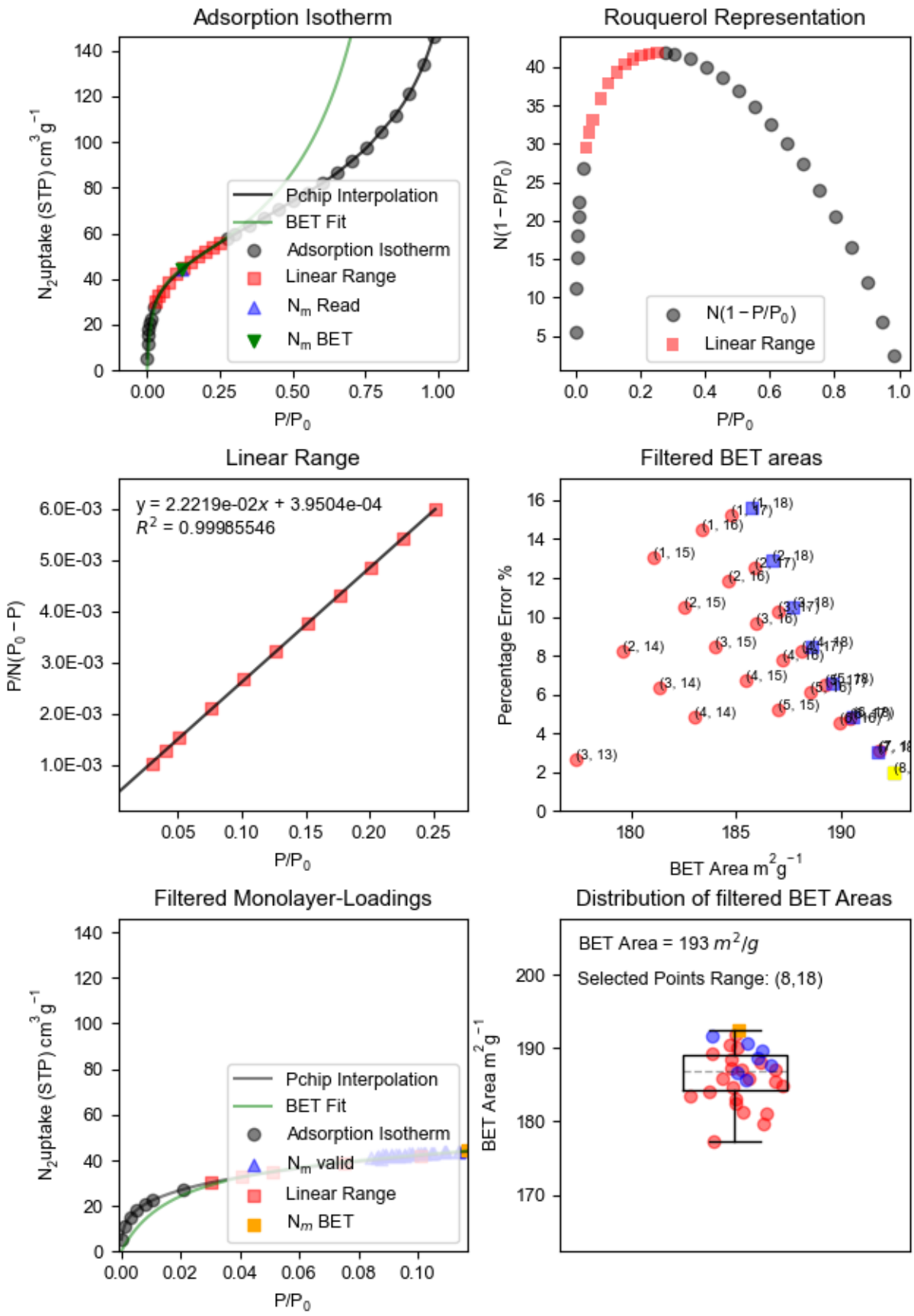

Figure S67. BETSI analysis of the coumarin/bix aerogel N_2 adsorption isotherm presented in **Figure 5b**.

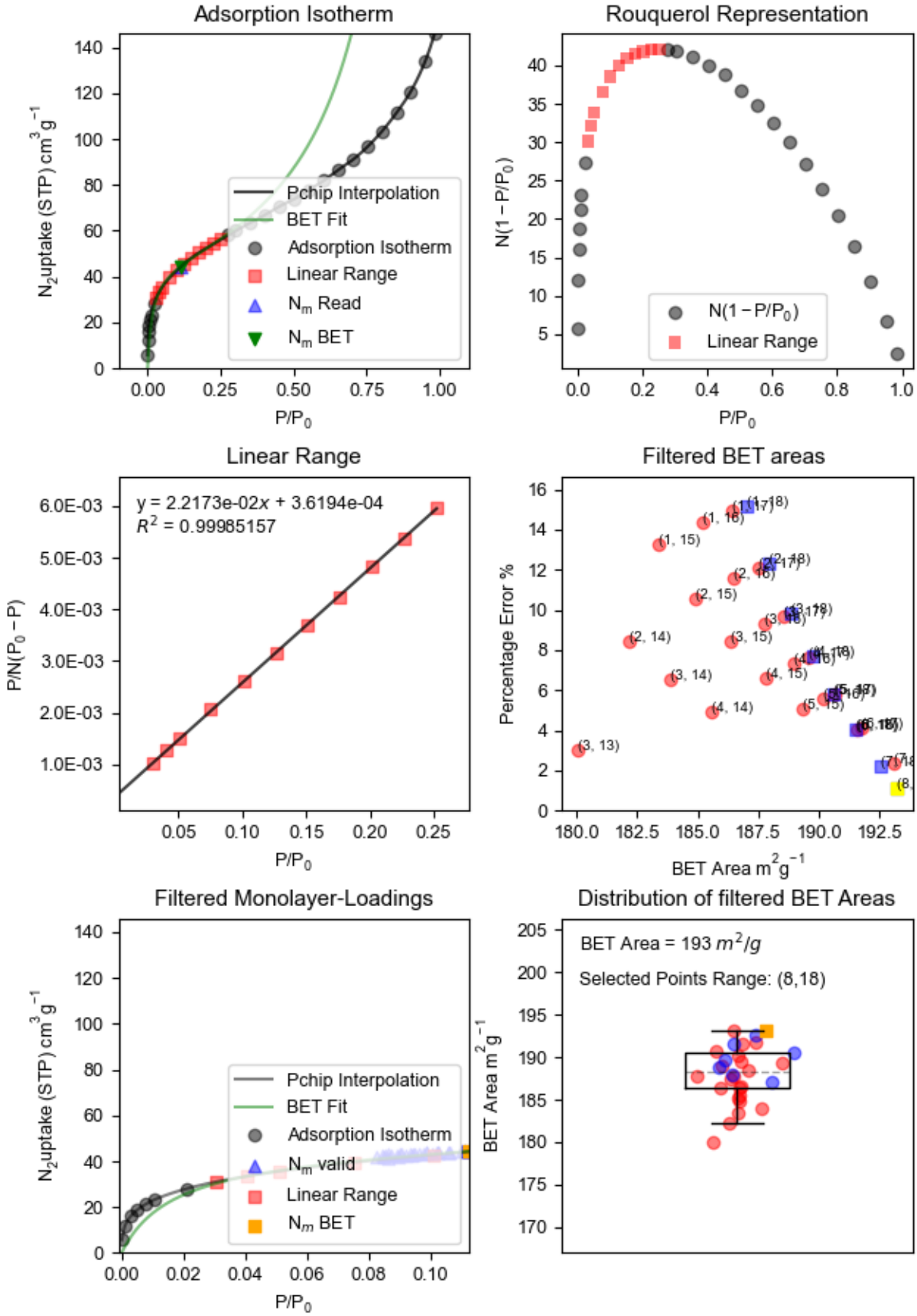

Figure S68. BETSI analysis of the coumarin aerogel N_2 adsorption isotherm presented in **Figure 5b**.

6. References

(1) J. W. M. Osterrieth, J. Rampersad, D. Madden, N. Rampal, L. Skoric, B. Connolly, M. D. Allendorf, V. Stavila, J. L. Snider, R. Ameloot, J. Marreiros, C. Ania, D. Azevedo, E. Vilarrasa-Garcia, B. F. Santos, X.-H. Bu, Z. Chang, H. Bunzen, N. R. Champness, S. L. Griffin, B. Chen, R.-B. Lin, B. Coasne, S. Cohen, J. C. Moreton, Y. J. Colón, L. Chen, R. Clowes, F.-X. Coudert, Y. Cui, B. Hou, D. M. D'Alessandro, P. W. Doheny, M. Dincă, C. Sun, C. Doonan, M. T. Huxley, J. D. Evans, P. Falcaro, R. Ricco, O. Farha, K. B. Idrees, T. Islamoglu, P. Feng, H. Yang, R. S. Forgan, D. Bara, S. Furukawa, E. Sanchez, J. Gascon, S. Telalović, S. K. Ghosh, S. Mukherjee, M. R. Hill, M. M. Sadiq, P. Horcajada, P. Salcedo-Abraira, K. Kaneko, R. Kukobat, J. Kenvin, S. Keskin, S. Kitagawa, K.-i. Otake, R. P. Lively, S. J. A. DeWitt, P. Llewellyn, B. V. Lotsch, S. T. Emmerling, A. M. Pütz, C. Martí-Gastaldo, N. M. Padial, J. García-Martínez, N. Linares, D. Maspoch, J. A. Suárez del Pino, P. Moghadam, R. Oktavian, R. E. Morris, P. S. Wheatley, J. Navarro, C. Petit, D. Danaci, M. J. Rosseinsky, A. P. Katsoulidis, M. Schröder, X. Han, S. Yang, C. Serre, G. Mouchaham, D. S. Sholl, R. Thyagarajan, D. Siderius, R. Q. Snurr, R. B. Goncalves, S. Telfer, S. J. Lee, V. P. Ting, J. L. Rowlandson, T. Uemura, T. Iiyuka, M. A. van der Veen, D. Rega, V. Van Speybroeck, S. M. J. Rogge, A. Lamaire, K. S. Walton, L. W. Bingel, S. Wuttke, J. Andreo, O. Yaghi, B. Zhang, C. T. Yavuz, T. S. Nguyen, F. Zamora, C. Montoro, H. Zhou, A. Kirchon and D. Fairen-Jimenez, How Reproducible are Surface Areas Calculated from the BET Equation?, *Adv. Mater.*, 2022, **34**, 2201502.

(2) S. Tokuda and S. Furukawa, Three-dimensional van der Waals open frameworks, *Nat. Chem.*, 2025, DOI: 10.1038/s41557-025-01777-0.

(3) A. Carné-Sánchez, G. A. Craig, P. Larpent, T. Hirose, M. Higuchi, S. Kitagawa, K. Matsuda, K. Urayama and S. Furukawa, Self-assembly of metal–organic polyhedra into supramolecular polymers with intrinsic microporosity, *Nat. Commun.*, 2018, **9**, 2506.

(4) J. Bae, K. Baek, D. Yuan, W. Kim, K. Kim, H.-C. Zhou and J. Park, Reversible photoreduction of Cu(ii)–coumarin metal–organic polyhedra, *Chem. Commun.*, 2017, **53**, 9250-9253.

(5) A. Carné-Sánchez, G. A. Craig, P. Larpent, V. Guillerm, K. Urayama, D. Maspoch and S. Furukawa, A Coordinative Solubilizer Method to Fabricate Soft Porous Materials from Insoluble Metal–Organic Polyhedra, *Angew. Chem. Int. Ed.*, 2019, **58**, 6347-6350.

(6) T. Wolff and H. Görner, Photodimerization of coumarin revisited: Effects of solvent polarity on the triplet reactivity and product pattern, *Phys. Chem. Chem. Phys.*, 2004, **6**, 368-376.

(7) J. A. Aguilar, R. W. Adams, M. Nilsson and G. A. Morris, Suppressing exchange effects in diffusion-ordered NMR spectroscopy, *J. Magn. Reson.*, 2014, **238**, 16-19.